Regulation of the Spore Cortex Lytic Enzyme SleB in *Bacillus anthracis*

Casey Brianne Bernhards

Dissertation submitted to the faculty of the Virginia Polytechnic Institute and State University in partial fulfillment of the requirements for the degree of

Doctor of Philosophy
In
Biological Sciences

David L. Popham, Chair
Florian D. Schubot
Ann M. Stevens
Richard A. Walker

July 25, 2014
Blacksburg, Virginia

Keywords: *Bacillus anthracis*, anthrax, spore germination, SleB, YpeB

Regulation of the Spore Cortex Lytic Enzyme SleB in *Bacillus anthracis*

Casey Brianne Bernhards

ABSTRACT

Bacillus anthracis is the causative agent of the disease anthrax and poses a threat due to its potential to be used as a biological weapon. The spore form of this bacterium is an extremely resistant structure, making spore decontamination exceptionally challenging. During spore germination, nutrient germinants interact with Ger receptors, triggering a cascade of events. A crucial event in this process is degradation of the cortex peptidoglycan by germination-specific lytic enzymes (GSLEs), resulting in cells that are easily killed. This work investigated the regulation of the GSLE SleB by other proteins in the spore. A full understanding of how GSLEs are held inactive in the dormant spore and are activated during germination could lead to development of simplified spore decontamination strategies in which spore germination is the first step.

It was found that SleB and YpeB are co-dependent. In the absence of one protein, the other is degraded during sporulation by an unidentified protease(s), although HtrC and SpoIVB are not likely responsible. Specific regions and residues of YpeB were also identified as being important to its relationship with SleB. While some evidence suggests that SleB and YpeB physically interact, a direct interaction was not observed *in vivo* or *in vitro*. YpeB was demonstrated to be proteolytically processed by HtrC during germination, resulting in stable products containing the YpeB C-terminus. The presence of inhibitory PepSY domains at the C-terminus of YpeB, coupled with YpeB degradation during germination, may suggest that YpeB processing results in SleB activation. Modification of the predominant YpeB cleavage sites or

deletion of *htrC* reduced proteolysis, but cleavage at other sites still resulted in YpeB instability. Additionally, these changes did not have a significant impact on SleB activity.

SleB regulation by other spore proteins was also examined. To test if SleB activation is Ger receptor-dependent, *Bacillus subtilis* strains lacking Ger receptors and/or GSLEs were germinated via non-nutrient means. Results indicated SleB can be activated independent of these proteins. *B. anthracis* homologs of the *B. subtilis* lipoproteins YlaJ and YhcN were also studied, but deletion of these genes did not result in significant changes in SleB stability or activity.

DEDICATION

I would like to dedicate this work to my entire tremendously supportive and loving family, without whom, none of this would be possible. I wonder if I would even be a college graduate without my mom and dad, Joelle and Wayne. My first week at Virginia Tech, I begged you to come and take me home. Thank you for not listening. You taught me how to stick it out when the going gets tough. You always believed in me, and your love and encouragement were never ending. To my sister Taylor, thank you for the phone calls when I needed to talk, and for always making sure I was healthy and happy. To my brother-in-law Nick, thanks for being a constant source of inspiration. To my sister- and brother-in-law, Kirsten and Evan, thank you for graciously letting me live with you for as long as I needed, and for not kicking me out when that turned out to be a long time.

Most importantly, I dedicate this to my best friend and wonderful husband Cory. Without you, I would never have decided to pursue a Ph.D. in microbiology. I love that I can talk with you about anything, including research. You provided me with the daily love and support I needed to finish, and your unfaltering belief in me got me through my moments of self-doubt. Thank you for handling our distance over the last year with love and encouragement rather than frustration, and for not letting me give up.

ACKNOWLEDGEMENTS

First of all, I would like to thank my advisor, David Popham, for allowing me the opportunity to be a part of your lab and to learn from you. I could not have asked for a better role model and mentor during my development as a scientist. I'm amazed by the depth of your knowledge on just about everything, and how you always seem to have some brilliant idea up your sleeve. At times, you seemed superhuman being able to juggle so much at once. You truly are the master of time management and organization, and your concern and respect for each one of your students is unparalleled. Your level of patience and understanding is also unique—I will never forget the time I was dreading telling you I had dropped and broken a gel power supply box on my way back from the cold room. When I told you, you just smiled and told me to use a cart next time. I don't think I will ever be able to adequately convey how much I appreciate everything you've done for me—the time you spent helping me study for prelims, listening to me practice presentations, and discussing my research with me; your excellent advice and words of encouragement; the countless abstracts, posters, manuscripts, and dissertation chapters you edited and provided feedback on in record time. I have so much respect and admiration for you, as both a scientist and a person.

I would also like to thank my other committee members, Florian Schubot, Ann Stevens, and Richard Walker. You provided me with encouragement, support, and ideas when my research hit a roadblock, and your high expectations and tough questions really pushed me to be better. I always felt that you were in my corner and wanted me to succeed, which made committee meetings just a little bit less intimidating.

My experience as a graduate student at Virginia Tech would not have been the same or nearly as enjoyable without each and every member of the Popham lab. To Jessica McElligott,

Jared Heffron, Emily Lambert, and Ben Orsburn, who were there when I first joined the lab, thank you for immediately making me feel so welcome and for creating such a great place to work everyday. Jessica, I'm grateful for all the initial training and help you gave me, as well as for your friendship and positive energy. Ben, your humor and crazy antics made lab interesting and fun. I'm still telling stories about you to the newer lab members. Emily and Jared, your success provided great examples of what to strive for as a grad student. I admired Emily's knack for organization and Jared's laid back approach to stressful situations. I worried what the future Popham lab would be like once they left, but in true Popham lab style, the next graduate students to join the lab were equally as awesome. Yan Chen and Sean Mury, you have been with me for the majority of my time in the Popham lab and I have appreciated your friendship tremendously. You both even helped me move! You are two of the nicest and most helpful people. Yan, I could always count on you for a good laugh with your various stories, especially one in particular involving a misunderstood student evaluation. I wish I could take you on job interviews since you are always saying the most complimentary things about me. Sean, not only did you supply me with chocolate and energy drinks on multiple occasions, but you actually drilled a hole in the tops of my breakfast shakes so that I would not repeatedly spill them on myself. I will also miss our discussions about the Bachelor and SYTYCD. To the newest addition to the lab, Cameron Sayer, you fit into our little lab family perfectly. Thanks for being easy to laugh and for helping me move too. I look forward to hearing about your journey in the Popham lab and know that you'll carry on the Popham lab traditions. If I could take you all with me to the next place I go, I would.

Thank you to the rest of the Micro Group faculty and grad students for making LSI such a warm and collaborative place to work. A special thank you to Andrea Hartman, my first friend

as a graduate student. I deeply appreciated your friendship and honesty. To Hualan Liu, you are one of the sweetest people I have even met and finding your cookies in the lunchroom always made my day a little better. I would still consider you an honorary Popham lab member even if you weren't married to Yan. To everyone in the teaching labs over the years, Katie Rodgers, Katrina Lasley, Carla Tyler, and Renee Irvin, thank you for your genuine care and concern for the GTAs and for helping things run smoothly so we could get back to research. To my friends in Blacksburg, Alison Heck and Susan Soccolich, thanks for keeping me sane and convincing me to get out of lab every once in awhile. Alison, thanks for always being my movie date, and Susan, thanks for your help with statistics.

Lastly, thank you to Blacksburg and Virginia Tech for being my home for the last 10 years. When I first came to VT as a freshman, I never would have dreamed I would spend both undergrad and grad school here. I grew to love VT, maroon and orange, and Hokie football so much that apparently I just couldn't leave. We've been through a lot together, which has helped shape the person I am, and I will always be proud to be a Hokie.

TABLE OF CONTENTS

LIST OF FIGURES

CHAPTER 1

CHAPTER 2

CHAPTER 3

CHAPTER 4

CHAPTER 5

LIST OF TABLES

CHAPTER 1

Introduction and Literature Review

Casey B. Bernhards and David L. Popham

ATTRIBUTIONS

The literature review sections involving spore peptidoglycan (PG) (General Aspects of PG Structure, Spore PG Layers: Germ Cell Wall versus Cortex, Cortex PG Structural Modifications, Relationships Between Spore PG Structure and Resistance Properties) and spore cortex degradation (Spore PG Lysis During Germination, SleB, CwlJ, SleL (YaaH), GSLEs in *Clostridiaceae*, SleC, SleM, Integration of Cortex Lysis With Other Germination Events), as well as Figures 1.3, 1.4, 1.5, and Tables 1.1 and 1.2 are taken from a book chapter co-authored by Casey B. Bernhards and David L. Popham:

Popham DL, Bernhards CB. 2015. Spore Peptidoglycan, In Press. *In* Driks A, Eichenberger P (ed.), The Bacterial Spore: From Molecules to Systems. ASM Press, Washington, D.C.

This book chapter has not yet been published and is currently in press. The remaining sections and figures were written and produced by Casey for the purpose of this dissertation.

Bacillus anthracis

Bacillus anthracis is a Gram-positive, rod-shaped, nonmotile, spore-forming bacterium that is normally found in soils (103). Anthrax, the disease caused by *B. anthracis,* predominantly affects herbivorous mammals; however, humans can also contract the disease (14). *B. anthracis* spores are the infectious agent, and disease is subsequently caused when the spores germinate into vegetative bacilli within a host and produce their deadly toxins (103). Genes for the main virulence factors, toxins and capsule, are found on two plasmids. Plasmid pXO1 contains genes for protective antigen (PA), edema factor (EF), and lethal factor (LF), while pXO2 contains the genes for capsule synthesis (103). PA combines with EF and LF to form edema toxin (EdTx) and lethal toxin (LeTx), respectively (103). EF is an adenylate cyclase; thus, EdTx increases intracellular cAMP levels which leads to edema through activation of a cAMP-dependent protein kinase (88). LF is a zinc-metalloprotease that cleaves mitogen-activated protein kinase kinases (MAPKKs) (79, 165). The effect of LeTx is shock and death (62).

Anthrax usually presents itself as one of three forms: cutaneous, gastrointestinal, and inhalation anthrax (41, 154). More recently, a fourth type of anthrax infection, injectional anthrax, has been described in heroine users in Europe (154). Most natural cases of the disease are associated with exposure to infected animals or contaminated animal products, generally resulting in cutaneous anthrax (151). Cutaneous anthrax, which accounts for 95% of all human cases, occurs when spores enter through a break in the skin (154). A black skin lesion at the site of infection, known as an eschar, is a hallmark of the disease (103, 151). With antibiotics, the mortality rate is less than 1% (41, 151, 154). Injectional anthrax differs from cutaneous anthrax in that spores are injected subcutaneously or intramuscularly and the mortality rate is 34%, despite antibiotic treatment (154). Gastrointestinal anthrax is relatively uncommon but is caused

by the ingestion of spores, usually by consuming contaminated meat (41, 154). Fatality rates are between 25 and 60% (41, 154). Inhalational anthrax occurs when spores are inhaled into the lungs. Alveolar macrophages phagocytize the spores and transport them through the lymphatic system where they can germinate, multiply, and disseminate into the blood and other organs (14, 41). The mortality rate of inhalational anthrax has generally been reported to be as low as 80% and as high as above 95%; however, during the 2001 exposure in the United States (see below), the fatality rate from inhalational anthrax was 45% (41, 151). While septicemia and death can result from any form of anthrax if prompt medical attention is not received, inhalation anthrax poses the greatest modern threat due to its severity and likelihood in regard to the use of *B. anthracis* as a biological weapon. This threat was realized in October of 2001 when letters containing *B. anthracis* spores were mailed in the United States, infecting 22 people (11 inhalational and 11 cutaneous) and resulting in 5 fatalities (41). The Centers for Disease Control and Prevention (CDC) continue to classify *B. anthracis* as a Category A select agent owing to the likelihood and ease of it being used again in an act of bioterrorism and the potential impacts.

One of the major concerns associated with the use of *B. anthracis* as a bioweapon is that *B. anthracis* spores are extremely resistant structures (see below). This makes antibiotic treatment of infected individuals and decontamination of contaminated sites difficult. Following exposure to *B. anthracis* in the context of bioterrorism, the CDC recommends a 60 day prophylactic course of antibiotics (generally ciprofloxacin or doxycycline) (33). While spores that have germinated are susceptible to antibiotics, dormant spores are not. Due to a possible prolonged period of latency during which dormant spores remain in the host, a long course of antibiotics is necessary (33, 151). Additionally, decontamination of buildings affected by the 2001 anthrax attacks involved fumigations with paraformaldehyde, chlorine dioxide, and

hydrogen peroxide (32). Not only did such fumigations take months and millions of dollars to complete, but the strong chemicals used to eliminate *B. anthracis* spores are toxic, carcinogenic, and/or corrosive (32). Clearly, there is a need for simpler treatment and decontamination strategies.

Bacterial Sporulation

During conditions of nutrient deprivation, members of *Bacillus* and *Clostridium* are capable of undergoing sporulation, a complex process by which vegetative cells become metabolically dormant spores until favorable conditions return. Spores are known for their resistance to environmental stresses, including heat, ultraviolet and ionizing radiation, pressure, chemicals, pH extremes, starvation, and desiccation (112, 147, 148). These resistance characteristics enable spores to persist for extended periods of time in adverse environmental conditions. There have even been reports of viable spores being recovered from thousand year old archeological sites, as well as from insects found within 25-40 million year old amber (57). Sporulation, which typically takes between eight and 10 hours to complete, can be divided into seven stages (not including vegetative cells at stage 0) involved in the transition from a vegetative cell to a free spore (174). After chromosomal replication has taken place, the two resulting chromosomes condense and form an axial filament in stage I (174). Stage II then follows, in which asymmetric septation occurs, dividing the cell into a mother cell and forespore. Engulfment of the forespore by the mother cell characterizes stage III, while cortex peptidoglycan (PG) is created in the intermembrane space between the inner and outer membranes of the engulfed forespore during stage IV (41, 174). Stage IV is also the stage in which pyridine-2,6-dicarboxylic acid (dipicolinic acid, DPA) synthesized in the mother cell is

transported and accumulates in the forespore (41, 148). Coat layers are added to the forespore in stage V, and stage VI is the time when spore maturation, including acquisition of heat resistance, other resistance characteristics, and refractility, occurs. The mother cell lyses releasing the dormant spore during the final step, stage VII (41, 174).

Sporulation is a tightly controlled process dependent upon sequential expression of a vast number of genes. Timing of each wave of gene expression is regulated by an interconnected cascade of sporulation-specific sigma factors. Following polar septation, σ^F becomes active in the forespore compartment leading to the subsequently activation of σ^E in the mother cell (82). Genes involved in forespore engulfment are under the control of these two sigma factors, as are the genes for σ^G and σ^K. Next, σ^G is activated in the forespore, dictating expression of proteins that protect the chromosome and will be necessary for the spore to respond to nutrients (82). Lastly, σ^K becomes active in the mother cell, and along with σ^E, directs expression of genes needed for spore cortex and coat synthesis (82).

Spore Structure

A bacterial spore is composed of different layers, many of which contribute to spore resistance and dormancy by maintaining the low water content of the spore and/or acting as a physical barrier. From the inside out, the layers include the spore core, inner forespore membrane, germ cell wall, cortex, outer forespore membrane, coats, and exosporium (Fig. 1.1). The spore core houses the nucleic acids and the majority of spore enzymes, as well as small, acid-soluble spore proteins (SASPs) that protect the DNA from damage against UV radiation, heat, and chemicals (148). The spore core also contains a large pool of DPA, which aids in DNA protection, protein stabilization, and is associated with the reduced water content of the core

(148). The inner forespore membrane surrounding the core is a lipid bilayer composed of lipid molecules that are compressed and immobile (42); thus, this inner membrane acts as a permeability barrier to water and chemicals (148). Two layers of PG surround this membrane. The inner layer, the germ cell wall, is a thin layer of PG with structural similarity to vegetative cell PG (10, 99). This layer becomes the initial cell wall during spore germination into a vegetative cell (10, 99). The outer layer, the cortex, is comprised of a thick layer of PG with a structure differing from that of vegetative cell and germ cell wall PG (172). Along with the inner membrane, the cortex serves to preserve spore dormancy by maintaining the reduced water content of the spore core (128, 129). The outer forespore membrane surrounds the spore cortex, while the proteinaceous coat layers provide an additional barrier and are necessary for complete protection from a number of chemicals (148). Spores from some species, including *B. anthracis*, have an additional outermost layer termed the exosporium (41). This loose-fitting layer comprised of protein may be an extension of the spore coats (148).

General Aspects of PG Structure

Certain aspects of PG structure are highly conserved across the domain of bacteria (Reviewed in (163, 166)). The glycan strands are composed of alternating N-acetylglucosamine (NAG) and N-acetyl muramic acid (NAM) residues. Attached to the lactyl groups of the NAM are peptide side chains. Disaccharide-pentapeptide precursors are synthesized in the cell cytoplasm and are linked to a bactoprenyl lipid carrier for movement across the membrane. The disaccharides are polymerized on the outer surface of the membrane to produce the PG glycan strands. The strands are then cross-linked via the peptide side chains. The terminal amino acid, generally D-Ala, is cleaved by a transpeptidase, and the new carboxyl terminal amino acid,

generally also D-Ala, becomes linked via a peptide bond to a diamino acid in the third position of a peptide side chain on a neighboring glycan strand. In some species an additional amino acid or short peptide crossbridge is placed between the cross-linked peptides, but this is less common in the Bacilli and has never been observed in spore PG. The diamino acid in the third position in vegetative cell PG is frequently diaminopimelic acid but can be lysine or, more rarely, other residues.

Spore PG Layers: Germ Cell Wall versus Cortex

Spore PG is described in terms of two layers: A thin inner layer called the germ cell wall and the thicker outer cortex layer. The primary distinction between the layers is functional, though the function is likely directly related to a structural difference. The germ cell wall is defined as a PG layer that is not degraded during germination and that functions as the initial wall of the outgrowing spore, while the cortex is the PG that is depolymerized during germination (10, 99). The germ cell wall is structurally more similar to the PG of vegetative cell walls (10, 99), as it contains more tripeptide side chains and a higher level of cross-linking than the cortex PG. The cortex possesses structural modifications that may determine functions and certainly determine its susceptibility to lytic enzymes active during germination (9, 99, 128). In all species in which the spore PG structure has been directly examined, the peptide side chains contain diaminopimelic acid (6, 7, 47, 115, 157, 172). There is some evidence that the germ cell wall of *Bacillus sphaericus* spores contains lysine, similar to the vegetative cell PG of this species (158), but there is no evidence that this aspect of PG structure has any effect on spore properties.

Cortex PG Structural Modifications

Cortex PG contains several structural modifications relative to vegetative cell PG. The major alteration is the removal of the peptide side chain from approximately 50% of the NAM residues and subsequent formation of muramic-δ-lactam (172). The majority of these residues are spaced quite regularly at every second NAM position along the glycan strands (170, 172). In most species, an additional 15-25% of the NAM residues have their side chains shortened to single L-Ala residues (6, 7, 47, 115, 157, 172). In *Clostridium perfringens*, these single L-Ala side chains are not present; instead, a small percentage of the side chains are reduced to dipeptides (115). Deacetylation of a subset of sugar residues in the cortex is observed in some species, but no physiological significance has been associated with this modification (6, 7, 47, 115). PG deacetylation contributes to lysozyme resistance of vegetative cells in several species (51, 131), but the level of deacetylation is generally higher than that observed in spore PG, and the permeability barrier of the spore coat layers is the primary mechanism of spore lysozyme resistance (49).

An outcome of modifications that remove or shorten the peptides is greatly reduced cross-linking of the spore PG. While 33-45% of NAM residues in vegetative cell walls of *Bacillus subtilis* carry peptides involved in cross-links (5, 171), only ~3% of NAM residues in spore PG carry cross-linked peptides (9). While the spore PG is clearly a relatively loosely cross-linked structure, some evidence indicates that the cross-linking varies across the span of the PG layers (99, 126). The germ cell wall layer appears to have the highest cross-linking level, while the cortex immediately exterior to this is extremely loosely cross-linked. The cross-linking then increases progressively toward the outermost region of the cortex.

Relationships Between Spore PG Structure and Resistance Properties

The aspect of spore PG structure that impacts spore resistance most clearly is the amount of PG per spore. Experimental reduction of accumulation of PG during spore formation resulted in increased spore hydration and a corresponding decrease in resistance to heat and organic chemicals (72). Comparisons across strains of a species and across multiple species have revealed a correlation between the ratio of core volume to core-plus-cortex volume and spore heat resistance and dehydration (17, 115). Variation of this ratio within a species is likely a measure of cortex PG abundance (115).

On the contrary, variation in spore PG structural parameters, such as muramic-δ-lactam abundance and peptide cross-linking, within a relatively broad range, has not revealed a clear correlation with spore dehydration and resistance properties. Spores that lack single L-Ala side chains and have a corresponding increased abundance of full-length peptide side chains are only slightly affected in their heat resistance (68). This spore PG alteration is accompanied by a very slight increase (< 2-fold) in PG cross-linking (68). Other mutations that increase spore PG cross-linking 5-fold (a *dacB* mutant) (9, 124) or 9-fold (a *cwlD dacB* double mutant) (130) do not produce major alterations of spore dehydration. These alterations also remove the gradient of cross-linking across the span of the cortex, with little effect on the ability of the spores to achieve normal dehydration (99). Only when the level of cross-linking rises to more extreme levels, in a *dacB dacF* double mutant, is the relative dehydration of the spore altered (126).

The low degree of cortex PG cross-linking is striking, and the lack of an effect of this structural parameter on spore properties is surprising. It is known that the relative cross-linking of PG affects the flexibility of the structure, with more loosely cross-linked structures exhibiting greater expansion and contraction (116). It was proposed that the flexibility of loosely cross-

linked spore PG could contribute to the process of spore core dehydration, either via cortex contraction (89) or anisotropic expansion (169), during spore formation. The observation that major changes in cortex PG cross-linking do not diminish dehydration (9, 124, 130) argues against this possibility. Perhaps the proper aspect of spore resistance has not been assayed relative to cortex cross-linking and flexibility. It has been demonstrated that spores expand and contract in response to changes in relative humidity of their environment (173). Presumably, a loosely cross-linked, flexible cortex might allow the spore PG layers to accommodate core volume changes. Such an ability may be very important in allowing spores to retain core dehydration, dormancy, and associated resistance properties while experiencing repeated cycles of humidity changes in their natural environment. Consistent with this idea, *B. subtilis dacB* mutant spores with increased cortex cross-linking are produced with a normal degree of core dehydration, but they are unable to maintain it and gain water content during heating (129). Interestingly, spores with increased cortex cross-linking could initiate the release of Ca^{2+}-DPA from the spore core more rapidly than wild type spores following exposure to germinants (178). This seems to indicate a direct effect of the cortex structure on the threshold for germination initiation within the spore.

The conversion of 50% of the NAM residues in cortex PG to muramic-δ-lactam is perhaps the most striking PG structural alteration found in the spore. Surprisingly, mutations that result in a complete lack of muramic-δ-lactam in spores do not have major effects on spore dehydration or heat resistance. Despite a > 2-fold increase in peptide side chain abundance and a > 2-fold increase in PG cross-linking that accompany the loss of muramic-δ-lactam, these spores are fully dehydrated and resistant (128). However, these same spores exhibit a > 10^4-fold decrease in ability to complete germination and produce colonies (10, 128, 142). Analyses of

spore PG degradation and release during germination indicate that spores lacking muramic-δ-lactam are unable to depolymerize the spore PG (10, 128). This led to the proposal, since borne out experimentally (see below), that the muramic-δ-lactam serves as a specificity determination for germination-specific lytic enzymes. The abundance of muramic-δ-lactam in cortex PG and its paucity in germ cell wall PG would therefore lead to the observed specific degradation of cortex during germination, leaving the germ cell wall intact.

Spore Germination

Following sporulation, dormant spores monitor the surrounding environment, lying in wait for conditions capable of sustaining growth to return. When nutrients, called germinants, become available again, the spores undergo a process known as germination in order to return to a vegetative state (Fig. 1.2) (147). In nature, germination is triggered by the binding of germinants to Ger receptors located in the inner membrane of the dormant spore (15, 70, 105, 118, 139). Each receptor is generally comprised of three protein subunits (A, B, and C) expressed from a tricistronic operon (139). A given species will commonly have multiple Ger receptors, each encoded by a separate operon, that respond to different classes of nutrients (139). Nutrient germinants can include amino acids (commonly L-alanine), sugars (such as glucose and fructose), purine nucleosides, or a combination (57, 147). Once germination is triggered in this manner, the spore becomes committed to proceed through germination, even if the germinant is subsequently removed (147). Spores have also been found to germinate in response to non-nutrient means, such as exogenous Ca^{2+}-DPA (135), lysozyme (following spore coat removal) (58), hydrostatic pressure (39), and cationic surfactants (especially dodecylamine (136, 137))

(138), although portions of the nutrient germination pathway may be bypassed in these instances (117, 119, 143, 147, 175).

Following the triggering of germination, stage I of the germination process occurs, in which ions and calcium DPA are rapidly released from the spore core, while the core is partially rehydrated by the uptake of water (147). Partial loss of some of the spore's resistance properties also occurs. Stage II is defined by the degradation of the cortex, causing cortical fragment release into the surrounding environment, as well as full rehydration and swelling of the core by inflowing water (147). The spore experiences loss of dormancy and further loss of resistance characteristics. Stage II is followed by a period of outgrowth, in which cell metabolism and protein synthesis resume (147).

Spore PG Lysis During Germination

Cortex degradation is necessary for full rehydration of the core and resumption of metabolism (128, 144). Spores in which the cortex cannot be degraded successfully initiate germination and release the large depot of Ca^{2+}-DPA stored within the spore core, though this release is slower than in wild type spores (178). The Ca^{2+}-DPA is replaced with a limited volume of water, which is accompanied by a decrease in spore refractility and a partial drop in optical density (128, 144). While these spores are able to complete stage I of germination, they cannot proceed any further. The intact cortex prevents the spore core from reaching rehydration levels necessary for metabolism to resume, and thus, the spores do not go through outgrowth to become vegetative cells (128, 144). Addition of lysozyme to these spores allows for the completion of germination and outgrowth, indicating the germination defect observed is due to intact cortex PG (128, 144).

Hydrolysis of the cortex during spore germination is due to the activity of germination-specific lytic enzymes (GSLEs). GSLEs can be subdivided into two categories: spore cortex-lytic enzymes (SCLEs), which preferentially degrade intact cortex PG, and cortex fragment-lytic enzymes (CFLEs), which have specificity for PG fragments that result from SCLE activity (94). Both groups require the presence of muramic-δ-lactam in the spore cortex to carry out their enzymatic activities, which ensures that the cortex is degraded while the germ cell wall remains unharmed (34, 94, 128). In addition, GSLEs must be expressed during spore formation, as they must be available to degrade cortex PG before there is any metabolism in the germinating spore (144, 145).

Bacillus species possess the GSLEs SleB, CwlJ, and SleL (YaaH). Although SleL and YaaH appear to be orthologs, they are referred to by separate names as a result of their distinct enzymatic activities. SleB and CwlJ must be SCLEs because either one alone is sufficient to allow completion of germination. Spores lacking both SleB and CwlJ have a severe germination defect. They release Ca^{2+}-DPA, but only lose a small percentage of their initial optical density (55, 63, 64, 117, 144, 145). Germination is arrested at the stage of cortex hydrolysis, resulting in no further loss of optical density, and no release of cortex muropeptides (55, 63, 64, 74, 145). SCLE-deficient spores cannot attain the level of rehydration necessary to resume metabolism (144, 145), and thus, their colony forming efficiency is significantly reduced by at least 10^3-fold (55, 63, 64, 74, 117, 145). SleL alone does not allow completion of germination but can accelerate the process of cortex degradation following the action of a SCLE; therefore, SleL is a CFLE.

SleB

The gene *sleB* is expressed under the control of σ^G, indicating SleB is synthesized in the developing forespore (23, 108). The arrangement of *sleB* in an operon upstream of *ypeB* is highly conserved across *Bacillus* species (23, 64, 108, 127). However, in *Bacillus anthracis* and others species of the *Bacillus cereus* group, a third gene follows *ypeB* in the operon and shows homology to the *ylaJ* and *yhcN* genes of *B. subtilis* (64). In *B. subtilis*, *ylaJ* and *yhcN* are not found in the *sleB* operon but elsewhere in the chromosome, where their transcription is also dependent on σ^G (12, 84). YlaJ is an uncharacterized sporulation-specific protein, while YhcN is predicted to be a membrane-anchored lipoprotein and appears to play a small role in spore germination or outgrowth (12, 84).

Spores lacking SleB exhibit a minor defect during germination. Studies have indicated that *sleB* mutant spores have a slight delay in loss of optical density, or they do not lose as much optical density as wild-type spores (23, 55, 64, 74, 109). In addition, spores of a *B. anthracis sleB* mutant release less cortex fragments and at a slower rate than wild-type spores (64). Despite their defect during germination, *sleB* mutant spores complete germination and produce viable colonies (23, 55, 64, 74). The ability of these mutant spores to form colonies indicates that SleB and CwlJ are partially redundant enzymes; the presence of one can compensate in the absence of the other.

SleB contains a classic signal sequence at its amino-terminus (Fig. 1.3) for translocation across the inner forespore membrane, and this signal sequence is cleaved during sporulation (65, 69, 108-110, 159). Thus, SleB is present in a mature yet inactive form within dormant spores. The ultimate location of SleB within the dormant spore has yet to be conclusively demonstrated (Fig. 1.4). Immunoelectron microscopy using anti-SleB antibodies detected SleB in the outer

cortex/outer forespore membrane region of spores from both *B. subtilis* and *B. cereus* (108). On the other hand, western blots of integument (consisting of spore coats, cortex, and outer membrane), inner membrane, and soluble spore fractions showed the presence of SleB in both the integument and inner membrane fractions (36). Compared with other GSLEs, the resistance of SleB within dormant spores to detergent, heat, and alkali treatments also suggests that SleB may be localized to a more inward, protected region of the spore (8, 36).

SleB possesses two recognizable protein domains (Fig. 1.3). The N-terminal half of SleB has tandem sequence repeats characteristic of a PG-binding domain (pfam01471), and this motif has been found in the noncatalytic region of other PG hydrolases (95, 109, 110). Using a series of SleB-GFP fusions, it was shown that the interaction between the PG-binding domain and muramic-δ-lactam in the spore cortex is necessary for SleB localization (95). However, this study did not utilize forms of SleB shown to retain any functional properties. *In vitro* assays using SleB overexpressed and purified from *E. coli* support the dominant role of the N-terminal domain in PG binding but suggest that the specificity for muramic-δ-lactam is actually contained in the C-terminal domain (65).

The C-terminal half of SleB contains the PG-cleaving enzymatic domain (pfam07486) (65, 90). SleB cleaves the glycan strands of the cortex PG between the NAM and NAG residues forming anhydromuropeptide products characteristic of a lytic transglycosylase (Fig. 1.5) (23, 64). Lytic transglycosylase products were demonstrated to be absent in the muropeptide profiles of *sleB* mutants, supporting this enzymatic classification of SleB (23, 37, 64). Assays of purified SleB *in vitro* demonstrated that while both protein domains are necessary for the most efficient lytic activity, the catalytic domain of SleB alone can act as a lytic transglycosylase without the PG-binding domain (65, 90).

Mutants lacking *sleB* or *ypeB* have similar germination phenotypes and cortex digestion patterns (19, 23). This is not surprising given that YpeB is required for the presence of SleB in spores, as SleB is absent in western blots of extracts from *ypeB* mutant spores in *B. subtilis* and *B. anthracis* (19, 36, 90). Similarly, SleB is required for the presence of YpeB in spores (19, 90). In the absence of the partner protein, both SleB and YpeB are produced and rapidly degraded during spore formation (19). Co-localization of SleB and YpeB (Fig. 1.4) is likely as the spore fractionation experiments that placed SleB in the integument and inner membrane fractions detected YpeB in the same fractions (36). YpeB possesses an N-terminal signal sequence (Fig. 1.3) that is likely uncleaved and anchors the protein to the inner forespore membrane (23, 36). In addition, YpeB contains three putative PepSY domains (pfam03413) (Fig. 1.3), which in some proteins are involved in the inhibition of proteolytic activity (177). The exact relationship between SleB and YpeB, as well as the contributions of the PepSY domains, have yet to be elucidated; however, interesting possibilities include involvement of YpeB in SleB localization, SleB stabilization against proteolysis and during prolonged spore dormancy, and holding SleB inactive prior to the triggering of spore germination. YpeB has been demonstrated to inhibit SleB activity in an *in vitro* assay, though a direct protein-protein interaction was not detected (90).

In the process of germinating, *B. cereus* spores release at least some SleB to the exudate, and this pool of SleB is active on decoated spores (93). Conversely, SleB is not released from germinating *B. subtilis* spores (36, 108, 109). SleB of a consistent size is detected in western blots throughout germination of *B. subtilis* spores, indicating SleB is stable and does not undergo proteolytic processing (36). While SleB is not processed during germination, there is evidence that YpeB may be proteolytically cleaved. Western blots of germinating *B. subtilis* spores show

a 51 kDa band corresponding to YpeB disappear within 10 minutes, at which point a 30 kDa YpeB fragment is detected (36). This processing is also observed in *B. anthracis*, and the stable YpeB fragment was found to contain the C-terminal PepSY domains (Chapter 3).

CwlJ

Unlike *sleB*, which is expressed in the forespore, *cwlJ* is a sporulation-specific gene expressed in the mother cell under the control of σ^E (74). *B. anthracis* contains two *cwlJ* homologs, *cwlJ1* and *cwlJ2* (55, 64). In many *Bacillus* species, *cwlJ* forms a bicistronic operon with *ywdL*, while in others, such as *B. subtilis*, the *cwlJ* gene is monocistronically transcribed, with *ywdL* being located elsewhere in the chromosome (Table 1.1) (74, 132). (In *B. subtilis*, *ywdL* was renamed *gerQ* (132), but there is a different gene called *gerQ* in the *B. cereus* group (16), so the *ywdL* designation is utilized here to avoid confusion.) The gene *ywdL* is also expressed in the mother cell under the control of σ^E in *B. subtilis* (132). In *B. anthracis*, *cwlJ1* is in a bicistronic operon upstream of *ywdL*, and *cwlJ2* is monocistronic (64).

CwlJ localizes to the spore coats (Fig. 1.4), and some studies suggest CwlJ may oligomerize (13, 36, 117, 132). CwlJ was detected in immunoblots of spore coat extracts, but not in decoated or *cotE* mutant spores in which the coat layers are disrupted or defective (13). The localization of CwlJ to the spore coats is fitting since CwlJ lacks a signal sequence necessary for transport from the mother cell across a membrane, and spore coat proteins are also synthesized in the mother cell compartment (36, 48, 74). In addition, CwlJ lacks transmembrane domains that would be characteristic of a membrane protein; thus, it is unlikely that CwlJ is associated with the outer membrane of the spore (13). Chirakkal *et al.* found CwlJ from *B. subtilis* to be present in western blots of germinated spore samples with no change in band size

or intensity (36). Conversely, results obtained by Bagyan and Setlow indicate CwlJ disappears during germination (13). These conflicting results may be due to the different methods of germination employed (the former study used L-alanine, while the latter used Ca^{2+}-DPA) or the use of CwlJ with a His-tag.

Similar to the dependence upon YpeB for the presence of SleB in the dormant, YwdL is required for the presence of CwlJ in spores (132). While CwlJ does not localize without YwdL, *cwlJ* is still expressed, suggesting YwdL plays a yet unknown role in CwlJ activity, localization, and/or stabilization (132). The relationship between the two proteins does not appear to be co-dependent as YwdL localizes properly in the absence of CwlJ (132). YwdL localizes to the inner spore coat layer (Fig. 1.4) in *B. subtilis* (73, 132) and to the inner layer of the exosporium in *B. cereus* (92, 155). In *B. subtilis*, YwdL is cross-linked into high-MW complexes, likely with other coat proteins, late in sporulation by Tgl, the spore transglutaminase (133). Three lysine residues near the N-terminus of *B. subtilis* YwdL are necessary for cross-linking, but cross-linking is not required for YwdL or CwlJ localization to the coats or function during germination (107, 132, 133). There is a lack of conservation of these YwdL lysine residues across *Bacillus* species, and it is unknown if YwdL is cross-linked to the spore coats in other species (107). Fluorescence microscopy has demonstrated that YwdL does not change location during germination and remains associated with the spore coats in *B. subtilis* (132).

CwlJ is necessary for germination via Ca^{2+}-DPA as *cwlJ* mutants fail to germinate in response to exogenous Ca^{2+}-DPA (117, 145). As expected due to its role in incorporation of CwlJ into spores, YwdL is also necessary for germination with Ca^{2+}-DPA (155). While CwlJ1 from *B. anthracis* is predominately responsible for response to Ca^{2+}-DPA, CwlJ2 plays a minor part in the process (63). Germination in response to Ca^{2+}-DPA requires intact coat layers,

providing further support that CwlJ is associated with the coats and is responsible for cortex hydrolysis in response to Ca^{2+}-DPA (117). Endogenous Ca^{2+}-DPA released from the spore core during the early stages of nutrient germination is essential to activate CwlJ to degrade the cortex, although it is unclear whether CwlJ activation by Ca^{2+}-DPA is direct or indirect (117).

Interestingly, CwlJ is homologous to the C-terminal catalytic domain of SleB (pfam07486) (Fig. 1.3), yet CwlJ does not appear to be a lytic transglycosylase and currently has no ascribed enzymatic function (36, 64, 74). The sequence similarity between CwlJ and SleB, and the shared cleavage site of lytic transglycosylases and muramidases (Fig. 1.5), raise the possibility that CwlJ could be a muramidase. Numerous muramidases and lytic transglycosylases belong to a very large family of related proteins (22, 140). Current methods of PG structural analysis involve hydrolysis using a commercially available muramidase (10, 47, 63), making detection of a small amount of such an activity problematic. Attempts by several research groups to purify active CwlJ have failed, so clear demonstration of enzymatic activity may await overcoming this roadblock.

SleL (YaaH)

During sporulation, *sleL (yaaH)* is expressed monocistronically under the control of σ^E in the mother cell (80, 85). The amino acid sequence of SleL (YaaH) does not contain a predicted signal sequence, which is consistent with its localization to the spore coats (Fig. 1.4) (34, 73, 80, 98). In support of the placement of SleL in the coat layers, western blotting experiments detected SleL in the coat fraction stripped from spores and not in the remaining decoated spores (34). More specifically, fluorescent microscopy and a dependence on SafA (a major inner coat protein) for localization, have demonstrated that YaaH resides in the inner spore coat (73, 98).

Studies in *B. cereus* and *B. subtilis* have indicated that following spore germination, active SleL (YaaH) is found in the exudate (34, 36).

At the N-terminus of SleL are two repeated sequences that have been implicated to be involved in cell wall binding (Fig. 1.3) (34). These sequences form LysM domains (pfam01476), which are widely distributed in nature, bind PG and chitin, a polymer of NAG, and are most frequently encountered in PG hydrolases (27). A glycosyl hydrolase family 18 domain (pfam00704) is found at the C-terminus of SleL (YaaH) (Fig. 1.3), but interestingly, this domain doesn't appear to have the same enzymatic activity across the *Bacillus* genus. HPLC analyses of muropeptides collected from germinating spores indicate YaaH has epimerase activity on cortex PG in *B. subtilis* and *B. megaterium* (57, 62). On the other hand, studies in *B. anthracis* and *B. cereus* have demonstrated SleL does not possess epimerase activity but is instead an N-acetyl-glucosaminidase that cleaves between NAG and muramic-δ-lactam (Fig. 1.5) (34, 85). A more recent study indicated that *B. megaterium* SleL can exhibit N-acetyl-glucosaminidase activity (161). Epimerase activity is a likely intermediate in the N-acetyl-glucosaminidase reaction (120), and the alternate production of epimerase versus N-acetyl-glucosaminidase products may be due to species and strain genetic variation (127). In *B. anthracis*, the glycosyl hydrolase domain can carry out N-acetyl-glucosaminidase activity alone; however, addition of the LysM domains results in increased affinity for its substrate resulting in greater PG degradation (86).

SleL is unique from the other *Bacillus* GSLEs in that it is only active on cortex fragments (34). Thus, the role of SleL, where it acts as an N-acetyl-glucosaminidase, is to break down larger PG fragments created first by SleB and CwlJ (63, 85). This small contribution of SleL is not crucial for spore germination, but does explain the rapid release of muropeptides from germinating *B. anthracis* spores and the retention of the majority of cortex material in Δ*sleL*

spores (63, 85). The epimerase activity of YaaH in *B. subtilis* and *B. megaterium* alters the stereochemistry of cortex fragments without hydrolyzing them, resulting in a much slower rate at which cortex material is released during germination (6, 10).

GSLEs in *Clostridiaceae*

While germination involves cortex hydrolysis in both *Bacillus* and *Clostridium* species, the mechanism through which cortex depolymerization is achieved is divergent. *Bacillus* species possess the major lytic enzymes SleB and CwlJ, either of which is sufficient to complete spore germination. Some *Clostridiaceae* contain *sleB* and *cwlJ* homologs in their genomes (Table 1.2), but to date, none of these homologs have been demonstrated to contribute to spore germination (127). This was found to be the case in *Clostridium difficile*, where a mutation in a *sleB*/*cwlJ* homolog had no effect on spore germination (28). Instead, many *Clostridium* species, including *C. perfringens* and *C. difficile*, contain SleC as the main GSLE (Table 1.2), which alone is necessary and sufficient to allow completion of germination (28, 122).

SleC acts on intact cortex PG and thus is classified as a SCLE (83, 102). Mutant strains lacking SleC have a severe germination defect. Spores without SleC experience only a small drop in optical density, release no hexosamine, and release Ca^{2+}-DPA more slowly during germination (122). In addition, these spores have a 10^3-fold decrease in colony-forming efficiency (122).

A smaller number of *Clostridiaceae*, including *C. perfringens*, also possesses a second GSLE, called SleM, which plays an auxiliary role in germination (127). Akin to the role of SleL in *Bacillus*, SleM is a CFLE with specificity for cortex fragments first produced by SleC (35, 83). SleM is not required for completion of germination, but an *sleC sleM* double mutant has an

even greater germination defect than a *sleC* mutant (122). Unlike the activation of CwlJ by Ca^{2+}-DPA in *Bacillus*, Ca^{2+}-DPA doesn't appear to trigger germination by activating SleC or SleM in *C. perfringens* (122).

SleC

In *C. perfringens*, SleC is expressed from a monocistronic gene in the mother cell compartment during sporulation (96). Unlike the GSLE counterparts in *Bacillus*, SleC is synthesized as a precursor containing N-terminal pre- and pro-sequences and a C-terminal pro-sequence (Fig. 1.3) that are processed during stages of sporulation and germination (101, 160). During spore formation, the N-terminal pre- and C-terminal pro-sequences are removed sequentially from the 50 kDa SleC precursor, and the resulting 35 kDa pro-SleC is incorporated into the dormant spore (101, 160). After cleavage, the N-terminal pre-peptide remains associated with pro-SleC and is necessary for proper folding of the pro-enzyme (114). The inactive pro-SleC requires proteolytic cleavage of the N-terminal pro-sequence during germination to become the active 31 kDa form of the enzyme (101). This mature form of the enzyme contains a PG-binding domain (pfam01471) (Fig. 1.3) similar to that found in SleB and other PG hydrolases (101), and was proposed to possess both lytic transglycosylase and N-acetylmuramoyl-L-alanine amidase activities (Fig. 1.5) (83, 101). The lytic transglycosylase activity of *C. difficile* SleC has also been demonstrated (60).

In a tricistronic operon just upstream of *C. perfringens sleC*, the genes *cspA*, *cspB*, and *cspC* encode the three proteases that make up the Germination-Specific Protease complex (GSP) needed to cleave pro-SleC to active SleC (96, 149). This is not the case for all strains of *C. perfringens* as some strains have only a single *cspB* gene upstream of *sleC* (111, 123), and this

single CspB is sufficient for the processing of pro-SleC to active SleC (123). The Csp proteases are also expressed in the mother cell and contain N-terminal pro-peptides (Fig. 1.3) that likely serve as intramolecular inhibitory chaperones (1, 96, 123, 149). These proteases belong to a family of subtilisin-like serine proteases possessing a highly conserved catalytic triad and an oxyanion binding region (149). Inactive pro-SleC and CspC localize outside the cortex, either in the inner coat or the outer membrane, within dormant spores (Fig. 1.4), and presumably this is also the location of the other Csp proteases (100, 101, 123, 149). After *C. perfringens* spores undergo germination, active SleC and the active Csp proteases are found in the germination exudate (100, 101, 160). The role of a CspB protease in germination-dependent processing of SleC has also recently been demonstrated in *C. difficile* (1).

SleM

Like *sleC, sleM* is transcribed monocistronically in the mother cell (96); however, SleM does not undergo proteolytic processing during sporulation or germination (Fig. 1.3) (35, 160). SleM is found as a mature enzyme within dormant spores, where it localizes outside the spore cortex to the outer forespore membrane or inner coat layers (Fig. 1.4) (35, 100). Release of active SleM from mechanically disrupted dormant spores provides evidence that SleM is not incorporated into the spore as a pro-enzyme that requires cleavage during germination (35). SleM is an N-acetylmuramidase (Fig. 1.5) and has specificity for cortex fragments rather than intact cortex PG (35). Thus, SleM is not essential for germination but likely further hydrolyzes cortex fragments first produced by SleC (83, 122). Unlike the loss of SleL in *Bacillus,* which causes spore retention of much of the muropeptides generated during germination (63, 85),

muropeptides appear to be released normally by *sleM* mutant spores (122). After germination, SleM is found as an active enzyme in the spore exudate (35, 100).

Integration of Cortex Lysis With Other Germination Events

Cortex degradation is a key step in completion of germination triggered by any stimulus, but the progression of germination events can differ based upon the type of stimulus. Nutrient-stimulated germination is almost certainly the predominant process in natural environments. Interaction of nutrient germinants with *Bacillus* Ger receptors at the inner spore membrane results in the release of ions, including Ca^{2+}-DPA, and some partial hydration of the spore core (104, 147). These events trigger SleB activity via an unknown mechanism. It may be via a return of fluidity to the inner spore membrane (42), via an allosteric regulation of SleB, or via an alteration of the cortex substrate conformation. The Ca^{2+}-DPA release triggers CwlJ activity. Similar initial steps take place during nutrient-stimulated germination of *Clostridium* spores (121), resulting in activation of the SCLEs present, either SleB, CwlJ, or SleC. SleC becomes active following cleavage of its pro-peptide by a Csp protease, but the regulation of this processing is unknown. The combined activities of SleB and CwlJ, or SleC, result in sufficient cortex depolymerization to allow core swelling and full rehydration. If a CFLE such as SleL or SleM is present, the further breakdown of cortex fragments can speed release of muropeptides into the surrounding medium.

Germination by exogenous Ca^{2+}-DPA proceeds by a different mechanism in *Bacillus*, where activation of CwlJ is the initial step (117). Cortex depolymerization by CwlJ apparently leads to eventual destabilization of the inner spore membrane, ion release, and a return of hydration and membrane fluidity to the core. It is likely that SleB becomes activated at some

point in this process, and SleL can act on cortex fragments produced by CwlJ (63). Germination of *C. perfringens* spores by exogenous Ca^{2+}-DPA occurs thorough an unknown mechanism that does not involve direct activation of a GSLE (122).

Regardless of the stimulus that initiates the germination process, in all cases some cortex degradation is essential for the resumption of metabolism and progression into spore outgrowth. From this discussion it is clear that the outstanding questions in this field concern the mechanisms by which the GSLEs are held inactive and stable in the dormant spore and the processes that result in their activation during germination. A full understanding of these enzymes can make them a target for efforts to stimulate highly efficient germination of spore populations followed by simplified decontamination treatments.

Study Objectives

The purpose of this research was to gain more insight into how the GSLE SleB is regulated by other spore proteins in *B. anthracis*. Previous studies have demonstrated the large contribution of SleB during spore germination and its precise enzymatic activity on cortex PG. What is still not understood is how SleB is held inactive in the dormant spore, and subsequently, how SleB is activated during spore germination. Chapter 2 examines the relationship between SleB and YpeB, a protein expressed from the same operon. SleB and YpeB were found to have a strongly co-dependent relationship, where without one, the other protein is degraded during sporulation. Further study revealed the necessity of regions in both N- and C-terminal portions of YpeB for SleB stability, as well as the importance of highly conserved residues within the YpeB PepSY domains for stability of both proteins.

Chapter 3 investigates the fate of YpeB during germination and how this may contribute to SleB activation. It was demonstrated that YpeB is cleaved into two stable products, both containing the C-terminal PepSY domains. The specific YpeB cleavage sites were determined, and a protease, HtrC, was shown to be involved in YpeB processing both *in vivo* and *in vitro*. Mutating the YpeB cleavage sites or deleting *htrC* did not prevent YpeB degradation completely, hindering the ability to determine the role of YpeB processing in SleB activation.

Another SleB activation theory was tested in Chapter 4 using *B. subtilis* as a model organism. To determine if the Ger receptors directly activate SleB, spores lacking all functional Ger receptors and/or GSLEs were germinated with the non-nutrient germinants Ca^{2+}-DPA and dodecylamine. Muropeptides specific to SleB activity were released during germination, indicating SleB does not require the Ger receptors or CwlJ for activation.

Experiments aimed at showing a direct physical interaction between SleB and YpeB *in vivo* and *in vitro* are presented in Chapter 5. The contributions of a protease, SpoIVB; and lipoproteins, YlaJ and YhcN, are also examined. SleB and YpeB do not interact *in vitro*, and a physical interaction *in vivo* could not be conclusively shown. Other proteases, besides SpoIVB, are involved in SleB and YpeB proteolysis during sporulation in the absence of YpeB or SleB, respectively. YlaJ and YhcN do not affect SleB or YpeB stability or significantly impact spore germination.

Knowledge of the mechanisms by which SleB is stabilized and held inactive in the dormant spore, as well as mechanisms for SleB activation during germination, could lead to development of decontamination methods that trigger germination by activating SleB. Such methods may directly target SleB or the proteins involved in its regulation. SleB activation

could result in very high levels of spore germination, producing vulnerable cells that are more easily killed.

Table 1.1. Identities of orthologous genes potentially involved in degradation of spore PG in a range of species spanning the family *Bacillaceae*[1].

B. subtilis **gene name**	***B. subtilis*** **gene ID**	***B. megaterium*** **QM B1551**	***B. anthracis*** **Ames**	***B. halodurans*** **C-125**	***Geobacillus kaustophilus*** **HTA426**	***Paenibacillus*** **sp. JDR-2**	***Oceanobacillus iheyensis*** **HTE831**
sleB	938979	8988788 P	1084998 P	891408 P	3184902 P	8126804 X 8124631 X	1018300 P
ypeB	938981	8988787 P	1086708 P	892552 P	3185430 P	8125141 X	1018299 P
cwlJ	938399	8989642 JY 8987672 X	1085358 JY 1087364 X	890546 JY	3184927 JY	8125961 X	1017903 JY
ywdL	937241	8989643 JY	1085359 JY	894423 JY	3184525 JY	8127416 X	1016708 JY
sleL/yaaH	937029	8984459 G	1089237 X	891826 X	3184040 X 3184810 X	8129825 X	1015055 P

[1]Each gene is identified by an NCBI Gene ID number. Orthologs were identified using tblastn and blastp searches (2) for similarity to the products of the indicated *B. subtilis* genes. In all cases, the identified ortholog exhibited the greatest amino acid sequence identity with the *B. subtilis* protein. Due to the presence of multiple genes within each class in some genomes, the genome context of each similar gene was examined to strengthen assignments of orthologs. A letter following the Gene ID number indicates the similarity of the genome context to that found in *B. subtilis*: G indicates a genome context match where the adjacent genes on both sides were shared; P indicates a partial genome context match where the adjacent genes on one side were shared; X indicates that the genome context was not shared with the *B. subtilis* gene; JY indicates that the *cwlJ* and *ywdL* genes were adjacent to one another, which is not the case in *B. subtilis*. Representative species were chosen to represent a broad phylogenetic spread across the family *Bacillaceae* (141).

Table 1.2. Identities of orthologous genes potentially involved in degradation of spore PG in a range of species spanning the family *Clostridiaceae*[1].

Gene	*C. perfringens* Strain 13	*C. difficile* 630	*C. lentocellum* DSM 5427	*C. leptum* DSM 753	*Thermoanaerobacter wiegelii* Rt8.B1	*Desultfotomaculum reducens* MI-1
sleC	990937	4916686 X	10331416 X	-	-	-
cspB	990939	4915699 X	10331412 X	-	-	-
sleM	989623	-	-	-	-	-
sleB	-	-	-	ZP_02079990.1 X	11084183 SY	4957310 SY
ypeB	-	-	-	ZP_02078794.1 X	11084182 SY	4958483 SY
sleL (yaaH)	-	-	10330877 X	ZP_02079199.1 X	11082049 X	4955511 X

[1]Each gene is identified by an NCBI Gene ID number. Orthologs were identified using tblastn and blastp searches (2) for similarity to the products of the indicated *C. perfringens* or *B. subtilis* genes. In all cases, the identified ortholog exhibited the greatest amino acid sequence identity with the query protein. Due to the presence of multiple genes within each class in some genomes, the genome context of each similar gene was examined to strengthen assignments of orthologs. A letter following the Gene ID number indicates the similarity of the genome context to that found for the query protein in its native species: SY indicates a partial genome context match where the *sleB* and *ypeB* genes are adjacent; X indicates that the genome context was not conserved. No clear *cwlJ* or *ywdL* orthologs were identified in these species. Representative species were chosen to represent a broad phylogenetic spread across the family *Clostridiaceae* (152).

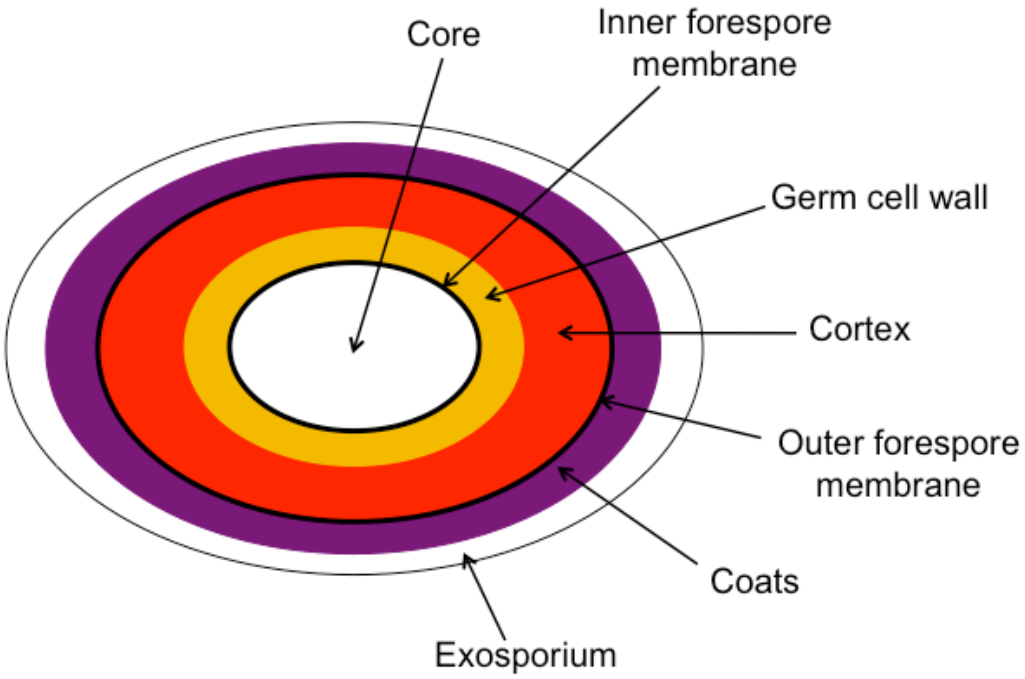

Figure 1.1. Spore structure. A simplified diagram depicting the layers of a bacterial spore. At the center is the spore core, which houses the nucleic acids. There are two membranes, the inner and outer forespore membranes. Between the two membranes are two layers of PG, the germ cell wall and the cortex. The coat layers and exosporium are the outermost layers of the spore. Note that the exosporium layer is absent in many species.

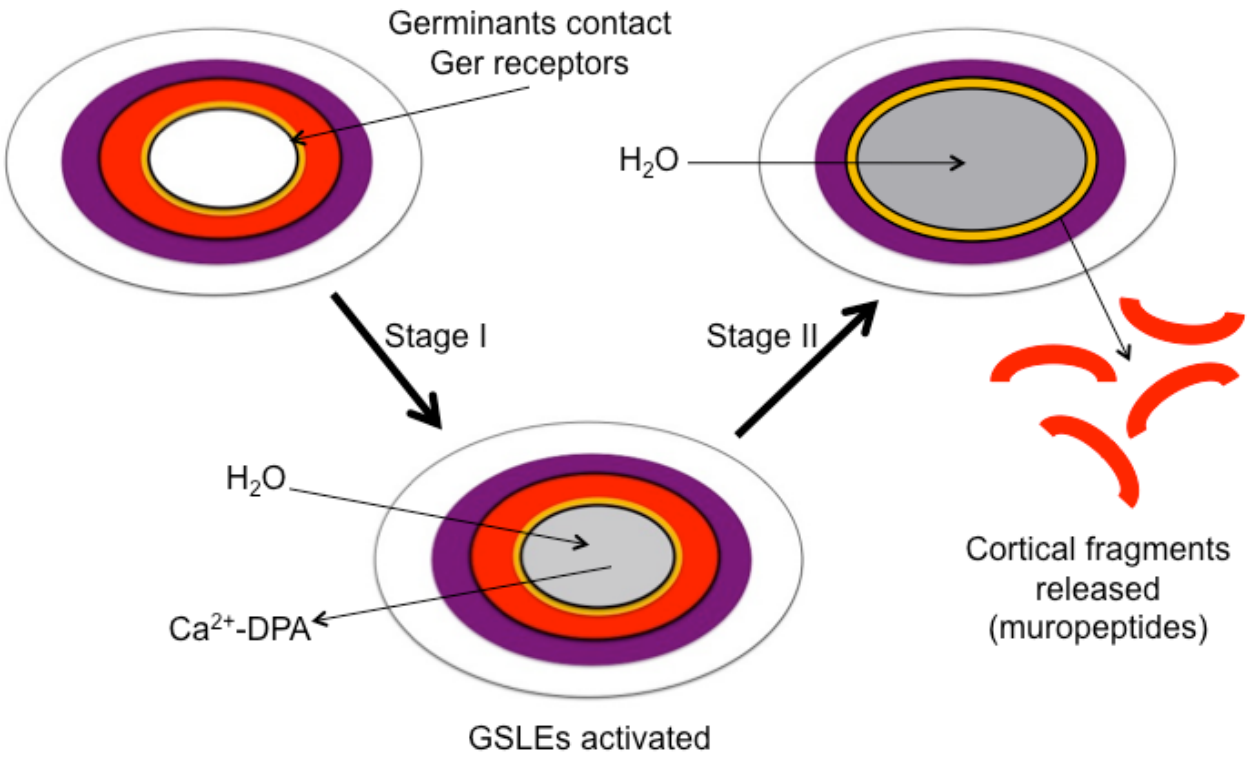

Figure 1.2. Spore germination. In nature, spore germination is initiated when nutrients, called germinants, interact with Ger receptors located at the inner forespore membrane. Germination can be divided into two stages, followed by a period of outgrowth (not shown). During stage I, a large pool of Ca^{2+}-DPA is released from the spore core, and the core becomes partially rehydrated with water (depicted as a darkening of the spore core). During stage II, the cortex PG is degraded through the action of germination-specific lytic enzymes (GSLEs). Cortex fragments are released to the external environment, and the core is free to expand as it fully rehydrates.

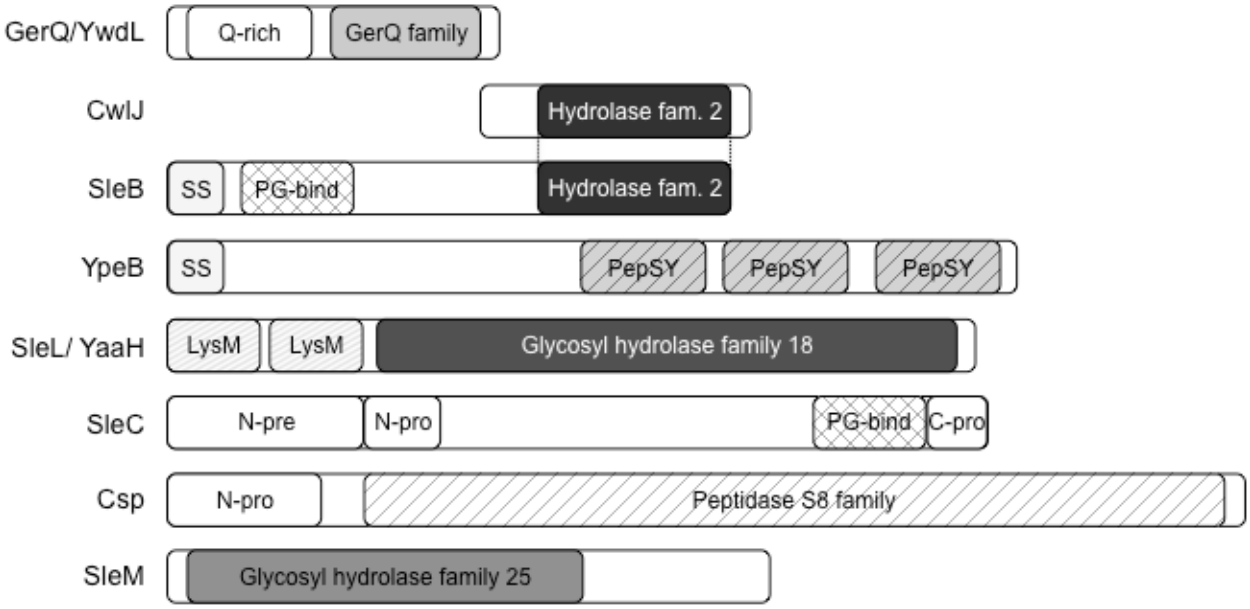

Figure 1.3. Domain architecture of GSLEs and interacting proteins. The proteins, along with the conserved domains and motifs shown, are drawn to scale. SleB and YpeB have signal sequences (SS) for export across the inner forespore membrane during sporulation. Both SleB and SleC have a PG-binding domain (PG-bind) (pfam01471), presumably to aid in protein localization or substrate affinity. The LysM domains (pfam01476) found in SleL/YaaH also recognize PG and are thought to play a similar role. The N-terminal pre- (N-pre) and pro- (N-pro), and C-terminal pro- (C-pro) sequences that are removed from SleC by Csp proteases during sporulation or germination are shown, as well as the N-terminal pro-sequence that is cleaved from Csp. YpeB contains three predicted PepSY domains (pfam03413), which play an unknown role; however these domains have been involved in the inhibition of peptidase activity in a number of PepSY-containing proteases. The C-terminus of YwdL/GerQ is highly conserved, and a glutamine-rich (Q-rich) region is found toward the N-terminus of the protein. The hydrolase family 2 (Hydrolase fam. 2) (pfam07486), glycosyl hydrolase family 18 (pfam00704), peptidase S8 family (pfam00082), and glycosyl hydrolase family 25 (pfam01183) domains contain the enzyme active sites.

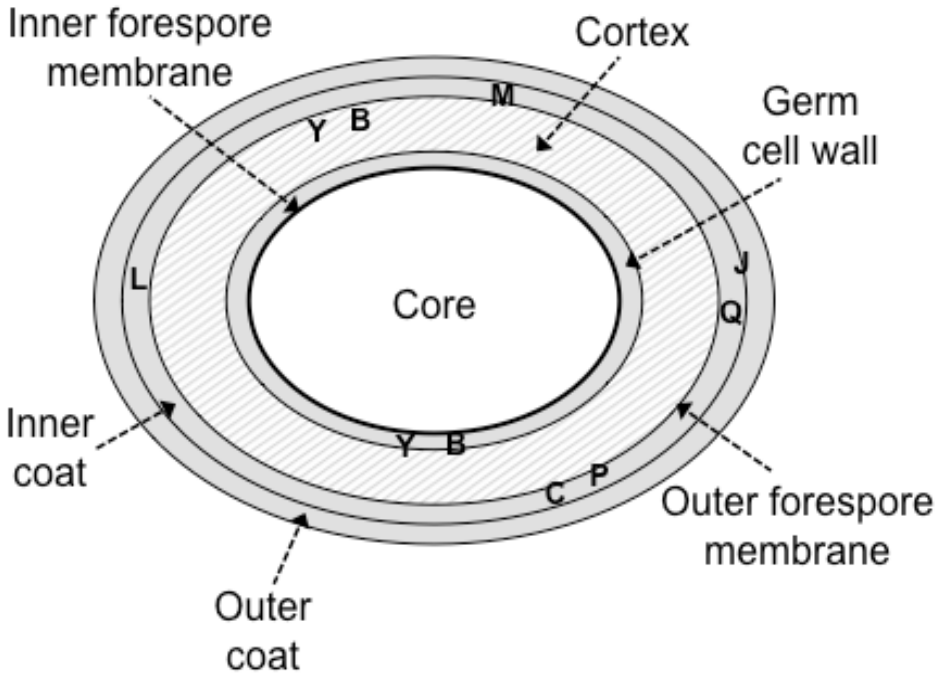

Figure 1.4. Localization of GSLEs and interacting proteins in dormant spores. SleB (B) and YpeB (Y) have been alternately demonstrated to be localized to the outer cortex/outer forespore membrane and the inner forespore membrane of dormant spores. The precise location of CwlJ (J) within the spore coat layers is unknown, but YwdL/GerQ (Q) is found within the inner coat. SleL/YaaH (L) has also been shown to be an inner coat protein. SleC (C), Csp proteases (P), and SleM (M) are located outside the cortex, either in the inner spore coat or outer forespore membrane. While these proteins are drawn within a single spore, in actuality, a spore only contains a subset of the proteins shown. B, Y, J, Q, and L are found in *Bacillaceae* and likely a few *Clostridiaceae*, while C, P, and M are found only in certain *Clostridiaceae*. Co-localization is shown for B-Y, J-Q, and C-P due to the requirement of YpeB and YwdL/GerQ for stable incorporation of SleB and CwlJ, respectively, into the dormant spore, and the processing of pro-SleC to active SleC by Csp proteases. However, it should be noted that there is currently no evidence that B-Y or J-Q directly interact.

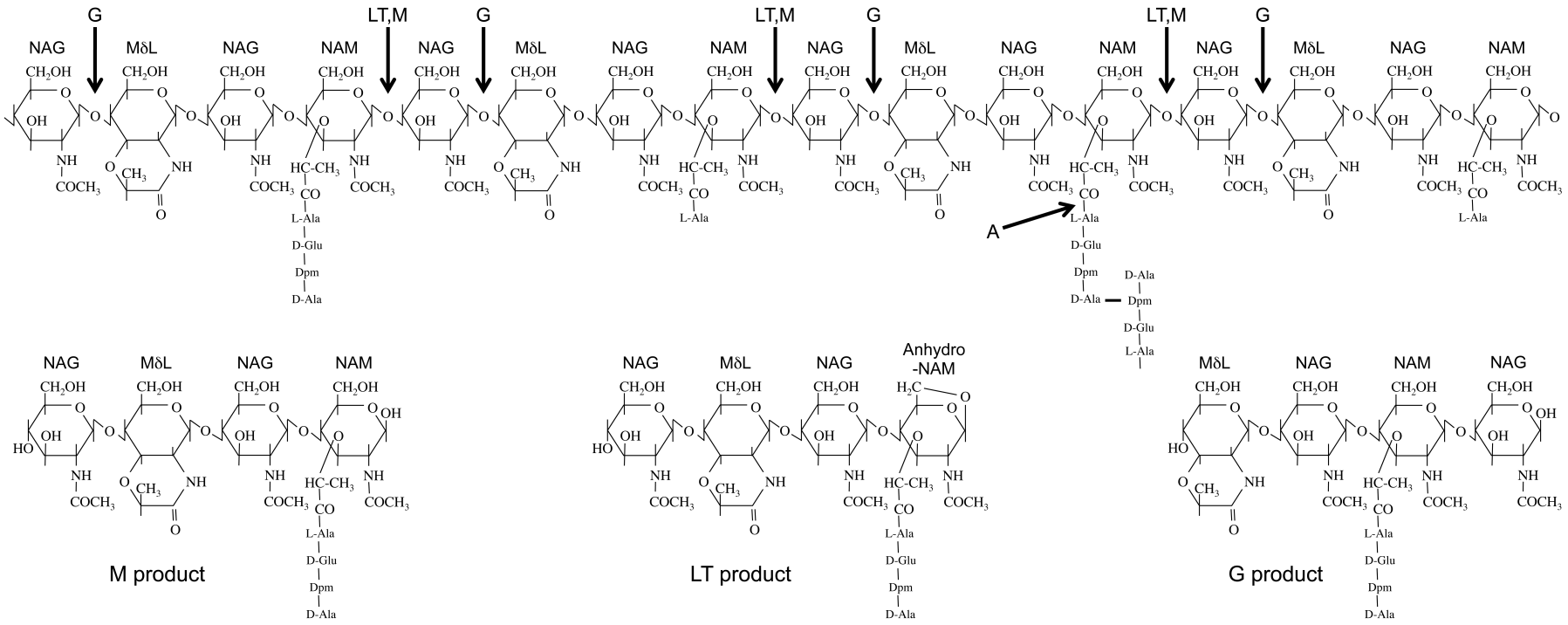

Figure 1.5. GSLE cleavage of cortex PG. A single strand of cortex PG is shown at the top, and the cleavage sites for the GSLE enzyme classes are indicated by arrows. A peptide cross-link to another strand is shown, but the second glycan strand is omitted. The proposed N-acetylmuramoyl-L-alanine amidase (A) activity of SleC can break peptide cross-links by cleaving a peptide from NAM. The cleavage sites and representative products (bottom) of N-acetyl-glucosaminidase (G, SleL), N-acetylmuramidase (M, SleM), and lytic transglycosylase (LT, SleB and SleC) are indicated.

CHAPTER 2

The role of YpeB in cortex hydrolysis during germination of *Bacillus anthracis* spores

Casey B. Bernhards and David L. Popham. 2014.

Journal of Bacteriology. In Press, Volume 196.

ATTRIBUTIONS

Casey B. Bernhards performed the research, experimentation, data analysis, and writing of the material presented herein. David L. Popham was the principle investigator. The manuscript has been accepted for publication in the Journal of Bacteriology.

ABSTRACT

The infectious agent of the disease anthrax is the spore of *Bacillus anthracis*. Bacterial spores are extremely resistant to environmental stresses, which greatly hinders spore decontamination efforts. The spore cortex, a thick layer of modified peptidoglycan, contributes to spore dormancy and resistance by maintaining the low water content of the spore core. The cortex is degraded by germination-specific lytic enzymes (GSLEs) during spore germination, rendering the cells vulnerable to common disinfection techniques. This study investigates the relationship between SleB, a GSLE in *B. anthracis*, and YpeB, a protein necessary for SleB stability and function. Results indicate that Δ*sleB* and Δ*ypeB* spores exhibit similar germination phenotypes, and the two proteins have a strict co-dependency for their incorporation into the dormant spore. In the absence of their partner protein, SleB and YpeB are proteolytically degraded soon after expression during sporulation, rather than escaping the developing spore. The three PepSY domains of YpeB were examined for their role in the interaction with SleB. YpeB truncation mutants illustrate the necessity of a region beyond the first PepSY domain for SleB stability. Furthermore, site-directed mutagenesis of highly conserved residues within the PepSY domains resulted in germination defects corresponding to reduced levels of both SleB and YpeB present in the mutant spores. These results identify residues involved in the stability of both proteins and reiterate their co-dependent relationship. By studying GSLEs and interacting proteins, it is hoped that GSLEs will be targets to efficiently activate spore germination and facilitate spore cleanup.

INTRODUCTION

Bacterial spores from the *Bacillus* and *Clostridium* genera are metabolically dormant and known for their extreme resistance to heat, desiccation, UV radiation, chemicals, and other insults (112, 147, 148). These resistance properties allow spores to survive for extended periods of time in the environment and have made eradication from contaminated sites incredibly difficult (57). Spore dormancy and wet heat resistance are largely dependent on spore core dehydration, which is maintained by a thick layer of modified peptidoglycan (PG) known as the cortex (54, 148). While vegetative cell wall PG consists of alternating *N*-acetylglucosamine (NAG) and *N*-acetylmuramic acid (NAM) sugars, approximately 50% of NAM residues in the cortex are converted to muramic-δ-lactam, while an additional portion of the NAM side chains are generally cleaved to a single L-alanine (6, 7, 9, 47, 124, 172).

The spore form of *Bacillus anthracis* is the etiological agent for all types of anthrax infections: inhalational, gastrointestinal, cutaneous, and the newest described form – injectional anthrax (103, 154). Upon sensing the availability of nutrients, such as when a spore enters a suitable host, spore germination is triggered, causing a chain of events that ultimately result in a vegetative cell capable of producing deadly toxins (103, 147). After germinant contact with receptors at the spore inner membrane, spores release their large pool of Ca^{2+}-DPA stored in the core, which becomes partially rehydrated through an influx of water (147). This is followed by cortex depolymerization, allowing the spore core to rehydrate to levels necessary for metabolism to resume (144). Spore germination concomitantly results in the loss of resistance properties; thus, triggering this process at a high efficiency is a potentially attractive approach for spore decontamination.

Cortex degradation during spore germination is accomplished by germination-specific lytic enzymes (GSLEs) already present within the dormant spore (94, 125). These enzymes exhibit specificity for PG containing the muramic-δ-lactam modification, ensuring that only the cortex PG is broken down (34, 35, 65, 86, 128). *Bacillus anthracis* contains the four GSLEs SleB, CwlJ1, CwlJ2, and SleL, where SleB and CwlJ1 are partially redundant enzymes responsible for the majority of cortex hydrolysis (55, 63, 64, 85). SleB or CwlJ1 alone is sufficient for cortex hydrolysis, and the absence of both proteins results in spores that are unable to degrade the cortex and complete germination (55, 63, 64). Identical roles for SleB and CwlJ have been demonstrated in *Bacillus subtilis* (36, 109, 117) and *Bacillus megaterium* (145). CwlJ2, a homolog of CwlJ1, appears to play a minor role during *B. anthracis* spore germination, at best, while SleL further breaks down PG fragments first generated by SleB and/or CwlJ1 (55, 63, 64, 85, 86).

The arrangement of *sleB* upstream of *ypeB* in an operon is highly conserved across *Bacillus* species, and in a few *Clostridiales* species possessing *sleB* (37, 64, 108, 125, 127). In the *Bacillus* species examined, SleB and YpeB are expressed during sporulation from the forespore under the control of σ^G, after which they are translocated across the inner membrane by way of their N-terminal signal sequences (23, 108-110). Unlike the YpeB signal sequence, which is not predicted to be cleaved, the SleB signal sequence is removed during sporulation and SleB is present in its mature form within the dormant spore (69, 108-110). The uncleaved signal sequence likely anchors YpeB to the inner membrane, which is supported by studies in *B. subtilis* that have found both SleB and YpeB associated with the inner membrane of the spore (36). The same study, as well as work in *B. cereus*, has placed SleB and YpeB at a second location near the outer region of the cortex (36, 108). Not only do SleB and YpeB appear to

localize within the same regions of the spore, but it was demonstrated in *B. subtilis* that YpeB is required for SleB activity and for stable incorporation of SleB into the spore (23, 36). Additionally, the relationship appears to be mutual, where SleB is also needed to stabilize YpeB (90).

Compared with YpeB, far more is known about SleB structure and function. At the N-terminus of the mature protein, SleB has a PG-binding domain (pfam01471), while the C-terminus contains a catalytic domain (pfam07486) (65, 95, 109, 110). As anticipated, the N-terminal domain plays the dominant role in PG-binding; however, the C-terminal domain appears to be responsible for both SleB lytic transglycosylase activity on cortex PG and its specificity for muramic-δ-lactam (65, 91, 95). Mutational analysis and crystal structure determination of the SleB C-terminal domain in *B. anthracis* (76) and *B. cereus* (91) revealed a conserved catalytic glutamate residue and unique substrate-binding cleft thought to mediate specificity for cortex PG. Apart from its signal sequence, the only recognizable features of YpeB are the three putative PepSY domains positioned in the C-terminal 60% of the protein (177). These domains are best characterized in the M4 family of metallopeptidases, where the PepSY domains serve as intramolecular inhibitors of protease activity until the protease is secreted out of the cell (177). Like a large number of other proteins containing PepSY domains, YpeB does not show homology with proteases; thus, the function of the PepSY domains is unknown in YpeB and the other proteins comprising this group (177).

The current study investigates the relationship between SleB and YpeB in *B. anthracis* and demonstrates the contribution of the PepSY domains to this interaction. The data solidify the co-dependent nature of this relationship and reveal that SleB and YpeB are rapidly degraded following expression in the absence of the other protein. The C-terminus of YpeB containing the

PepSY domains is critical for SleB stability and function, and certain highly conserved residues within the PepSY domains are important for the stability of both proteins. By understanding GSLEs and regulators of their activity, it may be possible to trigger germination at the stage of cortex hydrolysis, resulting in cells that are readily killed.

MATERIALS AND METHODS

Bacterial strains and general growth conditions. Strains and plasmids used are listed in Table 2.1. All *B. anthracis* strains in this study are derived from the Sterne strain 34F2 and were grown at 37°C in brain heart infusion (BHI; Difco) with 5 μg/ml erythromycin or 10 μg/ml tetracycline, where appropriate. *B. anthracis* strains maintaining pBKJ236-derived plasmids extrachromosomally were incubated at 25°C. Following plasmid integration into the chromosome (at 42°C in most instances), these strains were subsequently grown at 37°C. *Escherichia coli* strains were grown in LB at 37°C with 500 μg/ml erythromycin or 100 μg/ml ampicillin for strains involved in plasmid propagation, or 30 μg/ml chloramphenicol and 50 μg/ml ampicillin for strains used in protein overexpression.

Mutant construction. The sequences of all primers used during plasmid construction are listed in Table 2.2. All plasmids created were verified by DNA sequencing. To create a Δ*ypeB* strain, *ypeB* and approximately 500-bp flanking each side of the gene were PCR amplified from the *B. anthracis* chromosome. The PCR product was inserted into the vector pBKJ236 (75) by digesting with the restriction enzymes SacII and NotI and ligating the DNA to create pDPV388. Inverse PCR of the plasmid using primers with BglI restriction sites at the 3′ ends resulted in a linear PCR product with the majority of *ypeB* deleted, leaving only three codons from each end of the gene. Subsequent BglI digestion and ligation of the PCR product

formed pDPV392. This plasmid containing the *ypeB* deletion was introduced into *B. anthracis* using the markerless gene replacement strategy as previously described (75). Gene deletion was verified by PCR amplification and sequencing.

The *sleB* complementation strain published previously (DPBa57) contains an extrachromosomally-maintained pBKJ236 derivative with full-length *sleB* (pDPV346) (64). In order to achieve more complete complementation of the deletion phenotype by ensuring efficient plasmid partitioning into the forespore during spore formation, pDPV346 was integrated into the Δ*sleB* chromosome by shifting the temperature to 42°C. Plasmid integration through homologous recombination just upstream of Δ*sleB* in the chromosome was verified with PCR, and this new *sleB* complementation strain was designated DPBa134. To create a *ypeB* complementation plasmid that includes the native promoter, PCR was performed using the Δ*sleB* chromosome (64) as template. The resulting PCR product contained the promoter region for the *sleB* operon, followed by Δ*sleB*, *ypeB*, and approximately 500-bp downstream of *ypeB*. The DNA fragment was cloned into pBKJ236 by digesting with NotI and ligating to form pDPV416. This *ypeB* complementation plasmid was introduced into the Δ*ypeB* strain of *B. anthracis* via conjugation as done in the initial stages of the markerless gene replacement procedure (75). Subsequent plasmid integration within the 500-bp homologous region downstream of Δ*ypeB* in the chromosome was achieved by shifting the temperature to 42°C and was verified by PCR.

YpeB truncation and internal deletion mutations were designed using InterPro (71) to predict the locations of PepSY domains, and the Protean application of Lasergene 10.0 (DNAStar) to choose truncation/deletion sites based on high residue surface probability and residues not predicted to disrupt protein secondary structure. For the truncation mutations, inverse PCR of the *ypeB* complementation plasmid was performed using sets of two primers.

The tails of the forward primers contained codons encoding a hexahistidine tag followed by a stop codon and a BglII restriction enzyme recognition sequence. The tail of the reverse primer used to create all the truncation mutants also had a BglII site added. The linear PCR products from inverse PCR reactions were digested with BglII and ligated to recircularize the plasmids, generating pDPV421 through pDPV424. The internal deletion mutations were constructed using overlap extension PCR (66), followed by restriction-free cloning (162) to insert the PCR products into the plasmid encoding full-length YpeB with a C-terminal His_6 tag (pDPV424). The YpeB truncation and internal deletion plasmids were moved into the Δ*ypeB* strain of *B. anthracis* and integrated into the chromosome as described above. The 500-bp homologous region following *ypeB* in pDPV416 was removed during inverse PCR to create pDPV421-424; thus, these plasmids inserted into the Δ*ypeB* chromosome through homologous recombination upstream of *sleB*, as confirmed by PCR.

In order to predict residues of the YpeB PepSY domains that might be important for protein-protein interactions, the PepSY domain sequences from *B. anthracis* YpeB were aligned with a PepSY domain consensus sequence (45), other PepSY domain sequences (45, 53, 177), and the YpeB PepSY domain sequences from other *Bacillus* species using Clustal W sequence alignment software (156). Based on these alignments, highly conserved residues were identified as targets for mutagenesis. Site-directed mutagenesis by overlap extension PCR (66) was used to create point mutations in *ypeB*. The resulting PCR products were cloned into the *ypeB* complementation plasmid pDPV416 using restriction-free cloning (162). Successful plasmid construction was verified by screening for the gain or loss of a restriction site in *ypeB* that was designed as part of the mutagenic primers, followed by DNA sequencing. Plasmids were

mobilized into the Δ*ypeB* strain of *B. anthracis* and integrated into the chromosome downstream of Δ*ypeB* as described above for the *ypeB* complementation plasmid.

Spore preparation and decoating. *B. anthracis* strains were sporulated in modified G broth (78) with appropriate antibiotic at 37°C with aeration. After 3 to 4 days, dormant spores were harvested by centrifugation and repeatedly washed with deionized water. Any remaining vegetative cells were heat killed at 65°C for 25 min. Spores were further purified with a 50% sodium diatrizoate (Sigma) gradient as described previously (113). Decoated spores were prepared by suspending up to 30 OD units of spores in 1 ml decoating solution (50 mM Tris-HCl pH 8, 8 M urea, 1% SDS, 50 mM DTT). The spores were incubated at 37°C for 1 h and then centrifuged at 8,000 x *g* for 1 min to remove the decoating solution. The decoating procedure was repeated a second time, followed by five washes with 1 ml deionized water at room temperature. Untreated (native) and decoated spores were stored in deionized water at 4°C until analysis.

Spore and sporangia sample preparation for western blotting. Following spore purification, 7.5 to 10 OD units of dormant, native spores were pelleted, frozen at -80°C, and lyophilized. Dried spores were mechanically disrupted with 100 mg 0.1 mm glass beads and 20 pulses of 30 s each at 4,200 rpm using a Wig-L-Bug bead beater. Samples were placed on ice between pulses. Proteins were extracted from the broken material by adding 10 μl/OD unit of 1X sample loading buffer (62.5 mM Tris-HCl pH 6.8, 2% SDS, 10% glycerol, 5% β-mercaptoethanol, 0.05% bromophenol blue) and heating to 100°C for 5 min. Extracts were centrifuging at 15,800 x *g* for 1 min, and volumes of supernatants derived from equal starting OD units of spores were used for western blot analysis.

Strains grown in modified G broth with appropriate antibiotic were monitored spectrophotometrically until the OD_{600} indicated cells had entered stationary phase. This time point, termed t_0, coincides with the initiation of sporulation, and t_2 through t_6 designate 2 through 6 hours, respectively, past t_0. At hours t_2 through t_6 of sporulation, 10 ml sporangia samples were collected and centrifuged at 10,000 x *g* for 10 min at 4°C. Pellets were resuspended in 1 ml 8 mM $NaPO_4$ pH 7.0 and centrifuged at 15,800 x *g* for 1 min. The resulting pellets were flash frozen in liquid N_2 and lyophilized. Lyophilized sporangia were broken with glass beads and proteins extracted as described above, except that 100 µl of 1X sample loading buffer was used. Extract supernatants were used for western blotting using the average OD_{600} measured for a particular strain from t_2 through t_6 to adjust sample loading between strains.

Germination assays. To assess the rate of spore germination and outgrowth, decoated spores were heat activated at 70°C for 30 min and quenched on ice for 5 min. Heat-activated spores were diluted to an OD_{600} of 0.2 in liquid BHI at 37°C to initiate germination, and the change in OD_{600} was measured over time. For germination efficiency assays, decoated spores at an OD_{600} of 0.2 were heat activated at 70°C for 20 min and quenched on ice. Heat activated spores were serially diluted in deionized water, plated on BHI medium without antibiotics, and incubated at 37°C overnight. Colonies were counted to determine CFU/OD unit values. Unpaired, two-tailed Student's *t*-tests with unequal variance were used for statistical analyses of germination assays.

Protein expression and purification. The *ypeB* gene lacking the first 20 codons was amplified by PCR and inserted into a modified version of pDEST-HisMBP (11) containing a tobacco etch virus (TEV) cleavage site (pDEST-HisMBP-T) using restriction-free cloning (162). The resulting plasmid encoded an N-terminal His_6-tagged maltose binding protein (MBP) and

$YpeB_{21-446}$, separated by a TEV cleavage site. Successful plasmid construction was verified by sequencing. The His_6-MBP-$YpeB_{21-446}$ fusion protein was overexpressed in *Escherichia coli* BL21 (λDE3) (pLysS Cm^r) (Novagen) grown at 37°C until the OD_{600} reached 1.0, at which point isopropyl-β-D-thiogalactopyranoside was added to a final concentration of 1 mM and the culture was incubated at 10°C for an additional 16 h. Cells were harvested by centrifugation at 10,000 x *g* for 10 min at 4°C, and the pellet was resuspended in 5 ml/g Buffer A (50 mM NaCl, 50 mM Tris-HCl pH 7.5, 5% glycerol, 30 mM imidazole). Resuspended cells were lysed by sonication for 15 min and then centrifuged at 117,000 x *g* for 1 h at 4°C. Fusion protein in the soluble fraction was purified using a Ni-Sepharose HisTrap HP affinity column (GE Healthcare) equilibrated with Buffer A. Protein was eluted with a linear gradient of 30 to 500 mM imidazole in Buffer A, and elution fractions were dialyzed in Buffer A. Fusion protein was digested with 1 mg His_6-tagged TEV (S219V) protease (77) per 7 mg fusion protein at 15°C for 16 h, and the mixture was centrifuged at 117,000 x *g* for 20 min at 4°C to remove any precipitated protein. Cleavage of the fusion protein was verified by SDS-PAGE. $YpeB_{21-446}$ was purified from His_6-MBP and His_6-TEV using a second Ni-Sepharose HisTrap HP affinity column as described above. SleB overexpression and purification was performed as described previously (65).

Antibody preparation and western blot analysis. Polyclonal anti-SleB and anti-YpeB antibodies were raised in rabbits (Open Biosystems) using purified $SleB_{33-253}$ (65) or $YpeB_{21-446}$. SleB, YpeB, and derivatives were detected in western blots on Amersham Hybond-P (PVDF) membranes (GE Healthcare) using BM Blue POD Substrate, Precipitating (Roche) for colorimetric detection. Primary anti-SleB and anti-YpeB antibodies were generally used at 1:1,000 and 1:3,000 dilutions, respectively. Secondary goat anti-rabbit-HRP antibodies (Bio-Rad) were used at a 1:200,000 dilution. Western blot quantification was performed using Image

Lab Software (Bio-Rad). While efforts were made to ensure total protein load was identical for each strain, there is the inherent possibility of slight variations stemming from unequal protein extraction between samples and unequal sample loading. To account for experimental error, relative values were normalized using a highly reproducible non-YpeB background band detected in all strains, including the Δ*ypeB* strain. Similarly, SleB band intensities were normalized using a background band present on anti-SleB immunoblots.

RESULTS

Germination of Δ*ypeB* mutant spores. As previously reported by Heffron et al., a homolog of the *B. subtilis ypeB* gene (57% identity/77% similarity) exists as part of a putative tricistronic operon at locus BAS2561 in the *B. anthracis* chromosome (64). The *ypeB* homolog is the second gene in the operon, preceded by *sleB* (BAS2562) and followed by the open reading frame BAS2560 (64). BAS2560 shows homology to the *B. subtilis* genes encoding the lipoproteins YlaJ and YhcN, where YlaJ is an uncharacterized spore protein and YhcN plays an unknown role in spore germination or outgrowth (12, 64, 84). In this study, a deletion of the *ypeB* gene (BAS2561) in the *B. anthracis* chromosome was made using the markerless gene replacement strategy (75). The effects of this *ypeB* deletion, and of an *sleB* deletion, are not due to polar effects on expression of BAS2560, because: A) a BAS2560 deletion results in no change in spore germination, specifically in SleB activity (data not shown), B) as shown below, all effects of a *ypeB* deletion can be complemented by the *ypeB* gene alone, and C) as shown below and in Heffron et al. (64), all effects of an *sleB* deletion can be complemented by *sleB* alone.

In assays in which purified spores were germinated in BHI and the change in OD_{600} measured over time, the germination phenotype of Δ*ypeB* spores was essentially identical to that

of Δ*sleB* spores (64). This could be seen in assays using native spores, in which Δ*ypeB* and Δ*sleB* spores produced a shallower germination curve, indicative of a slightly less efficient germination response, and also showed a slower rate of outgrowth (data not shown). The germination defect in Δ*ypeB* and Δ*sleB* spores, alike, was more pronounced in assays using decoated spores, where the other GSLEs localized to the outer periphery of the spore are removed or inactivated, and SleB alone is responsible for cortex hydrolysis during germination (Fig. 2.1A). Both Δ*ypeB* and Δ*sleB* decoated spores proceeded through stage I of germination similar to wild-type, where the initial OD decreases as the spores uptake water and release their large deposit of Ca^{2+}-DPA. Decoated wild-type spores continued to lose nearly half of their initial OD as the cortex peptidoglycan was degraded during stage II of germination, followed by an increase in OD as germination was completed and outgrowth into vegetative cells began. Conversely, germination was arrested for Δ*ypeB* and Δ*sleB* decoated spores at the stage of cortex hydrolysis, where Δ*ypeB* and Δ*sleB* spores never lost more than 34 percent of their initial OD and did not proceed to outgrowth (Fig. 2.1A). This germination deficiency is also illustrated in spore plating efficiency assays, where Δ*ypeB* and Δ*sleB* decoated spores showed greater than a 10^4-fold reduction in their ability to germinate and form colonies on rich medium, relative to wild-type spores (Table 2.3). A wild-type germination phenotype was achieved in both germination rate and plating efficiency assays using spores from a *ypeB* complementation strain (DPBa113, *ypeB*$^+$), in which *ypeB,* provided on a plasmid downstream of its native promoter, was integrated into the Δ*ypeB* chromosome. HPLC analyses of muropeptides collected during spore germination revealed the complete absence of SleB-specific lytic transglycosylase products identified by Heffron et al. (64) in both Δ*sleB* and Δ*ypeB* spores, with restoration of these peaks during germination of *ypeB*$^+$ spores (data not shown). Consistent with the results observed from

a *ypeB* deletion in *B. subtilis* (23, 90), these results indicate YpeB is necessary for SleB lytic activity on spore cortex peptidoglycan in *B. anthracis*.

Stability of SleB and YpeB in spores and sporangia. Not only is YpeB needed for SleB activity, but western blots of Δ*ypeB* spore extracts demonstrated YpeB is also required for SleB incorporation into the spore (Fig. 2.2). SleB was essentially not detected in Δ*ypeB* spore extracts, and this could be complemented. As in *B. subtilis* (90), this relationship is mutual, where SleB was also needed for the stable incorporation of YpeB into the spore (Fig. 2.2). Immunoblots of Δ*sleB* spore extracts revealed significantly diminished levels of YpeB when SleB was absent, which could also be complemented. Miniscule levels of SleB and YpeB detected in western blots of Δ*ypeB* and Δ*sleB* spores, respectively, could be attributed either to the expression of the proteins during spore formation followed by rapid proteolysis in the absence of their stabilizing partner, or to escape of the proteins from the developing spore. The former proposal is supported by western blot analyses of whole sporangia samples taken throughout sporulation (Fig. 2.3). In wild-type and *ypeB*$^+$ strains, significant amounts of SleB and YpeB were detected beginning 3 h after the initiation of sporulation (t_3) (Fig. 2.3A and B). This is consistent with previous β-galactosidase activity assays performed in *B. anthracis* which show *sleB* transcription reaches its peak near $t_{3.5}$ (64). During spore formation in Δ*sleB* and Δ*ypeB* strains, some YpeB and SleB, respectively, could be seen at t_3 and t_4, but were not strongly detected thereafter (Fig. 2.3A and B). The expression of YpeB at t_3 and t_4 coincided with the production of large quantities of two YpeB-specific degradation products in Δ*sleB* sporangia (and to a lesser degree in wild-type and *ypeB*$^+$ sporangia, data not shown), indicating protein degradation occurred immediately following protein expression (Fig. 2.3C). Specific SleB degradation products were not observed during sporulation of any of the strains tested (data

not shown). The protease(s) responsible for degradation of SleB and YpeB during spore formation are unknown. Elimination of SpoIVB, which is known to be active in the forespore intermembrane space in *B. subtilis* (43, 168), had no effect on stability of SleB in the absence of YpeB (Chapter 5, Fig. 5.7). Elimination of BAS5314 (HtrC), which in *B. subtilis* is expressed in the forespore and possesses a signal sequence/membrane anchor (50), had no effect on stability of SleB and YpeB in the absence of the partner protein (Chapter 3, Fig. 3.9).

Analyses of YpeB PepSY domain truncation mutants. InterPro (71) predicted the presence of three PepSY domains in *B. anthracis* YpeB from residues 218-282, 291-358, and 375-436. To assess the individual contributions of the three putative PepSY domains located at the C-terminus of YpeB, strains were constructed expressing truncated forms of YpeB with a C-terminal His_6 tag. Plasmids expressing YpeB from its native promoter were integrated into the Δ*ypeB* chromosome; the resulting strains expressed YpeB with zero PepSY domains ($YpeB_{1-208}$-His_6), one PepSY domain ($YpeB_{1-283}$-His_6), two PepSY domains ($YpeB_{1-368}$-His_6), or all three PepSY domains (full-length YpeB, $YpeB_{1-446}$-His_6). In decoated spore germination rate assays in liquid BHI and in decoated spore plating efficiency assays, spores containing YpeB with zero, one, or two PepSY domains were similar to Δ*ypeB* spores (Fig. 2.1B and Table 2.3). Like Δ*ypeB* spores, these spores containing truncated versions of YpeB were arrested during germination and showed greater than a 10^3-fold reduction in plating efficiency in the case of the $YpeB_{1-208}$-His_6 mutant, but generally greater than a 10^4-fold decrease. The reason for the similarity was revealed in western blots of dormant spore extracts, which show that YpeB is unstable in many of the truncated forms (Fig. 2.4A). In fact, YpeB and SleB were both stable only in strains possessing all three YpeB PepSY domains. In spores with highly unstable YpeB ($YpeB_{1-208}$-His_6 and $YpeB_{1-368}$-His_6), as anticipated, SleB was also unstable (Fig. 2.4A). Interestingly, although

YpeB with only the first PepSY domain ($YpeB_{1-283}$-His_6) appeared somewhat stable in the anti-YpeB western blot, SleB was unstable (Fig. 2.4A), and these spores had germination phenotypes like those of Δ*ypeB* spores (Fig. 2.1B and Table 2.3). This suggests that the C-terminal region of YpeB, more specifically a region beyond the first PepSY domain, is critical for SleB stability, and thus spore germination.

Analysis of YpeB internal deletion mutants. In order to determine what other areas of YpeB may be necessary for YpeB function in stabilizing SleB and SleB activity during germination, internal deletions of different lengths were made between the N-terminal signal sequence and C-terminal PepSY domains. Deletion endpoints were chosen based on software predictions of transitions between secondary structural elements. The created strains expressed YpeB without residues 25-203 ($YpeB_{\Delta 25-203}$-His_6), 67-203 ($YpeB_{\Delta 67-203}$-His_6), 119-203 ($YpeB_{\Delta 119-203}$-His_6), or 156-203 ($YpeB_{\Delta 156-203}$-His_6). Immunoblots of dormant spore extracts revealed that $YpeB_{\Delta 25-203}$-His_6 and $YpeB_{\Delta 67-203}$-His_6 are at least moderately stable, while $YpeB_{\Delta 119-203}$-His_6 and $YpeB_{\Delta 156-203}$-His_6 are not; however, SleB was not stably incorporated into spores of any of these internal deletion strains (Fig. 2.4B). Even $YpeB_{\Delta 25-203}$-His_6, which appears to accumulate in dormant spores to similar levels as full-length YpeB ($YpeB_{1-446}$-His_6), failed to stabilize SleB. Thus, the N-terminal half of YpeB, likely a region between residues 67 and 203, also must play a role in stabilizing SleB.

Analyses of YpeB PepSY domain point mutants. As an alternative approach to study the PepSY domains while attempting to maintain YpeB stability, site-directed mutagenesis was performed on selected highly conserved residues within the three PepSY domains. Y254 within the first PepSY domain, Y329 in the second PepSY domain, and T377, Y410, and G430, all in the third and last PepSY domain, were selected to be individually changed to alanine. Spores

with YpeB^{Y329A} or YpeB^{T377A} showed no significant decrease in either germination rate in liquid BHI or plating efficiency compared with *ypeB*$^{+}$ spores (Figs. 2.1C and 2.5). Spores with YpeB^{Y254A} or YpeB^{G430A} showed a delay in germination, reaching their lowest OD 40 min and 50 min, respectively, later than *ypeB*$^{+}$ spores (Fig. 2.1C). While YpeB^{Y254A} and *ypeB*$^{+}$ spores each lost 59-60% of their initial OD, YpeB^{G430A} spores had a shallower germination curve, losing 51% of initial OD (Fig. 2.1C). Both YpeB^{Y254A} and YpeB^{G430A} spores showed a slight but significant ($P < 0.007$) decrease in plating efficiency, but less than a 10-fold reduction in CFU/OD was seen (Fig. 2.5). The most dramatic effect on spore germination was seen in YpeB^{Y410A} spores, where spores showed a significant delay in germination and a shallower germination curve (Fig. 2.1C). YpeB^{Y410A} spores lost only 50% of their initial OD, and this point was reached 105 min after *ypeB*$^{+}$ spores lost 59% of their initial OD (Fig. 2.1C). YpeB^{Y410A} spores also showed a significant decrease ($P < 0.004$) in their ability to form colonies on BHI plates with a nearly 100-fold reduction (Fig. 2.5).

The trend seen for the YpeB point mutants in germination rate and plating efficiency assays was mirrored by the levels of YpeB and SleB seen in western blots of dormant spore extracts (Fig. 2.5). Relative YpeB band intensities for each strain were computed by comparison to the YpeB band from the *ypeB*$^{+}$ strain. Similarly, SleB band intensities relative to the SleB band detected in *ypeB*$^{+}$ spores were determined. The strains that appeared most similar to *ypeB*$^{+}$ spores in germination rate and plating efficiency assays (YpeB^{Y329A} and YpeB^{T377A}) contained 101 and 99% of the YpeB protein levels and 102 and 93% of the SleB protein levels, respectively, detected in *ypeB*$^{+}$ spores. Likewise, YpeB^{Y254A} and YpeB^{G430A} spores, which showed minor defects during the other assays tested, possessed 69 and 75% of native YpeB levels and 70 and 65% of native SleB levels, respectively. Immunoblots of YpeB^{G430A} dormant

spore extracts also revealed the presence of two stable YpeB-specific degradation products (not shown) that are similar to those observed during sporulation of a Δ*sleB* strain (Fig. 2.3C). Of the point mutants, the lowest levels of the two proteins were seen for YpeB^{Y410A}, with 60% YpeB levels and 40% SleB levels of those found in *ypeB*$^{+}$ spores. This corresponds well with the more severe deficit in germination phenotypes demonstrated by YpeB^{Y410A} spores. While the correlation between YpeB and SleB band intensities was not perfect, the trend was quite clear, where YpeB abundance, SleB abundance, and germination rate decreased in concert in all strains tested.

DISCUSSION

This study investigated the relationship between SleB and YpeB in *B. anthracis* for the first time. Consistent with findings in *B. subtilis* (23), germination of decoated Δ*sleB* and Δ*ypeB* spores of *B. anthracis* was blocked after the initial steps of germination, these spores exhibited greater than a 10^4-fold decrease in colony forming ability, and lytic transglycosylase products were absent in germinating spores, confirming that YpeB is needed for the lytic activity of SleB on cortex peptidoglycan *in vivo*. The current work clearly demonstrates that not only is YpeB required for SleB incorporation in the dormant spore, as in *B. subtilis* (36, 90), but YpeB has a reciprocal requisite for SleB. This mutual dependency was also discovered recently using a *B. subtilis* strain ectopically-expressed YpeB in a *cwlJ sleB ypeB* mutant background (90). In that strain, YpeB was only detected in western blots of spore inner membrane fractions if SleB was also expressed (90). It should be noted since only the inner membrane fraction was analyzed in those immunoblots, there's a possibility the absence of SleB may have resulted in the mislocalization of YpeB. The western blots in the present study utilized entire spore extracts

derived from strains in which *sleB* or *ypeB* were deleted or expressed from the native operon. Thus, these results provide more conclusive evidence that YpeB is indeed absent in Δ*sleB* spores. Furthermore, it is demonstrated that in the absence of their stabilizing partner, SleB and YpeB are expressed and degraded during early sporulation, rather than simply failing to localize within the developing spore.

Li et al. suggested that both the N- and C-terminal domains of YpeB are necessary for SleB lytic activity during spore germination, as a *cwlJ sleB ypeB* deficient strain of *B. subtilis* ectopically expressing individual *ypeB* domains ($YpeB^{N}$ or $YpeB^{C}$) with full-length *sleB* ($SleB^{FL}$) could not complement the germination defect in these spores (90). While these results were hampered by an inability to determine if $YpeB^{N}$ or $YpeB^{C}$ were stably incorporated into the spore, Li et al. did demonstrate that the C-terminus of YpeB fused to its signal sequence (memseg-$YpeB^{C}$) was stable and yet could not complement when expressed with $SleB^{FL}$, indicating the N-terminus of YpeB is needed (90). Results obtained through the current study, in which stretches of residues between the YpeB signal sequence and PepSY domains were deleted, support the necessity of a region within the N-terminal portion of YpeB. This critical region occurs within the span of residues 67 and 203, as $YpeB_{\Delta 67\text{-}203}$-$His_6$ was moderately stable in the dormant spore yet could not stabilize SleB. Deletion of regions corresponding to the PepSY domains at the C-terminus of YpeB also add to what is known about the portions of YpeB needed for SleB stability. While many of the truncated YpeB variants were unstable, $YpeB_{1\text{-}283}$-His_6, which contained the first predicted PepSY domain, was moderately stable, yet SleB was not detected in western blots and germination phenotypes resembled those of Δ*ypeB* spores. These results clearly show that a region beyond the first YpeB PepSY domain is also essential for SleB stabilization. Taken together with the findings by Li et al. (90), it's apparent that both

the N-terminus and PepSY domain-containing C-terminus of YpeB are required for stable incorporation of SleB in the spore.

In studying the effects of *ypeB* point mutations on SleB stability and function, the co-dependency between the two proteins observed in Δ*sleB* and Δ*ypeB* spores was reinforced. There was a strong correlation between SleB and YpeB protein levels present within spores of individual strains, and protein abundance matched well with observed germination phenotypes. This intrinsic co-dependency becomes a complicating factor in determining which YpeB residues are actually important for the interaction with SleB, and which are just important for proper YpeB folding. In the former scenario, alteration of a residue mediating the interaction between YpeB and SleB would destabilize the interaction, resulting in decreased levels of both proteins. In the latter scenario, a mutation effecting YpeB protein folding would likely decrease YpeB stability, subsequently decreasing the stability of SleB. Residue Y410 of YpeB clearly plays a large role in YpeB and SleB stability, and this residue is one of the most highly conserved across PepSY domains (45, 177). While the Y410A substitution had a large effect on spore germination, the tyrosine residues at similar positions in the other two PepSY domains did not prove to be as important. The Y254A substitution in the first PepSY domain resulted in a milder spore germination defect, and the Y329A replacement in the second PepSY domain produced spores that germinated equally as well as *ypeB*$^{+}$ spores. Additionally, of the three mutations made in the region encoding the third PepSY domain of YpeB, two resulted in observable phenotypes, indicating the relative importance of this third PepSY domain. The three *ypeB* point mutations that produced phenotypic changes (Y254A, Y410A, G430A) affect residues that are 100% conserved in an alignment of YpeB proteins from 13 *Bacillus* species, while those mutations that produced no phenotypic changes were less conserved. This could

point to the three PepSY domains being unequal, with the third being the most crucial but the first also playing a role. Without an alternative means of stabilizing YpeB and SleB *in vivo*, such as via inhibition of proteolysis within the developing sporangium, further *in vivo* genetic study of the relationship between these proteins is difficult.

Analysis of YpeB point mutants also indicated that reduced amounts of SleB in spores not only resulted in reduced germination rates, but also hindered the ability of spores to complete outgrowth and form colonies. A similar phenomenon was evident in *B. subtilis cwlJ sleB* mutants expressing *sleB* ectopically in addition to a low level of *ypeB* expression through apparent read-through of an *sleB* insertion mutation (90). While the amounts of SleB and YpeB present in spores of these *B. subtilis* strains were not explicitly quantified, immunoblots clearly showed a reduction in SleB and YpeB levels. These same spores exhibited greater than a 50% decrease in colony forming ability (90). One might expect that even limited quantities of SleB within a given spore would allow the spore to germinate, albeit at a slower rate. This finding may suggest heterogeneity within a population of dormant spores from an individual mutant strain with respect to absolute SleB levels present or the portion of SleB capable of being activated.

The simplest explanation for how SleB and YpeB are able to stabilize each other is that the two proteins physically interact; yet such a direct interaction has not been demonstrated. Li et al. did not observe an interaction using *in vitro* affinity pull-down assays involving various forms of *B. cereus* and *B. megaterium* SleB and YpeB purified from *E. coli* and *Lactococcus lactis* (90). Similarly, in conjunction with the work presented here, affinity pull-down assays were performed using His_6-MBP-$YpeB_{1-446}$ or His_6-MBP-$YpeB_{21-446}$ and untagged $SleB_{33-253}$, and reciprocally, His_6-MBP-$SleB_{33-253}$ and untagged $YpeB_{21-446}$. No interaction between SleB

and YpeB was observed (data not shown). A logical explanation for the lack of *in vitro* interaction is that if SleB and YpeB do indeed physically interact, it likely occurs during spore formation as the proteins are co-expressed and translocated in their unfolded forms across the inner forespore membrane via the Sec pathway. Thus, the proteins may need to be co-translocated and/or co-folding or, as postulated by Li et al., a membrane might be necessary for the interaction to occur (90). Protein co-expression is likely not the only variable missing from the equation, as assays performed using cell extracts from *E. coli* in which SleB and YpeB were co-expressed, still failed to show an interaction between the two proteins (90), although it's feasible the N-terminal affinity tags on both proteins impeded an interaction.

As YpeB does not have any homologs of known function, one of the major clues in determining the precise nature of the relationship between SleB and YpeB may lie in PepSY domains at the C-terminus of YpeB, which this study has demonstrated are clearly important. While these domains have an unknown function in many proteins, they have been found in the pro-peptide region of M4 class proteases and function as inhibitors of protease activity (177). Another potential model, where SleB and YpeB do not bind and YpeB instead forms an inhibitory interaction with the protease(s) responsible for SleB degradation in the absence of YpeB, fails to explain how SleB stabilizes YpeB. It's possible PepSY domains are capable of inhibiting a broader range of enzymatic activities, as they belong to a superfamily of bacterial protein domains sharing a β-lactamase inhibitor protein (BLIP)-like fold (45). Members of this superfamily have been associated with various inhibitory roles, including inhibition of β-lactamases, and have also been proposed to mediate protein-protein interactions (45). The potential for PepSY domains to inhibit enzymatic activities outside their known niche makes YpeB a prime candidate for a way by which SleB is held inactive in the dormant spore. It has

been demonstrated in *B. subtilis* that YpeB is cleaved during spore germination (36), so such cleavage could release SleB from the inhibitory interaction with YpeB, thereby activating SleB for cortex degradation. Recent *in vitro* experiments using various forms of exogenous SleB and YpeB from *B. cereus* have demonstrated the inhibition of SleB activity in the presence of YpeB (90). While the *in vitro* experiments performed by Li et al. (90) support an inhibitory role of YpeB, more work is needed to further elucidate the relationship between SleB and YpeB. Such studies should aim to clarify the function of the PepSY domains, and the mechanism by which YpeB, and specifically $YpeB^{N}$, are able to inhibit SleB activity. YpeB processing during germination should also be investigated to determine if this event is required for SleB activation, or merely part of the process whereby unneeded spore proteins are broken down and recycled for new protein synthesis during outgrowth.

ACKNOWLEDGEMENTS

Research reported in this publication was supported by the National Institute of Allergy and Infectious Disease of the National Institutes of Health under award number AI060726. The content is solely the responsibility of the authors and does not necessarily represent the official views of the National Institutes of Health.

Table 2.1. Bacterial strains and plasmids.

Strain or plasmid	Relevant genotype/phenotype [a]	Construction [b]	Source
E. coli			
DPVE13	BL21 (λDE3) pLysS (Cm^r)		Novagen
DPVE440	pDPV426 (His_6-MBP-$YpeB_{21-446}$ Amp^r) Cm^r	pDPV426→DPVE13	This study
B. anthracis			
Sterne 34F2	$pXO1^+$ $pXO2^-$		P. Hanna
DPBa38	Δ*sleB*		(64)
DPBa57	Δ*sleB*, pDPV346 (*sleB*$^+$ Er^r)		(64)
DPBa89	Δ*ypeB*	pDPV392→34F2	This study
DPBa113	Δ*ypeB*::pDPV416 (*ypeB*$^+$ Er^r)	pDPV416→DPBa89	This study
DPBa124	Δ*ypeB*::pDPV421 ($YpeB_{1-208}$-His_6 Er^r)	pDPV421→DPBa89	This study
DPBa125	Δ*ypeB*::pDPV422 ($YpeB_{1-283}$-His_6 Er^r)	pDPV422→DPBa89	This study
DPBa126	Δ*ypeB*::pDPV423 ($YpeB_{1-368}$-His_6 Er^r)	pDPV423→DPBa89	This study
DPBa127	Δ*ypeB*::pDPV424 ($YpeB_{1-446}$-His_6 Er^r)	pDPV424→DPBa89	This study
DPBa134	Δ*sleB*::pDPV346 (*sleB*$^+$ Er^r)	DPBa57 integration	This study
DPBa143	Δ*ypeB*::pDPV435 ($YpeB^{Y410A}$ Er^r)	pDPV435→DPBa89	This study
DPBa144	Δ*ypeB*::pDPV436 ($YpeB^{G430A}$ Er^r)	pDPV436→DPBa89	This study
DPBa148	Δ*ypeB*::pDPV432 ($YpeB^{T377A}$ Er^r)	pDPV432→DPBa89	This study
DPBa149	Δ*ypeB*::pDPV433 ($YpeB^{Y254A}$ Er^r)	pDPV433→DPBa89	This study
DPBa150	Δ*ypeB*::pDPV434 ($YpeB^{Y329A}$ Er^r)	pDPV434→DPBa89	This study
DPBa158	Δ*ypeB*::pDPV448 ($YpeB_{Δ25-203}$-His_6 Er^r)	pDPV448→DPBa89	This study
DPBa159	Δ*ypeB*::pDPV449 ($YpeB_{Δ67-203}$-His_6 Er^r)	pDPV449→DPBa89	This study
DPBa160	Δ*ypeB*::pDPV450 ($YpeB_{Δ119-203}$-His_6 Er^r)	pDPV450→DPBa89	This study
DPBa161	Δ*ypeB*::pDPV451 ($YpeB_{Δ156-203}$-His_6 Er^r)	pDPV451→DPBa89	This study
Plasmids			
pBKJ236	Er^r *ori*(Ts)		(75)
pBKJ223	Tet^r Amp^r, P_{amy}-I-SceI		(75)
pDEST-HisMBP-T	His_6-MBP, Amp^r Cm^r		F. Schubot
pDPV346	*sleB*$^+$	pBKJ236::*sleB*	(64)
pDPV388	*ypeB*$^+$	pBKJ236::*ypeB*	This study
pDPV392	Δ*ypeB*	pBKJ236::Δ*ypeB*	This study
pDPV416	*ypeB*$^+$	pBKJ236::Δ*sleB ypeB*	This study
pDPV421	$YpeB_{1-208}$-His_6	pBKJ236::Δ*sleB* $ypeB_{1-208}$-His_6	This study
pDPV422	$YpeB_{1-283}$-His_6	pBKJ236::Δ*sleB* $ypeB_{1-283}$-His_6	This study
pDPV423	$YpeB_{1-368}$-His_6	pBKJ236::Δ*sleB* $ypeB_{1-368}$-His_6	This study
pDPV424	$YpeB_{1-446}$-His_6	pBKJ236::Δ*sleB* $ypeB_{1-446}$-His_6	This study
pDPV426	His_6-MBP-$YpeB_{21-446}$	pDEST-HisMBP-T::$ypeB_{21-446}$	This study
pDPV432	$YpeB^{T377A}$	pBKJ236::Δ*sleB* $ypeB^{T377A}$	This study
pDPV433	$YpeB^{Y254A}$	pBKJ236::Δ*sleB* $ypeB^{Y254A}$	This study
pDPV434	$YpeB^{Y329A}$	pBKJ236::Δ*sleB* $ypeB^{Y329A}$	This study
pDPV435	$YpeB^{Y410A}$	pBKJ236::Δ*sleB* $ypeB^{Y410A}$	This study
pDPV436	$YpeB^{G430A}$	pBKJ236::Δ*sleB* $ypeB^{G430A}$	This study
pDPV448	$YpeB_{Δ25-203}$-His_6	pBKJ236::Δ*sleB* $ypeB_{Δ25-203}$-His_6	This study
pDPV449	$YpeB_{Δ67-203}$-His_6	pBKJ236::Δ*sleB* $ypeB_{Δ67-203}$-His_6	This study
pDPV450	$YpeB_{Δ119-203}$-His_6	pBKJ236::Δ*sleB* $ypeB_{Δ119-203}$-His_6	This study
pDPV451	$YpeB_{Δ156-203}$-His_6	pBKJ236::Δ*sleB* $ypeB_{Δ156-203}$-His_6	This study

[a] Cm^r, chloramphenicol resistance; Amp^r, ampicillin resistance; Er^r, erythromycin resistance; *ori*(Ts), temperature-sensitive origin of replication; Tet^r, tetracycline resistance.
[b] Strains were constructed by conjugation or electroporation. The designation preceding the arrow is the plasmid, while the designation following the arrow is the recipient strain. Single strain designations indicate the existing plasmid was integrated into the chromosome.

Table 2.2. Primer sequences.

Plasmid constructed	Primer name	Sequence 5′ to 3′ [a]
pDPV388	442	CGCCCGCGGGTTGATGGTTTAGCTGGAGC
	443	CGCGCGGCCG*C*ACTTGTGGCATTACACGGCC
pDPV392	444	GCCCGCGCGGCTCGTAACATAGTTCCACCTCCGCTC
	445	AGCCGCGCGGGCTATGATTAAACTTTAATGGTAAAGT
pDPV416	288	CGCGCGGCCGCCTCGTCTTCTGGAACGACAC
	443	
pDPV421	494	CGCAGATCT*TTA***ATGATGATGATGATGATG**TTTATTTTTTTGTGCACTTGTAAAGGTAGG
	498	CGCAGATCTGCCACCGCGGTGGAGCTC
pDPV422	495	CGCAGATCT*TTA***ATGATGATGATGATGATG**ATTCATAACCCAAATTGGATATCCGC
	498	
pDPV423	496	CGCAGATCT*TTA***ATGATGATGATGATGATG**TTTTTGATGTGACGCTAAATATTCTTTTGC
	498	
pDPV424	497	CGCAGATCT*TTA***ATGATGATGATGATGATG**ATCATAAATTTTTTCAACAGCCTGC
	498	
pDPV426	511	*CCACTTTGTACAAGAAAG*TTGCATTGCTTTAATCATAAATTTTTTCAACAGCC
	512	***GTGGAGAACCTGTACTTCCAGGGT***TATAAAGAGCATCAAGAGAAGAATGC
pDPV432	538	CGAACAGTTCCATCAGCAAAACTAGCGGCAGCAGAAGCAA
	539	TTGCTTCTGCTGCCGCTAGTTTTGCTGATGGAACTGTTCG
	554	CGTGATCCTGCCGACAATACAATTATTGACGGACTAAAGACAGTAG
	555	GCTAGATGATCCGCTGCTTTTTCATTTGGCTTATTTGACTTATTCG
pDPV433	534	AAGTGGAAAAGGTGCAAAAGAATCTTTCGCGAGTGTGAAAATTAAAGATGAAGCAACG
	535	CGTTGCTTCATCTTTAATTTTCACACTCGCGAAAGATTCTTTTGCACCTTTTCCACTT
	554, 555	
pDPV434	536	CTCACAATATGATAATGTTGGAGTATTTACAGCTGTAGTAAATGTGAATGGCGTACGAATTTA
	537	TAAATTCGTACGCCATTCACATTTACTACAGCTGTAAATACTCCAACATTATCATATTGTGAG
	554, 555	
pDPV435	540	AATGATCTGCATAATGAAGTACTTTGCGCAGAATTTGTAGGTACGTTAGGGAAAGAT
	541	ATCTTTCCCTAACGTACCTACAAATTCTGCGCAAAGTACTTCATTATGCAGATCATT
	554, 555	
pDPV436	542	CAAATCTTCATTAATGCAAATAGCGCTGCAGAAGAAAAAGTGAAGAAAATGC
	543	GCATTTTCTTCACTTTTTCTTCTGCAGCGCTATTTGCATTAATGAAGATTTG
	554, 555	
pDPV448	595	GGGTACTGGGGCTATAAAGAGGCACAAAAAAATAAAAAAGGTGGATTTGAAGCAGAAGG
	596	CCTTTTTTATTTTTTTGTGCCTCTTTATAGCCCCAGTACCCTGTGCCGAC
	603	GTCTTCTTTACATAAAAGCGAGCCTTTTACAAAACATAACC
	604	GCTTTACGTTCTTCCATAACTTTCACATCTGGATTG
pDPV449	597	CGCTTGCGATGAATTCACGTGCACAAAAAAATAAAAAAGGTGGATTTGAAGCAGAAGG
	598	CCTTTTTTATTTTTTTGTGCACGTGAATTCATCGCAAGCGTTGTACC
	603, 604	
pDPV450	599	CCGTGCAGCTATTCGTGATGCACAAAAAAATAAAAAAGGTGGATTTGAAGCAGAAGG
	600	CCTTTTTTATTTTTTTGTGCATCACGAATAGCTGCACGGTAACTAAAATCACCG
	603, 604	
pDPV451	601	GTGCAACATCTTGTTTTGAAAGCACAAAAAAATAAAAAAGGTGGATTTGAAGCAGAAGG
	602	CCTTTTTTATTTTTTTGTGCTTTCAAAACAAGATGTTGCACTTTTCTTAGTTCATCTTG
	603, 604	

[a] Restriction sites are underlined, TEV cleavage site regions of pDEST-HisMBP-T are italicized and in bold, *att*R2.1 regions of pDEST-HisMBP-T are italicized and underlined, added stop codons are italicized, and His_6 encoding codons are in bold.

Table 2.3. Decoated spore plating efficiencies for *sleB* and *ypeB* mutants.

Strain	Genotype/Phenotype	CFU/OD_{600} [a]
34F2	wild-type	8.4×10^7
DPBa38	Δ*sleB*	8.3×10^3 [b]
DPBa89	Δ*ypeB*	$< 5.8 \times 10^3$ [b]
DPBa113	$ypeB^+$	8.7×10^7
DPBa124	$YpeB_{1\text{-}208}$-His_6	9.7×10^3 [b]
DPBa125	$YpeB_{1\text{-}283}$-His_6	$< 3.5 \times 10^3$ [b]
DPBa126	$YpeB_{1\text{-}368}$-His_6	$< 4.5 \times 10^3$ [b]
DPBa127	$YpeB_{1\text{-}446}$-His_6	1.1×10^8

[a] Values are averages of three independent spore preparations.

[b] Value is significantly different from that of wild-type and $ypeB^+$ spores with P values of < 0.006 and < 0.02, respectively.

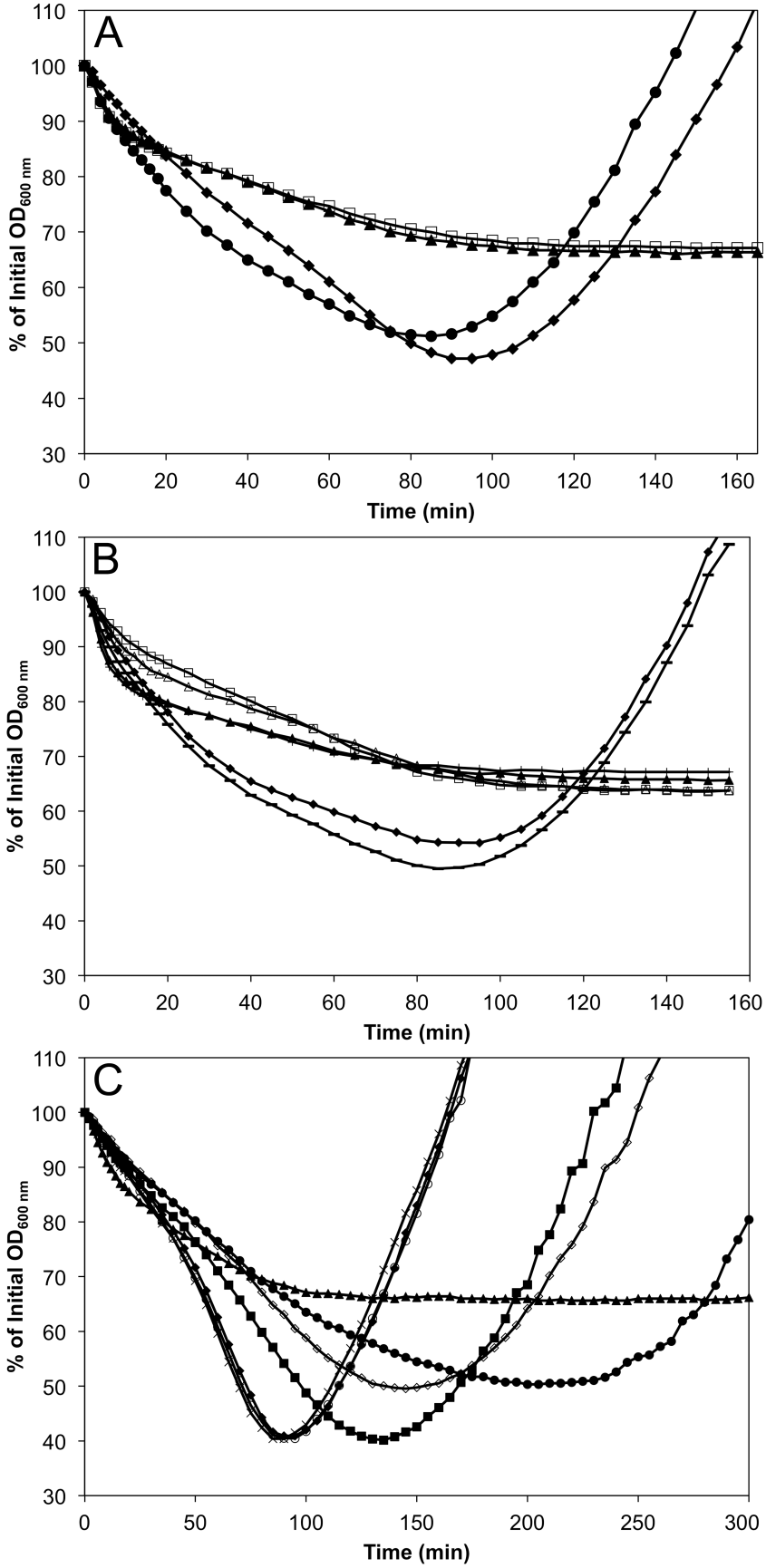
A
B
C
% of Initial OD600 nm
Time (min)
110
100
90
80
70
60
50
40
30
0
20
40
60
80
100
120
140
160
0
50
100
150
200
250
300

Figure 2.1. Effects of a variety of *ypeB* mutations on germination and outgrowth of decoated *B. anthracis* spores. Decoated spores were heat activated and germinated in BHI medium at 37°C. Data shown are averages of results from three independent spore preparations; error bars are omitted for clarity. (A) Germination and outgrowth are blocked in decoated Δ*ypeB* spores. Wild-type (●), Δ*sleB* (□), Δ*ypeB* (▲), and *ypeB* complementation (*ypeB*$^+$,◆) strains were analyzed. Germination of Δ*sleB* and Δ*ypeB* spores was statistically indistinguishable ($P > 0.23$), as was germination of wild-type and *ypeB*$^+$ spores ($P > 0.08$). Both Δ*sleB* and Δ*ypeB* spores were significantly different ($P < 0.04$) from wild-type and *ypeB*$^+$ spores during stage II of germination from 45-95 min. (B) Truncations removing YpeB PepSY domains block decoated spore germination. Δ*ypeB* (▲), $YpeB_{1\text{-}208}$-His_6 (△), $YpeB_{1\text{-}283}$-His_6 (+), $YpeB_{1\text{-}368}$-His_6 (□), $YpeB_{1\text{-}446}$-His_6 (−), and *ypeB*$^+$ (◆) strains were analyzed. Germination of *ypeB*$^+$ and $YpeB_{1\text{-}446}$-His_6 spores is not statistically different ($P > 0.08$); likewise, germination of Δ*ypeB* and $YpeB_{1\text{-}283}$-His_6 spores is statistically indistinguishable ($P > 0.49$). $YpeB_{1\text{-}208}$-His_6 and $YpeB_{1\text{-}368}$-His_6 spores do not differ ($P > 0.05$) from Δ*ypeB* spores during germination, except at 55 min, and from 45-55 min, respectively ($P < 0.05$). Germination of $YpeB_{1\text{-}208}$-His_6, $YpeB_{1\text{-}283}$-His_6, and $YpeB_{1\text{-}368}$-His_6 spores is not statistically different ($P > 0.11$) from 4 min onward. (C) Point mutations in YpeB PepSY domain conserved residues slow decoated spore germination. Δ*ypeB* (▲), $YpeB^{Y254A}$ (■), $YpeB^{Y329A}$ (×), $YpeB^{T377A}$ (○), $YpeB^{Y410A}$ (●), $YpeB^{G430A}$ (◇), and *ypeB*$^+$ (◆) strains were analyzed. Statistical analysis of *ypeB* point mutants is complex due to the greater variability of germination rates of decoated spore preparations, as well as the fact that spores of some strains are initiating outgrowth while others are still germinating. Focusing on stage II of germination, between 45 and 95 min, $YpeB^{Y329A}$ and $YpeB^{T377A}$ spores are not significantly different from *ypeB*$^+$ spores ($P > 0.38$). Germination of $YpeB^{Y254A}$ spores from 80-90 min, $YpeB^{Y410A}$ spores from 45-55 min and 70-95 min, and $YpeB^{G430A}$ spores at 50 min and from 75-95 min, are significantly different from *ypeB*$^+$ spores ($P < 0.05$).

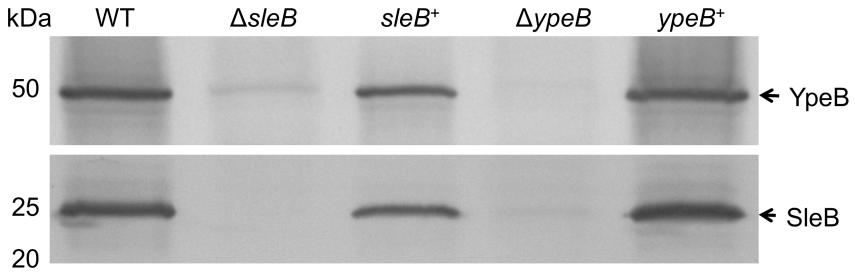

Figure 2.2. *B. anthracis* SleB and YpeB are co-dependent for incorporation into dormant spores. Dormant wild-type (WT), Δ*sleB*, *sleB* complementation (*sleB*$^+$), Δ*ypeB*, and *ypeB* complementation (*ypeB*$^+$) spores were mechanically disrupted and proteins extracted with sample loading buffer for western blot analysis. Blots were probed with anti-YpeB antibodies (top) and anti-SleB antibodies (bottom). The predicted molecular weights of mature SleB lacking its signal sequence and YpeB are 24.1 and 50.0 kDa, respectively. The positions of molecular weight marker proteins (not shown) are indicated on the left.

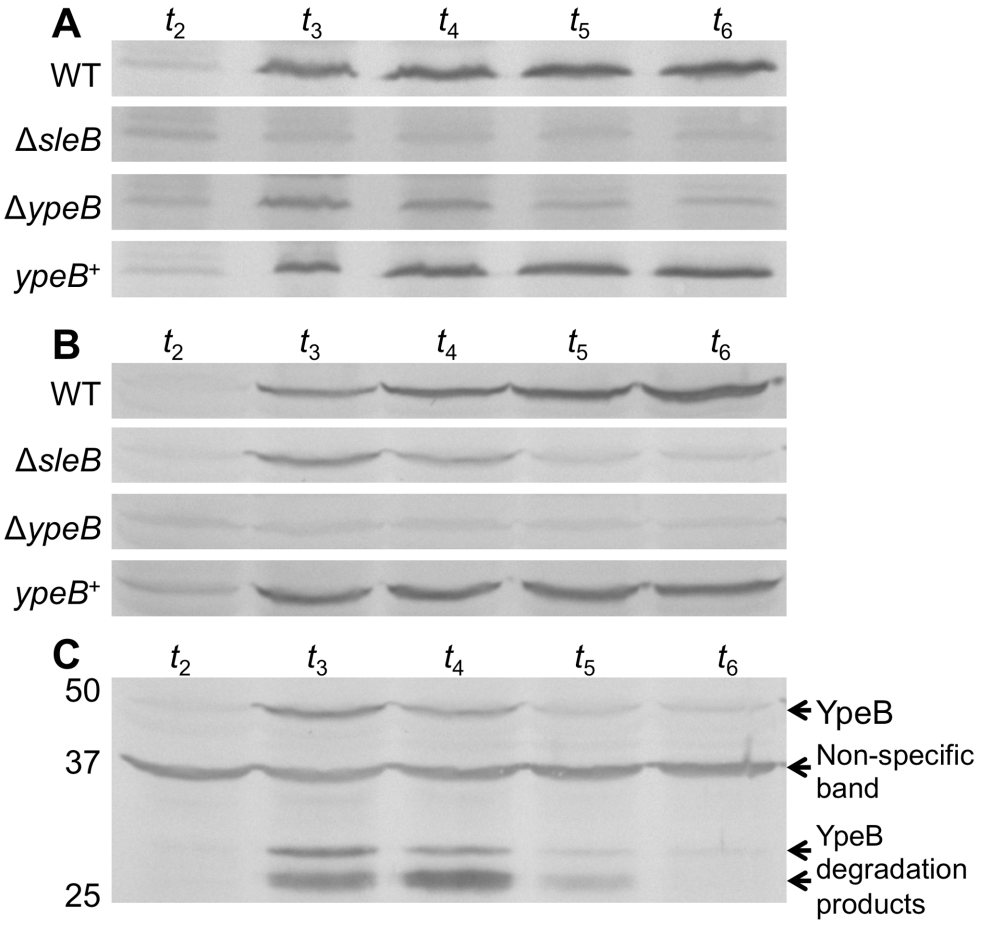

Figure 2.3. *B. anthracis* SleB and YpeB are degraded during spore formation in the absence of their partner protein. Wild-type (WT), Δ*sleB*, Δ*ypeB*, and *ypeB* complementation (*ypeB*$^+$) strains were grown in modified G broth at 37°C, and samples collected during sporulation were used for western blot analysis. Values t_2 through t_6 indicate hours since the initiation of sporulation. (A) Sporangia probed with anti-SleB antibodies. (B) Sporangia probed with anti-YpeB antibodies. (C) Sporangia from the Δ*sleB* strain probed with anti-YpeB antibodies. The positions of molecular weight marker proteins (kDa) (not shown) are indicated on the left.

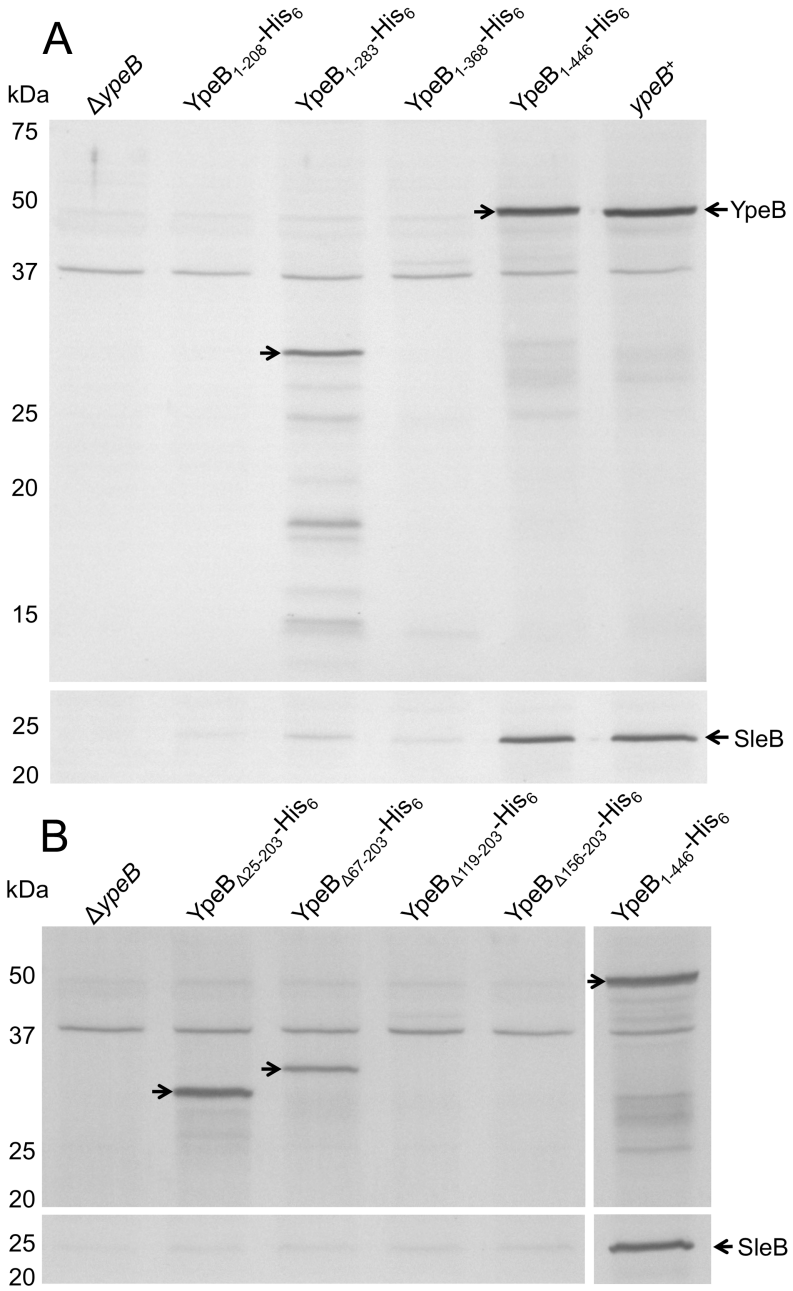

Figure 2.4. Effects of *ypeB* truncation and internal deletion mutations on stability of YpeB and SleB. Dormant spores were mechanically disrupted and proteins extracted with sample loading buffer for western blot analysis. Samples were probed with anti-YpeB antibodies (top panels) and anti-SleB antibodies (bottom panels). Rightward pointing arrowheads indicate YpeB derivatives. The positions of molecular weight marker proteins (not shown) are indicated on the left. (A) Truncations removing YpeB PepSY domains destabilize both YpeB and SleB. $YpeB_{1-208}$-His_6, $YpeB_{1-283}$-His_6, $YpeB_{1-368}$-His_6, and $YpeB_{1-446}$-His_6 have predicted molecular weights of 24.3, 32.5, 42.1, and 50.9 kDa, respectively. (B) Internal deletions in the YpeB N-terminal domain destabilize SleB. Lanes intervening between lanes 5 and 6 were removed for clarity. $YpeB_{\Delta 25-203}$-His_6, $YpeB_{\Delta 67-203}$-His_6, $YpeB_{\Delta 119-203}$-His_6, $YpeB_{\Delta 156-203}$-His_6, and $YpeB_{1-446}$-His_6 have predicted molecular weights of 30.6, 35.5, 41.2, 45.6, and 50.9 kDa, respectively.

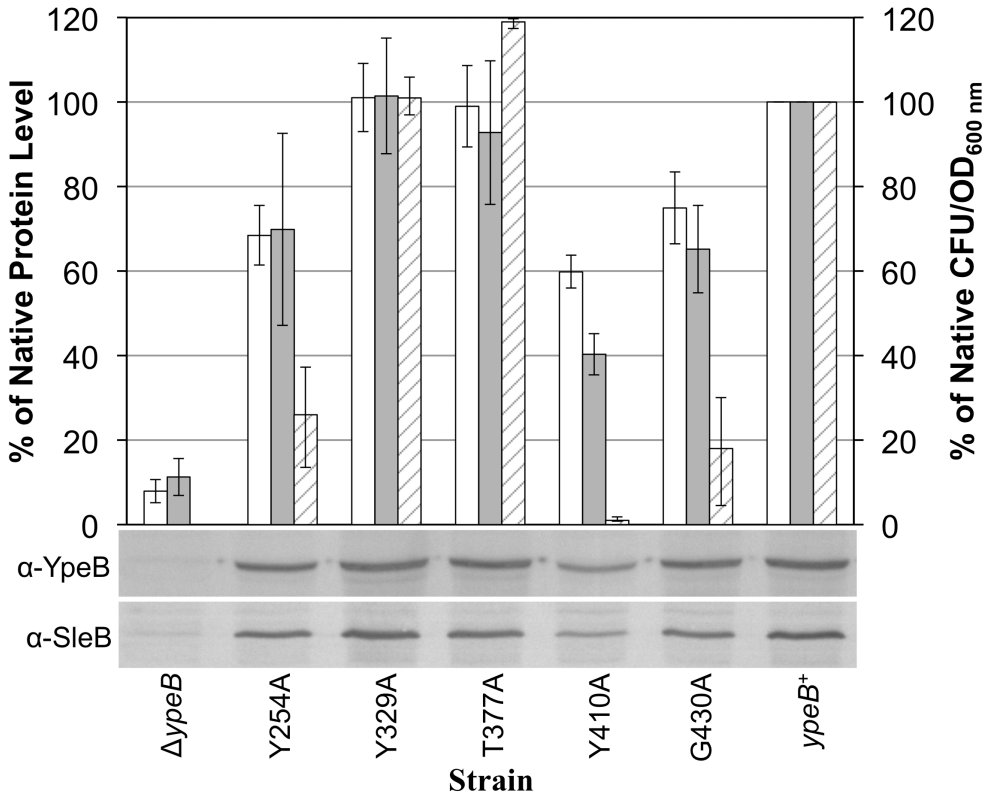

Figure 2.5. Protein stability and plating efficiency in YpeB point mutant spores. Dried, dormant Δ*ypeB*, YpeB^{Y254A} (Y254A), YpeB^{Y329A} (Y329A), YpeB^{T377A} (T377A), YpeB^{Y410A} (Y410A), YpeB^{G430A} (G430A), and *ypeB* complementation (*ypeB*$^{+}$) spores were broken, and extracted proteins were analyzed through western blots with anti-SleB antibodies (α-SleB) or anti-YpeB antibodies (α-YpeB). Band intensities were quantified and are depicted as levels of YpeB (white bars) and SleB (gray bars) present in spores, relative to the native protein levels found in *ypeB*$^{+}$ spores, which were set at 100%. Spores of the same strains were heat activated, serially diluted, and plated on BHI medium. Following incubation, colonies were counted and % native CFU/OD values (stripped bars) were determined by comparison to the CFU/OD value of *ypeB*$^{+}$ spores, which was set at 100%. Plating efficiency and western blot quantification data shown are averages from three independent spore preparations with error bars representing the standard deviation. Western blots pictured are representative results from one of the replicates.

CHAPTER 3

HtrC is involved in proteolysis of YpeB during germination of *Bacillus anthracis* and *Bacillus subtilis* spores

Casey B. Bernhards, Yan Chen, Hannah K. Toutkoushian, and David L. Popham

Manuscript in preparation

ATTRIBUTIONS

Casey B. Bernhards and Yan Chen contributed equally to the research, experimentation, and data analysis of the material presented herein. Casey is responsible for the work presented in Figures 3.1, 3.2, 3.3, 3.4, and 3.9. Yan is responsible for the work presented in Table 3.3 and Figures 3.5, 3.6, 3.7, 3.8. Hannah K. Toutkoushian performed germination rate assays involving *htrC* mutants and provided laboratory assistance. David L. Popham was the principle investigator. Casey, Yan, and David all contributed to the writing of the manuscript.

ABSTRACT

Bacterial endospores can remain dormant for decades, yet can respond to nutrients, germinate, and resume growth within minutes. An essential step in the germination process is degradation of the spore cortex peptidoglycan wall, and the SleB protein in *Bacillus* species plays a key role in this process. Stable incorporation of SleB into the spore requires the YpeB protein, and some evidence suggests that these two proteins interact within the dormant spore. Early during germination, YpeB is proteolytically processed to a stable fragment. In this work, the primary sites of YpeB cleavage were identified in *Bacillus anthracis*, and it was shown that the stable products are comprised of the C-terminal domain of YpeB. Modification of the predominant YpeB cleavage sites reduced proteolysis, but cleavage at other sites still resulted in loss of full-length YpeB. A *B. anthracis* strain lacking the HtrC protease did not generate the same stable YpeB products. In *B. anthracis* and *Bacillus subtilis htrC* mutants, YpeB was partially stabilized during germination but was still degraded at a reduced rate by other unidentified proteases. Purified HtrC cleaved YpeB to a fragment similar to that observed *in vivo*, and this cleavage was stimulated by Mn^{2+} or Ca^{2+} ions. A lack of HtrC did not stabilize YpeB or SleB during spore formation in the absence of the partner protein, indicating other proteases are involved in their degradation during sporulation.

INTRODUCTION

Endospores produced by Gram-positive genera such as *Bacillus* and *Clostridium* possess extreme resistance properties and can remain in a fully dormant state for years. The dormant state and resistance properties are dependent on the maintenance of the spore core (cytoplasm) in a relatively dehydrated state, and this in turn depends on the intact state of the inner spore membrane and the cortex peptidoglycan (PG) wall surrounding that membrane (148). Upon exposure to nutrient germinants, spores begin to release low molecular weight solutes, including a large depot of Ca^{2+}-dipicolinic acid (Ca^{2+}-DPA), and take up water (146). Degradation of the cortex PG by germination-specific lytic enzymes (GSLEs) is required for full expansion of the membrane, full hydration of the core, and resumption of metabolism (9, 128, 142, 144). As GSLEs hydrolyze the cortex PG before new protein synthesis can occur, they must be produced during spore formation and held stable and inactive in the dormant spore until germination is triggered (127).

Bacillus species possess two major, partially redundant GSLEs: CwlJ and SleB (127). CwlJ is produced in the mother cell of the developing sporangium (74), is associated with the spore coats on the outer surface of the cortex (13, 36, 117, 132), and becomes active when exposed to a high concentration of Ca^{2+}-DPA—normally when that solute is released from the germinating spore (63, 117, 145). SleB is produced within the developing forespore (23, 108) and is located interior to the cortex in the dormant spore, most likely in close association with the inner spore membrane (36, 81). The mechanisms by which SleB is held inactive during spore dormancy and released to become active during germination are unclear.

A potential factor in regulation of SleB activity is YpeB, which is encoded in an operon with *sleB* and possesses a transmembrane anchor sequence that should also localize it to the

outer surface of the inner spore membrane (19, 23, 64). SleB and YpeB exhibit a co-dependence for their stable incorporation into the dormant spore (19, 36, 90). In the absence of their partner protein, both SleB and YpeB are produced and rapidly degraded during spore formation (19). It has also been observed that YpeB is proteolytically processed during spore germination (36), and it has been suggested that this processing could be involved in the initiation of SleB activity during germination (90).

The current study examined the cleavage sites generating the stable YpeB products during germination and identified HtrC as the protease responsible for these cleavage events. The resulting cleavage products were shown to contain the C-terminus and PepSY domains of YpeB. Strains lacking HtrC or with mutations at the YpeB cleavage sites were constructed to evaluate the role of YpeB processing in SleB activation. In the absence of HtrC, YpeB was degraded in a more non-specific manner during germination, and activity of SleB was not significantly affected.

MATERIALS AND METHODS

Strains, culture conditions, and spore preparation. *Escherichia coli* strains used for plasmid propagation were grown at 37°C in LB medium with 500 μg/ml erythromycin or 20 μg/ml kanamycin. Strains used for protein overexpression were grown in LB with 30 μg/ml chloramphenicol and 50 μg/ml ampicillin. *Bacillus anthracis* strains were derived from the Sterne strain 34F2 and were grown on brain heart infusion (BHI; Difco) agar plates with 5 μg/ml erythromycin or 20 μg/ml kanamycin, where appropriate. *B. anthracis* strains maintaining pBKJ236-derivatives extrachromosomally were grown at 25°C, while those in which the plasmid was integrated into the chromosome were grown at 37°C. *Bacillus subtilis* strains were derived

from PS832, a prototrophic laboratory derivative of strain 168, and were grown on 2xSG medium (87) with 0.5 μg/ml erythromycin and 12.5 μg/ml lincomycin (MLS resistance), and/or 10 μg/ml tetracycline, when appropriate. Spores were prepared in Modified G (78) broth for *B. anthracis*, or 2xSG (87) broth for *B. subtilis* with appropriate antibiotics. After 72 h incubation at 37°C, spores were harvested, washed in deionized water for several days, and any remaining vegetative cells were heat killed at 65°C for 25 min. *B. anthracis* spores were further purified by centrifugation through a 50% sodium diatrizoate (Sigma) layer as described (113). Where indicated, *B. anthracis* spores were decoated as previously detailed (19, 124). All spores used in this work were 99% free of vegetative cells and were stored in deionized water at 4°C until analysis.

Mutant strain construction. All strains and plasmids used are listed in Table 3.1, and the primer sequences used for plasmid construction are listed in Table 3.2. Construction of DPBa127, a *B. anthracis* strain expressing YpeB-His_6, was published previously (19). In this strain, the plasmid pDPV424 encoding YpeB-His_6 was integrated into the Δ*ypeB* chromosome. Strains in which the YpeB T202-S203 or A168-S169 cleavage sites were changed to E202-L203 or E168-L169 were created by site-directed mutagenesis of *ypeB* using overlap extension PCR (66). The PCR products were subsequently cloned into pDPV424 through restriction-free cloning (162), generating plasmids encoding $YpeB^{T202E/S203L}$-His_6 (pDPV447) and $YpeB^{A168E/S169L}$-His_6 (pDPV454). To construct a strain in which both cleavage sites had been mutated, pDPV447 was used as template for overlap extension PCR, and the PCR product was cloned into pDPV447, producing pDPV455. Plasmids pDPV447, pDPV454, and pDPV455 were screened for the gain or loss of a restriction site in *ypeB* that was designed as part of the mutagenic primers, and were also verified by DNA sequencing. Plasmids were introduced into

the Δ*ypeB* strain of *B. anthracis* (19) by conjugation, as in the initial steps of the markerless gene replacement procedure (75), and chromosomal integrants were selected by shifting the temperature to 42°C. PCR amplification and sequencing verified plasmid integration within the 500-bp homologous region downstream of Δ*ypeB* in the chromosome and confirmed the presence of the desired cleavage site mutations.

To create a *B. anthracis* Δ*htrC* strain, *htrC* and approximately 500-bp flanking each side of the gene were PCR amplified from chromosomal DNA. The PCR product was inserted into the vector pBKJ236 (75) by digesting with the restriction enzymes BamHI and PstI and ligating the DNA to create pDPV459. Inverse PCR of the plasmid using primers with BglII restriction sites at the 3′ ends resulted in a linear PCR product with the majority of *htrC* deleted, leaving only the first five and last two codons of the gene. Subsequent BglII digestion and ligation of the PCR product produced pDPV460. This plasmid containing the *htrC* deletion was introduced into *B. anthracis* using the markerless gene replacement strategy as previously described (75), except plasmid pSS4332 (21) was used for I-SceI expression in place of pBKJ223. Gene deletion was verified by PCR amplification and sequencing. Complementation of the Δ*htrC* mutation was achieved by introduction and chromosomal integration of pDPV459. To create Δ*sleB* Δ*htrC* and Δ*ypeB* Δ*htrC* double deletion strains, pDPV460 was used to introduce the *htrC* deletion into Δ*sleB* (DPBa38, (64)) and Δ*ypeB* (DPBa89, (19)) strains of *B. anthracis* using the markerless gene replacement strategy (75) with pSS4332 (21). Gene deletions were verified by PCR amplification and sequencing.

To create a *B. subtilis* Δ*htrC* strain, approximately 1000-bp flanking each side of the gene were PCR amplified from chromosomal DNA and linked to the *ermC* Macrolide-Lincosamide-Streptogramin (MLS) antibiotic resistance gene cassette by long-flanking homology PCR (167).

The PCR product was transformed into *B. subtilis* PS832 with selection for MLS resistance to produce DPVB668, in which all but the first 7 and last 8 codons of the *htrC* coding sequence were deleted and replaced by the MLS cassette. Chromosomal DNA from FB111 (117) was transformed into *B. subtilis* DPVB668 with selection for tetracycline resistance to produce DPVB669.

Spore germination assays. The rate of germination and outgrowth of spores in liquid BHI (*B. anthracis*) or 2xYT (*B. subtilis*) was assessed by monitoring the change in optical density at 600 nm (OD) as described previously (19). For germination efficiency assays, spores at an OD of 0.2 were heat activated at 70°C for 20 min and quenched on ice. Heat activated spores were serially diluted in deionized water, plated on BHI or 2xSG medium without antibiotics, and incubated at 37°C overnight. Colonies were counted to determine CFU/OD unit values. Statistical analyses of spore germination rates were performed using unpaired, two-tailed Student's *t*-tests with unequal variance.

Preparation and analysis of spore fractions. Sporangia samples were collected at hours 2 through 6 of sporulation from strains grown in modified G broth, as described previously (19). To prepare germinated spores for western blot analysis, a suspension of dormant spores at a concentration of 5 OD units per ml in 10 mM Tris-HCl pH 7.0 were heat activated at 70°C for 30 min (*B. anthracis*) or 75°C for 30 min (*B. subtilis*) and cooled on ice for 10 min. Chloramphenicol was added to a final concentration of 10 μg/ml to inhibit protein synthesis and 7.5 OD units of spores were removed for the dormant spore sample. The spore suspension was briefly prewarmed before spores were germinated at 37°C with shaking at 250 rpm by the addition of 10 or 100 mM L-alanine with 1 mM inosine (*B. anthracis*) or 10 mM L-valine (*B. subtilis*). Samples equivalent to 7.5 OD units based on the starting OD were collected at various

times after the addition of germinants and centrifuged at 15,800 x *g* for 2 min. The resulting pellets were flash frozen in liquid N_2 and lyophilized.

Dried spores or sporangia were pulverized with 100 mg of 0.1 mm glass beads in a dental amalgamator (Wig-L-Bug) at 4,200 rpm for 20 pulses of 30 s each. Samples were put on ice for at least 30 s between pulses. Proteins were extracted from broken material with 75 μl (dormant and germinated spores) or 100 μl (sporangia) of 1X sample loading buffer (62.5 mM Tris-HCl pH 6.8, 2% SDS, 10% glycerol, 5% β-mercaptoethanol, 0.05% bromophenol blue). Following heating at 100°C for 5 min, extracts were centrifuged at 15,800 x *g* for 1 min, and supernatants were analyzed by western blotting. In some cases, proteins were extracted in sample loading buffer without bromophenol blue and quantified using amino acid analyses (56).

To extract and purify His_6-tagged YpeB cleavage products for N-terminal sequencing, 250 OD units of DPBa127 or DPBa157 spores in a final volume of 100 ml 10 mM Tris-HCl pH 7.0 were heat activated and germinated with 100 mM L-alanine and 1 mM inosine as described above. Spores were germinated for approximately 1 h, or until ≥ 90% of spores had germinated, as determined by phase contrast microscopy. The germinated spores were collected by centrifugation at 10,000 x *g* for 10 min at 4°C and washed with 5 ml Buffer A (50 mM NaCl, 50 mM Tris-HCl pH 7.5, 5% glycerol, 30 mM imidazole). Following another centrifugation, the pellet was resuspended in 5 ml Buffer A, split between 4 microcentrifuge tubes, and centrifuged at 15,800 x *g* for 2 min. The pellets were frozen at -80°C, lyophilized, and broken with glass beads as described above. Proteins were extracted by resuspending and combining samples in a total of 5 ml Buffer B (500 mM NaCl, 50 mM Tris-HCl pH 7.5, 30 mM imidazole, 8M urea) and incubating at 4°C with slow rocking for at least 2 h. The sample was centrifuged at 6,800 x *g* for 10 min at 4°C, and the supernatant containing soluble extracted proteins was filtered and loaded

on a 1-ml Ni-Sepharose HisTrap HP affinity column (GE Healthcare) equilibrated with Buffer B. YpeB cleavage products were eluted with Buffer C (500 mM NaCl, 50 mM Tris-HCl pH 7.5, 500 mM imidazole, 8M urea). To precipitate the affinity-purified cleavage products, deoxycholate and TCA (0.05% and 20% final concentrations, respectively) were added to the pooled elution fractions, which were then incubated on ice overnight. The mixture was centrifuged at 15,000 x *g* for 10 min at 4°C, and the pellet was washed 3 times with 1 ml ice-cold 100% acetone. The pellet was dried and mixed with 25 µl 1X sample loading buffer, and additional 0.5 M Tris-HCl pH 6.8 was added until the sample was blue again.

The entire precipitated sample was run on a SDS-PAGE gel that had first been incubated overnight in 1X Tris-Glycine SDS Running Buffer with 0.1 mM sodium thioglycolate. Sodium thioglycolate scavenges free radicals, thereby protecting the N-termini of proteins from modification. The proteins were transferred to Immobilon-PSQ PVDF membrane (Millipore) in CAPS transfer buffer (10 mM CAPS pH 11.0, 10% methanol), and the membrane was briefly washed with deionized water before being stained with 0.1% Coomassie Brilliant Blue R-250 (Jersey Lab Supply) for 30 s. The membrane was destained repeatedly with 50% methanol until bands were visible. Bands corresponding to YpeB cleavage products were cut from the membrane, washed with deionized water, dried, and stored at -80°C. N-terminal sequencing via automated Edman degradation was performed on extracted bands using an ABI 494 Protein Sequencer (Tufts University Analytical Core Facility).

Western blot analysis. Polyclonal antibodies raised in rabbits against *B. anthracis* SleB and YpeB (19), and monoclonal mouse anti-His (C-term) antibodies (Invitrogen) were used for detection of SleB, YpeB, and derivatives in western blots. Anti-SleB and anti-YpeB antibodies were used at 1:1,000 and 1:3,000 dilutions, respectively, while anti-His antibodies were used at a

1:5,000 dilution. Secondary goat anti-rabbit-HRP antibodies (Bio-Rad) were used at a 1:5,000 (cat. #166-2408) or 1:200,000 (cat. #170-6515) dilution, while goat-anti-mouse-HRP antibodies (PerkinElmer) were used at a 1:5,000 dilution. Western blots utilized Amersham Hybond-P (PVDF) membranes (GE Healthcare), and antibody detection was carried out using colorimetric (BM Blue POD Substrate, Precipitating; Roche) or chemiluminescent (Amersham ECL Prime Western Blotting Detection Reagent; GE Healthcare) substrates.

HtrC and YpeB purification and assay. The *B. anthracis htrC* coding sequence, lacking the first 44 codons containing the predicted transmembrane anchor, was PCR-amplified and introduced into the entry vector pDonR201 (Invitrogen) and then the destination vector pDEST-HisMBP-T (a modified version of pDEST-HisMBP (11) containing a tobacco etch virus (TEV) cleavage site). The resulting plasmid, pDPV458, encoding an N-terminal His_6-tagged maltose binding protein (MBP) fused to a TEV cleavage site and HtrC lacking its signal sequence/membrane anchor, was verified by DNA sequencing. Overexpression strain DPVE501 was cultured at 37°C until the OD reached ~0.8, at which point isopropyl-β-D-thiogalactopyranoside was added to a final concentration of 0.7 mM, the culture temperature was reduced to 12°C, and incubation was continued for 16 h.

Cells were harvested by centrifugation, resuspended in Buffer D (50 mM NaCl, 50 mM Tris-HCl pH 7.5, 5% glycerol, 25 mM imidazole) and lysed using sonication. Soluble and insoluble protein fractions were separated by centrifugation at 117,000 x *g* for 1 h. Soluble His_6-MBP-$HtrC_{45-391}$ was purified using a Ni-Sepharose HisTrap HP affinity column equilibrated with Buffer D. Protein was eluted with a step gradient of Buffer D containing 100 mM increasing concentrations of imidazole and fractions were dialyzed in Buffer D. His_6-MBP-$HtrC_{45-391}$ at a concentration of ~1.5 mg/ml was incubated with 0.5 mg/ml His_6-tagged TEV (S219V) protease

(77) at 15°C for 16 h. Cleavage was verified by SDS-PAGE analysis. $HtrC_{45-391}$ was separated from His_6-TEV, His_6-MBP, and undigested protein using a Ni-Sepharose HisTrap HP affinity column. Fractions containing $HtrC_{45-391}$ were dialyzed in Buffer D, flash frozen, and stored at -80°C. $YpeB_{21-446}$ overexpression and purification was performed as described previously (19).

Protease activity of HtrC was assayed in 50 mM Tris-HCl pH 8.0 with 1 μM $HtrC_{45-391}$ and 6 μM $YpeB_{21-446}$ at 37°C for 4 h, unless indicated otherwise. The reaction was terminated by adding 2X SDS-PAGE sample loading buffer to a final concentration of 1X and incubating at 100°C for 5 min. Proteins were separated using SDS-PAGE and were stained with Coomassie Brilliant Blue.

RESULTS

***B. anthracis* YpeB is proteolytically processed during spore germination.** A previous study indicated that YpeB of *B. subtilis* is proteolytically cleaved during spore germination (36). A *B. anthracis ypeB* deletion mutant was previously complemented with a gene expressing YpeB with a C-terminal His_6 tag (19). This His_6-tagged protein accumulated in spores to an abundance equivalent to that of the wild-type, complemented fully for stabilization of SleB in the dormant spore, and allowed a wild-type germination rate (19). Spores of this *B. anthracis* YpeB-His_6 strain (DPBa127) were germinated and extracted at various times for western blotting to examine YpeB processing. By the 45 min time point, spores had lost at least 50% of their initial OD, and examination by phase-contrast microscopy indicated that > 95% of the spores in each preparation had germinated. Full-length 51 kDa YpeB-His_6 diminished during germination, with the appearance of an abundant stable product at ~28 kDa product and a minor ~32 kDa product (Fig. 3.1, upper panel). The same banding pattern was observed during germination of wild-type *B.*

anthracis spores (not shown). Western blotting of the same YpeB-His_6 germinating spore fragments using anti-His_6 antibodies indicated that the 28 and 32 kDa YpeB fragments possessed the His_6 tag (Fig. 3.1, lower panel), and were therefore C-terminal portions of YpeB. The abundant 28 kDa YpeB-His_6 fragment was purified from germinated spores using metal-affinity chromatography, and the N-terminal sequence was determined to be SAQKN. The sequence indicated cleavage between residues T202 and S203 of YpeB (Fig. 3.2). In an effort to block this specific cleavage event, the *ypeB*-His_6 allele was mutagenized to change residues T202-S203 to E202-L203. The altered YpeB-$^{T202E/S203L}$-His_6 protein accumulated to levels equivalent to YpeB-His_6 in the spore and complemented for SleB stabilization and for germination rate (Figs. 3.3A and 3.4). YpeB-$^{T202E/S203L}$-His_6 protein was not cleaved to the 28 kDa fragment during germination, indicating that the mutation at the cleavage site succeeded in blocking proteolysis, but the stability of full-length YpeB during germination was not increased; rather, the abundance of the 32 kDa product increased (Fig. 3.3A and C). In addition, a small amount of a new ~29 kDa cleavage product, slightly larger than the original 28 kDa fragment, was observed (Fig. 3.3A and C). The 32 kDa product was purified from germinated YpeB-$^{T202E/S203L}$-His_6 spores and the N-terminal sequence was determined to be SNRDP, indicating processing between residues A168 and S169 (Fig. 3.2). Once again, the amino acids flanking this cleavage site were changed by site-specific mutagenesis, allowing the expression of YpeB-$^{A168E/S169L}$-His_6 and YpeB-$^{A168E/S169L,\ T202E/S203L}$-$His_6$. Both of these proteins accumulated to normal levels in the spore (Fig. 3.3B) and both allowed normal spore germination (Fig. 3.4). Western blotting of germinating spore samples indicate that the A168E/S169L change prevented proteolysis at that site (Fig. 3.3B and C). YpeB-$^{A168E/S169L}$-His_6 was instead processed to the dominant 28 kDa fragment (Fig. 3.3B and C). Stable cleavage products were not as strongly detected during germination of YpeB-

$^{A168E/S169L,\ T202E/S203L}$-$His_6$ spores, but the full-length protein still diminished during germination (Fig. 3.3B and C). Two less stable products of ~29 and ~33 kDa were produced (Fig. 3.3B and C).

Identification of candidate *B. anthracis* proteases that might cleave YpeB. A variety of data sources were used to identify a protease, herein called HtrC, as a candidate to be involved in YpeB cleavage. Recent studies of *B. anthracis* and *B. subtilis* spore membrane proteomes indicated that this protease might be associated with the membrane that YpeB is embedded in (Chen, Y. and D.L. Popham, unpublished). A transcriptome study had indicated that *htrC* (BAS5314) was expressed during the latter stages of *B. anthracis* sporulation (18). In *B. subtilis*, the apparent ortholog (*yycK/htrC*) is expressed during sporulation under the control of σ^G, which would place it in the forespore compartment (50) along with *sleB-ypeB* expression (108). Studies of HtrC and paralogs in other species have indicated that these proteases cross and remain associated with the outer surface of the cytoplasmic membrane due to an uncleaved signal sequence/membrane anchor (44). HtrC expressed in the developing spore would therefore be expected to remain on the outer surface of the inner spore membrane, in the same location as YpeB. While multiple proteases in each species possess some properties consistent with a role in YpeB processing, the HtrC proteins of *B. anthracis* and *B. subtilis* were considered the strongest candidates.

Strains lacking HtrC are altered in YpeB proteolysis. *B. anthracis* and *B. subtilis* strains carrying null mutations in *htrC* were constructed, and YpeB cleavage was examined by western blotting using antisera against *B. anthracis* YpeB (19). The *B. anthracis* Δ*htrC* mutant lost full-length YpeB during germination more slowly than the wild-type and did not accumulate the specific 27 and 31 kDa cleavage products (Fig. 3.5A) (These cleavage products are slightly

smaller than those in Fig. 3.1 because they lack the His_6 tag). In some cases, western blots exhibited a heavier background in the 30-50 kDa range for germinating Δ*htrC* spores (Fig. 3.5A), suggested that YpeB might be degraded to non-specific products, but this has not been further confirmed. While the antibodies did not recognize the cleavage products of *B. subtilis* YpeB, the *htrC* mutant maintained increased amounts of full-length YpeB during germination relative to the wild-type strain (Fig. 3.5B).

The germination of *htrC* mutant spores was examined to determine if slowed degradation of YpeB resulted in decreased SleB activity. This was done in *B. anthracis* decoated spores and in a *B. subtilis* Δ*cwlJ* background in order to render the function of SleB more easily observed (55, 63). In both *Bacillus* species, the germination rates of Δ*htrC* spores were not significantly different from those of the wild-type spores (Fig. 3.6A and B). In both species, the colony-forming efficiency of Δ*htrC* spores lacking CwlJ activity was also not different from the corresponding wild-type spores (Table 3.3).

***In vitro* cleavage of YpeB by HtrC**. *B. anthracis* HtrC, lacking its signal sequence/membrane anchor, was expressed in *E. coli* as a His_6-MBP fusion protein and was purified by metal-affinity chromatography. Following purification of His_6-MBP-$HtrC_{45-391}$, the His_6-MBP domain was removed using TEV protease, and $HtrC_{45-391}$ was purified (Fig. 3.7). The pure protease exhibited little activity against a generic substrate (fluorescently-labeled casein, data not shown) and, initially, very little activity against purified *B. anthracis* YpeB (Fig. 3.8, lanes 8, 10, and 15-16). Assay attempts using a wide variety of conditions revealed that HtrC-catalyzed cleavage of YpeB to produce an ~27 kDa fragment, as observed *in vivo*, was greatly stimulated by the presence of Mn^{2+} (Fig. 3.8, lanes 10-13) and, to a lesser degree, by Ca^{2+} (Fig. 3.8, lanes 16-19), but not by Mg^{2+}, Zn^{2+}, Na^{+}, or K^{+} (Fig. 3.8, lanes 1-10). Relatively high

concentrations of Mn^{2+} or Ca^{2+} were required to achieve maximum HtrC activity (Fig. 3.8, lanes 10-13 and 16-19). Metal-stimulated HtrC activity was inhibited by EDTA, a chelator of divalent cations (Fig. 3.8, lanes 16, 18, and 20). The presence of an equimolar concentration of DPA, another strong chelator, blocked the positive effect of Ca^{2+} on HtrC (Fig. 3.8, lanes 22-26). HtrC action on YpeB was found to be maximal at pH 7-9 (data not shown).

HtrC is not an important factor in SleB or YpeB degradation during spore formation. To determine if HtrC is involved in degradation of SleB and/or YpeB in the absence of the partner protein during spore formation, Δ*sleB* Δ*htrC* and Δ*ypeB* Δ*htrC* double mutants were constructed in *B. anthracis*. As demonstrated previously (19), in a Δ*sleB* mutant, YpeB failed to accumulate during spore formation, and in a Δ*ypeB* mutant, SleB did not accumulate (Fig. 3.9A and B). The additional deletion of *htrC* from these strains still resulted in the degradation of YpeB or SleB, respectively, during sporulation (Fig. 3.9), indicating that other proteases are likely active in their degradation during spore formation. Additionally, the production of YpeB during Δ*sleB* Δ*htrC* spore formation coincided with the appearance of YpeB-specific degradation products (Fig. 3.9C), similar to those seen during sporulation of the Δ*sleB* strain (19) and to specific cleavage products seen during spore germination. This finding indicates that, at least during sporulation, other proteases are capable of producing similar cleavage products.

DISCUSSION

B. anthracis YpeB is processed to a relatively stable fragment during germination, as in *B. subtilis* (36). The ultimate N-termini of the stable YpeB fragments were determined to be in a region between an undefined N-terminal YpeB domain and the C-terminal region containing

three putative PepSY domains. This C-terminal fragment persists well into the germination process. The N-terminal cleavage product was observed neither in western blots of germinating spore extracts nor in *in vitro* reactions using purified proteins. While this might be due to poor recognition of this domain by the antiserum and/or poor staining of the domain, it raises the possibility that this domain is subject to more rapid degradation to smaller fragments. Interestingly, the YpeB N-terminal domain was recently shown to exert an inhibitory effect on SleB activity *in vitro* (90). Processing of YpeB could play a role in the activation of SleB during germination.

Deletion of *htrC* was found to result in the disappearance of specific YpeB degradation products in both species, though the amount of full-length YpeB still decreased during germination. This indicates that multiple proteases are active in this region of the spore during germination. The degradation of YpeB during germination may be a multistep process, carried out by multiple proteases, with the ultimate stable products being produced by HtrC. However, initial cleavage of YpeB by another protease is apparently not a requirement for HtrC action, as the action of HtrC was reproducible *in vitro* using purified proteins.

The inability to fully block YpeB degradation during germination precludes demonstration of a role of YpeB instability in SleB activation during germination. Even when YpeB degradation was slowed by the loss of HtrC, the spore germination rate was not significantly affected. Under the experimental conditions tested, germination was dependent on SleB activity (64, 117). A previous study indicated that a 30% decrease in SleB abundance resulted in an observable germination defect (19), so the delay in YpeB degradation observed here must not have inhibited SleB to this degree. This may indicate that YpeB degradation is not required for SleB activation and that YpeB degradation is merely the natural disposal of this

protein following the breakage of spore dormancy. Alternatively, the slowed kinetics of YpeB degradation may not have been sufficient to affect the outward assays of germination progression. Unfortunately, strains in which N-terminal regions of YpeB were deleted, including the identified HtrC cleavage sites and potential upstream cleavage sites, did not retain stable SleB in the dormant spore (19), and thus could not be used to determine what effect a non-cleavable YpeB has on SleB activity during germination.

Alteration of the dominant HtrC cleavage sites in YpeB resulted in the appearance of alternative dominant *in vivo* cleavage sites in the same region of the protein. Several pieces of evidence suggest that the C-terminal domain of YpeB is relatively protease resistant, while the N-terminal domain is more sensitive, and the region linking the domains may be especially sensitive. The N-terminal domain was observed in neither *in vivo* nor *in vitro* experiments where the C-terminal domain could be detected. In the absence of SleB, YpeB is degraded during spore formation, producing dominant cleavage products similar in size to those produced during germination (19). Similar YpeB cleavage products were produced during sporulation of a Δ*sleB* Δ*htrC* mutant, indicating that another protease(s) targets this same region between the YpeB domains. These experiments also revealed that proteases other than HtrC must be involved in the degradation of both YpeB and SleB when produced in the absence of SleB or YpeB, respectively, during spore formation. The use of multiple protease-deficient strains to block SleB and YpeB degradation during sporulation, and potentially during germination, is challenging, as multiple proteases present in the intermembrane space of the developing spore are necessary for proper spore formation (31, 97).

B. anthracis HtrC, expressed and purified from *E. coli*, cleaved YpeB *in vitro* but with relatively poor kinetics. A four-hour digestion was required to achieve catalysis of

approximately three YpeB molecules per HtrC molecule. This activity was dependent on the presence of relatively high concentrations of Mn^{2+} or Ca^{2+} ions. The high ion concentrations required suggests that their function is not directly in catalysis, which is consistent with the absence of a metal role in catalysis by this class of serine protease (38). Interestingly, HtrC action on YpeB coincides closely with the release of a large amount of Ca^{2+}-DPA from the spore core during germination. The local Ca^{2+}-DPA concentration is apparently quite high at this time, as it can activate CwlJ activity, a process that requires > 20 mM Ca^{2+}-DPA (119). While most of the Ca^{2+} released during germination is likely bound to DPA, and our findings indicate that the Ca^{2+}-DPA complex is ineffective in promoting HtrC activity, it is possible that enough free Ca^{2+} is present to increase HtrC activity during germination. Spores also contain significant amounts of Mn^{2+} (59, 150), which is likely complexed with DPA and released during germination, and could thus play a role in stimulating HtrC.

Chemicals that function as protease inhibitors have been shown to block spore germination at different stages, suggesting that protease activity is critical during germination (24-26, 40). While it has not been shown that this activity is actually due to inhibition of a protease rather than another protein function or what specific germination processes are affected, these results raise the possibility that initiation of cortex hydrolysis could require a protease activity. Proteolytic processing of a Clostridial GSLE, SleC, is required for induction of activity during germination, but this GSLE is unrelated to *Bacillus* GSLEs. Further study of the roles of proteases in spore germination, and of their potential direct effect on activation of cortex hydrolysis, may allow the improvement of spore decontamination or application methods.

ACKNOWLEDGEMENTS

Research reported in this publication was supported by the National Institute of Allergy and Infectious Disease of the National Institutes of Health under award number R21AI088298. The content is solely the responsibility of the authors and does not necessarily represent the official views of the National Institutes of Health. We thank Roger Plaut and Scott Stibitz for the gift of plasmid pSS4332. Dr. Florian Schubot contributed reagents and Jessica Blackwood provided laboratory assistance.

Table 3.1. Bacterial strains and plasmids.

Strain or plasmid	Relevant genotype/phenotype [a]	Construction [b]	Source
E. coli			
DPVE13	BL21 (λDE3) pLysS (Cm^r)		Novagen
DPVE501	pDPV458 (His_6-MBP-$HtrC_{45-391}$ Amp^r) Cm^r	pDPV458→DPVE13	This study
B. anthracis			
Sterne 34F2	$pXO1^+$ $pXO2^-$		P. Hanna
DPBa38	Δ*sleB*		(64)
DPBa89	Δ*ypeB*		(19)
DPBa113	Δ*ypeB*::pDPV416 (*ypeB*$^+$ Er^r)		(19)
DPBa127	Δ*ypeB*::pDPV424 (YpeB-His_6 Er^r)		(19)
DPBa157	Δ*ypeB*::pDPV447 (YpeB$^{T202E/S203L}$-His_6 Er^r)	pDPV447→DPBa89	This study
DPBa167	Δ*ypeB*::pDPV454 (YpeB$^{A168E/S169L}$-His_6 Er^r)	pDPV454→DPBa89	This study
DPBa168	Δ*ypeB*::pDPV455 (YpeB$^{A168E/S169L,\ T202E/S203L}$-$His_6$ Er^r)	pDPV455→DPBa89	This study
DPBa178	Δ*htrC*	pDPV460→34F2	This study
DPBa182	Δ*htrC*::pDPV459 (*htrC*$^+$ Er^r)	pDPV459→DPBa178	This study
DPBa187	Δ*sleB* Δ*htrC*	pDPV460→DPBa38	This study
DPBa188	Δ*ypeB* Δ*htrC*	pDPV460→DPBa89	This study
B. subtilis			
PS832	Prototrophic derivative of strain 168		P. Setlow
FB111	Δ*cwlJ*::Tet^r		(117)
DPVB668	Δ*htrC*::MLS^r	PCR→PS832	This study
DPVB669	Δ*cwlJ*::Tet^r Δ*htrC*::MLS^r	FB111→DPVB668	This study
Plasmids			
pBKJ236	Er^r *ori*(Ts)		(75)
pSS4332	Kan^r, I-SceI, AmCyan		(21)
pDEST-HisMBP-T	His_6-MBP, Amp^r Cm^r		F. Schubot
pDPV416	*ypeB*$^+$		(19)
pDPV424	YpeB-His_6		(19)
pDPV447	YpeB$^{T202E/S203L}$-His_6	pBKJ236::Δ*sleB ypeB*$^{T202E/S203L}$-His_6	This study
pDPV454	YpeB$^{A168E/S169L}$-His_6	pBKJ236::Δ*sleB ypeB*$^{A168E/S169L}$-His_6	This study
pDPV455	YpeB$^{A168E/S169L,\ T202E/S203L}$-$His_6$	pBKJ236::Δ*sleB ypeB*$^{A168E/S169L,\ T202E/S203L}$-$His_6$	This study
pDPV458	His_6-MBP-$HtrC_{45-391}$	pDEST-HisMBP-T::*htrC*$_{45-391}$	This study
pDPV459	*htrC*$^+$	pBKJ236::*htrC*	This study
pDPV460	Δ*htrC*	pBKJ236::Δ*htrC*	This study

[a] Cm^r, chloramphenicol resistance; Amp^r, ampicillin resistance; Er^r, erythromycin resistance; Tet^r, tetracycline resistance; MLS^r, macrolide-lincosamide-streptogramin B resistance; *ori*(Ts), temperature-sensitive origin of replication; Kan^r, kanamycin resistance.

[b] Strains were constructed by conjugation or electroporation for *B. anthracis*, or transformation for *B. subtilis*. The designation preceding the arrow is the plasmid or source of donor DNA, while the designation following the arrow is the recipient strain.

Table 3.2. Primer sequences.

Plasmid/Strain constructed	Primer name	Sequence 5′ to 3′ [a]
pDPV447	593	CTTCGGACCTACCTTTGAATTAGCACAAAAAAATAAAAAAGGTGG
	594	CCACCTTTTTTATTTTTTTGTGCTAATTCAAAGGTAGGTCCGAAG
	603	GTCTTCTTTACATAAAAGCGAGCCTTTTACAAAACATAACC
	604	GCTTTACGTTCTTCCATAACTTTCACATCTGGATTG
pDPV454	605	GTTGAGATGGCACTCGAGTTAAATCGTGATCCTGCCG
	606	CGGCAGGATCACGATTTAACTCGAGTGCCATCTCAAC
	603, 604	
pDPV455	603, 604, 605, 606	
pDPV458	612	***GTGGAGAACCTGTACTTCCAGGGT***TCAAATGATACGGGCGC
	613	*CCACTTTGTACAAGAAAGTTGCATT*TTAATACTTTTGAATGCCTAGTTTAAC
pDPV459	614	CGCGGATCCGATATTGAGGTCGAGTCATTTG
	615	CGCCTGCAGCAATGACATGCGTATCATCAG
pDPV460	616	CGCAGATCTAAAGGACATATTTGTTCACCTATC
	617	CGCAGATCTAAGTATTAAAAACAGGAGGGCCTAC
DPVB668	607	ACAAGTACGCAGGTGCTGGC
	608	CGATTATGTCTTTTGCGCAGTCGGCCCTCACGTTCGTAATCCACC
	609	GAGGGTTGCCAGAGTTAAAGGATCCCTCCGCAGACCAATTAGGC
	610	GATACACCGATTGACGTACG

[a] Restriction sites are underlined, TEV cleavage site regions of pDEST-HisMBP-T are italicized and in bold, and *att*R2.1 regions of pDEST-HisMBP-T are italicized and underlined.

Table 3.3. Germination efficiencies of Δ*htrC B. anthracis* and *B. subtilis* spores.

Species	Strain	Genotype	CFU/OD_{600} [a]
B. anthracis	DPBa2	WT	6.7×10^7
	DPBa178	Δ*htrC*	6.0×10^7
	DPBa182	*htrC*$^+$	6.3×10^7
B. subtilis	PS832	WT	1.7×10^8
	FB111	Δ*cwlJ*	3.0×10^8
	DPVB668	Δ*htrC*	1.9×10^8
	DPVB669	Δ*cwlJ* Δ*htrC*	2.0×10^8

[a] Decoated spores were used for *B. anthracis* studies. Values are averages of three independent spore preparations.

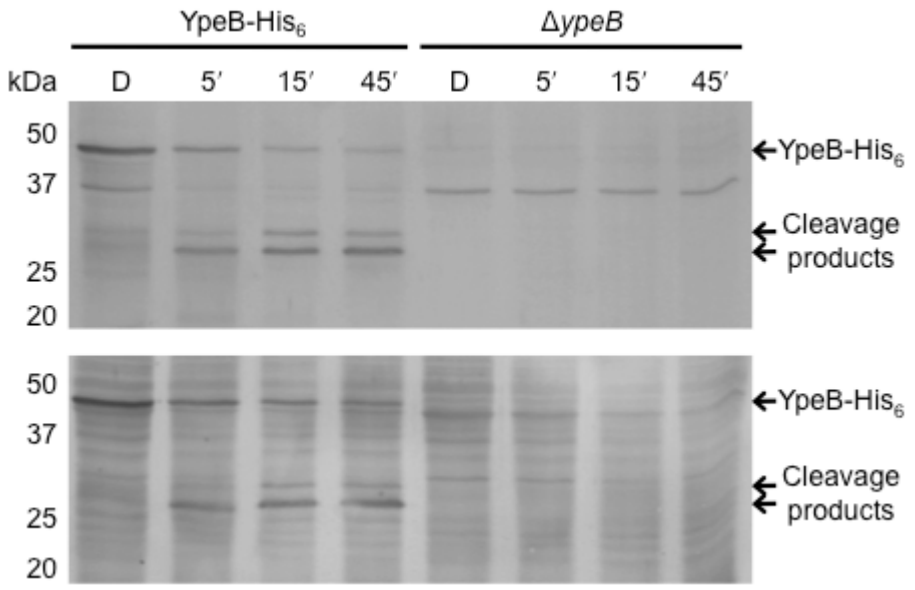

Figure 3.1. YpeB is cleaved during germination of *B. anthracis* spores. Dormant (D) DPBa127 (YpeB-His_6) and DPBa89 (Δ*ypeB*) spores were germinated with 100 mM L-alanine and 1 mM inosine at 37°C, and samples were collected at 5 (5′), 15 (15′), and 45 (45′) min. Extracted proteins were probed with anti-YpeB (top panel) and anti-His_6 (bottom panel) antibodies. The predicted molecular weight of YpeB-His_6 is 51 kDa. The positions of the molecular weight marker proteins (not shown) are indicated on the left.

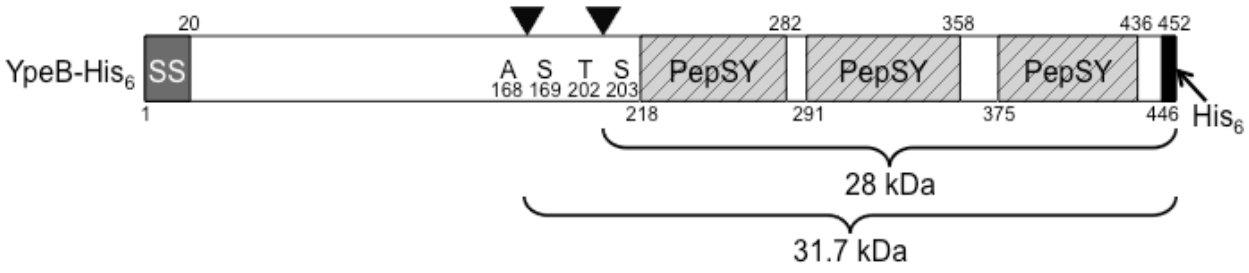

Figure 3.2. Locations of major *B. anthracis* YpeB cleavage sites. Scale drawing of the domain architecture of YpeB showing the N-terminal signal sequence (SS), C-terminal PepSY domains, and YpeB cleavage sites (▼) with predicted molecular weights of C-terminal cleavage products. Residue numbers designate amino acid positions of domain boundaries and positions of YpeB cleavage during spore germination.

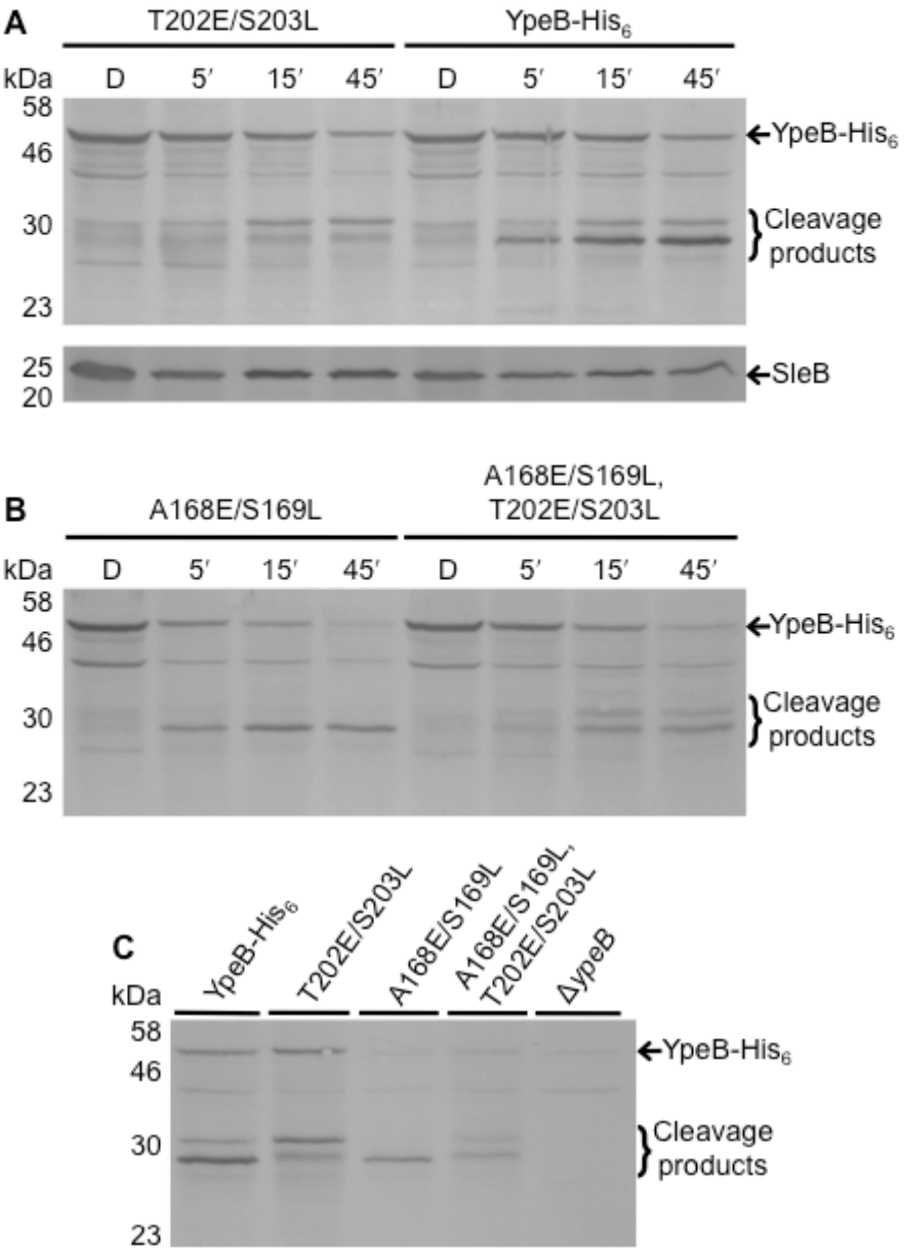

Figure 3.3. YpeB cleavage during germination of *B. anthracis* mutant spores. Dormant (D) spores were germinated with 100 mM L-alanine and 1 mM inosine at 37°C, and samples were collected at 5 (5′), 15 (15′), and 45 (45′) min. (A) DPBa157 (T202E/S203L) and DPBa127 (YpeB-His_6) sample extracts probed with anti-YpeB (top panel) and anti-SleB (bottom panel) antibodies. (B) DPBa167 (A168E/S169L) and DPBa168 (A168E/S169L, T202E/S203L) sample extracts were probed with anti-YpeB antibodies. (C) Extracts from 45 min-germinated spores from each strain were probed with anti-YpeB antibodies. The predicted molecular weight of YpeB-His_6 and derivatives is approximately 51 kDa. The positions of the molecular weight marker proteins (not shown) are indicated on the left.

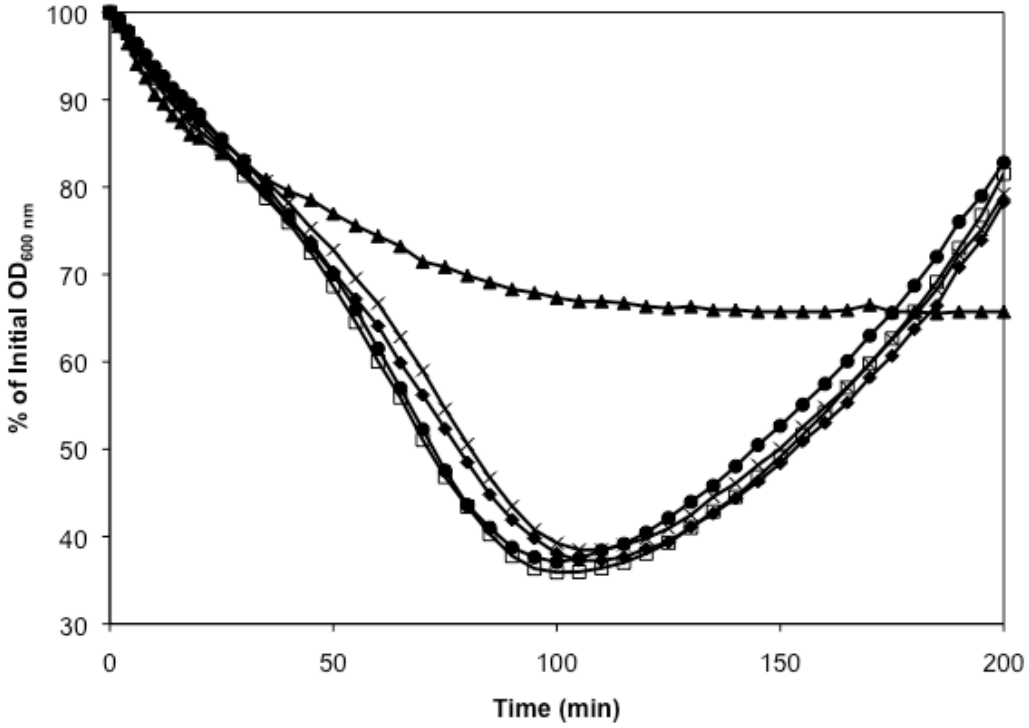

Figure 3.4. Altered YpeB proteolysis does not slow spore germination and outgrowth. Decoated Δ*ypeB* (▲), YpeB$^{T202E/S203L}$-His$_6$ (□), YpeB$^{A168E/S169L}$-His$_6$ (◆), YpeB$^{A168E/S169L, T202E/S203L}$-His$_6$ (×), and YpeB-His$_6$ (●) *B. anthracis* spores were heat activated and germinated in BHI medium at 37°C; germination and outgrowth were tracked as changes in OD. Data shown are averages of results from three independent spore preparations; error bars are omitted for clarity. Germination of YpeB$^{T202E/S203L}$-His$_6$, YpeB$^{A168E/S169L}$-His$_6$, and YpeB$^{A168E/S169L, T202E/S203L}$-His$_6$ spores is not significantly different ($P > 0.06$) at any time point. Likewise, germination of YpeB-His$_6$ and YpeB$^{T202E/S203L}$-His$_6$ spores is not significantly different ($P > 0.07$) at any time point. Focusing on stage II of germination, from 45 to 95 min (19), YpeB$^{A168E/S169L}$-His$_6$ and YpeB-His$_6$ spores do not significantly differ ($P > 0.07$), whereas YpeB$^{A168E/S169L, T202E/S203L}$-His$_6$ and YpeB-His$_6$ spores are not significantly different ($P > 0.05$), except from 75 to 80 min ($P < 0.05$).

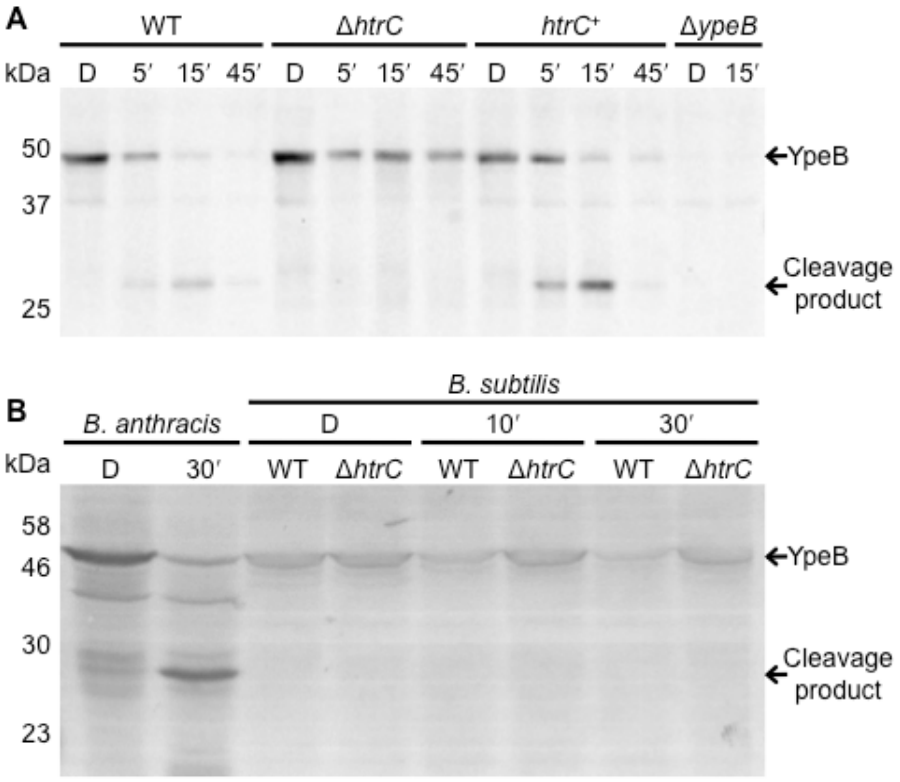

Figure 3.5. HtrC cleaves YpeB during germination of *B. anthracis* and *B. subtilis* spores. Spores were prepared, germinated, and analyzed by western blot with *B. anthracis* anti-YpeB antibodies as described in materials and methods. (A) *B. anthracis* spores were dormant (D) or collected 5 (5′), 15 (15′), and 45 (45′) min after addition of germinants. Strains were DPBa2 (WT), DPBa178 (Δ*htrC*), DPBa182 (*htrC*$^{+}$), and DPBa89 (Δ*ypeB*). (B) *B. anthracis and B. subtilis* spores were dormant (D) or collected 10 (10′) and 30 (30′) min after addition of germinants. Strains were DPBa2 (*B. anthracis* WT), PS832 (*B. subtilis* WT), and DPVB668 (*B. subtilis* Δ*htrC*). The predicted molecular weights of YpeB from *B. anthracis* and *B. subtilis* are 50 and 51 kDa, respectively. The positions of the molecular weight marker proteins (not shown) are indicated on the left.

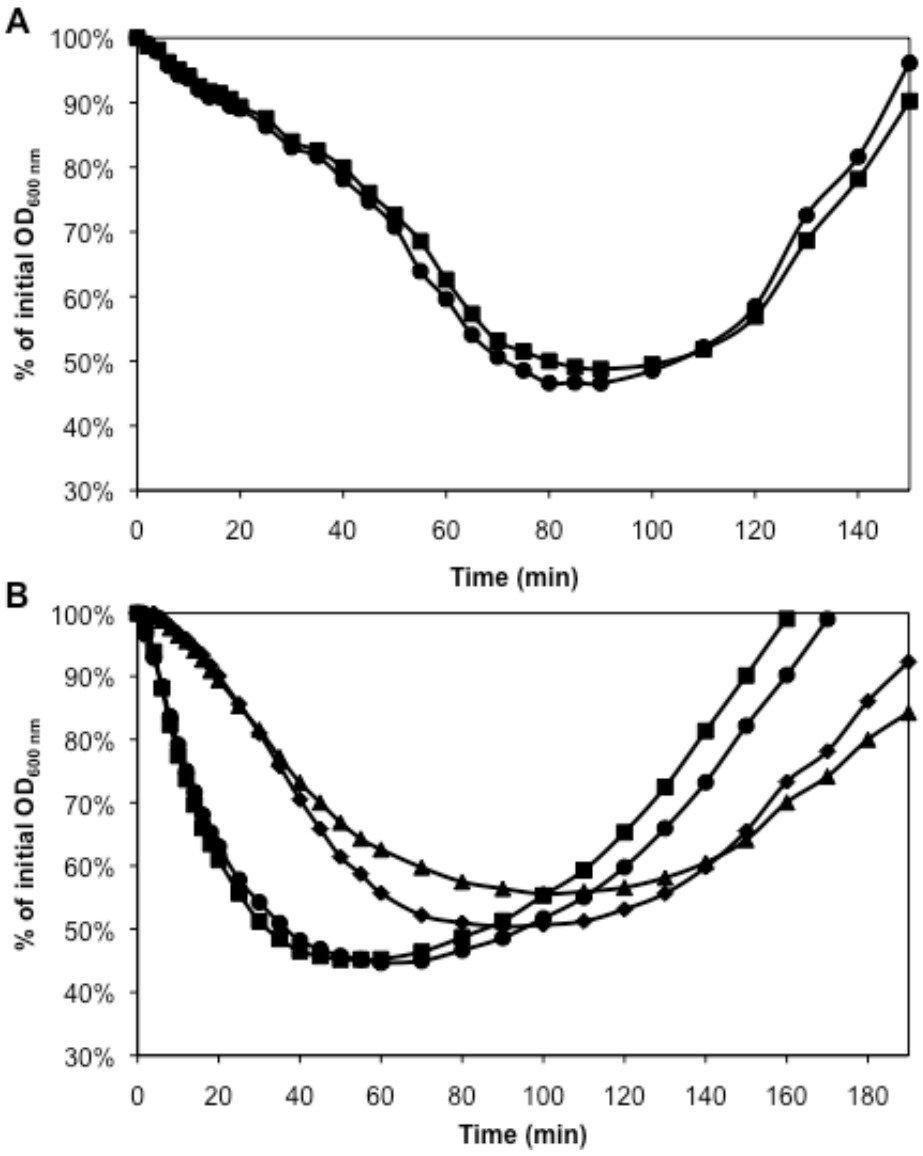

Figure 3.6. Loss of HtrC does not alter the germination rates of *B. anthracis* and *B. subtilis* spores. Spores were heat activated and germinated in rich medium as described in materials and methods; germination and outgrowth were tracked as changes in OD_{600}. Data shown are averages of results from three (*B.anthracis*) or two (*B. subtilis*, preliminary results) independent spore preparations; error bars are omitted for clarity. (A) *B. anthracis* wild-type (DPBa2, ■) and Δ*htrC* (DPBa178, ●) spores were decoated and germinated in BHI broth. The two strains were not statistically different from one another ($P > 0.3$) at any time point. (B) *B. subtilis* wild-type (PS832, ■), Δ*cwlJ* (FB111, ◆), Δ*htrC* (DPVB668, ●), and Δ*cwlJ* Δ*htrC* (DPVB669, ▲) spores were germinated in 2xYT broth. Wild-type and Δ*htrC* strains were not significantly different, and Δ*cwlJ* and Δ*cwlJ* Δ*htrC* strains were not significantly different ($P > 0.19$) at any time point. The two Δ*cwlJ* strains were not significantly different from the two $cwlJ^+$ strains ($P > 0.05$) at any time point.

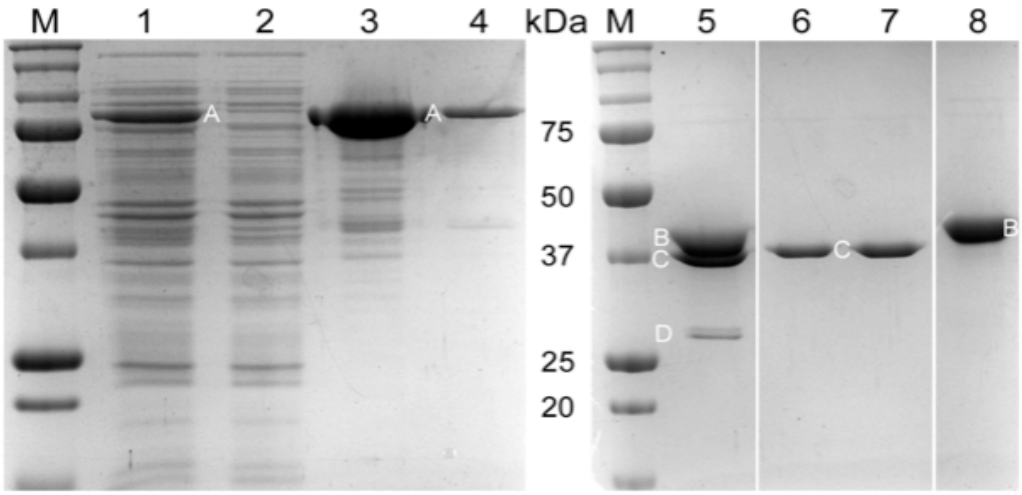

Figure 3.7. Purification of *B. anthracis* HtrC. A His_6-MBP-$HtrC_{45-391}$ fusion protein was overexpressed in *E. coli*, purified by metal-affinity chromatography, cleaved with TEV protease, and separated from the His_6-MBP tag and His_6-TEV using a second metal-affinity column. Samples were soluble protein extracts of induced (lane 1) and uninduced cells (lane 2), eluate fractions from the metal-affinity column containing His_6-MBP-$HtrC_{45-391}$ (A) (lanes 3 and 4), His_6-MBP-$HtrC_{45-391}$ digested with His_6-TEV protease (D) (lane 5), flow-through fractions from the second metal-affinity column containing $HtrC_{45-391}$ (C) (lanes 6 and 7), and eluate from the second metal-affinity column containing His_6-MBP (B) (lane 8). Lanes 1-4 and 5-8 are from two different gels; intervening lanes between 5-6 and 7-8 were removed for clarity. Masses of standard proteins (M) are indicated in the center.

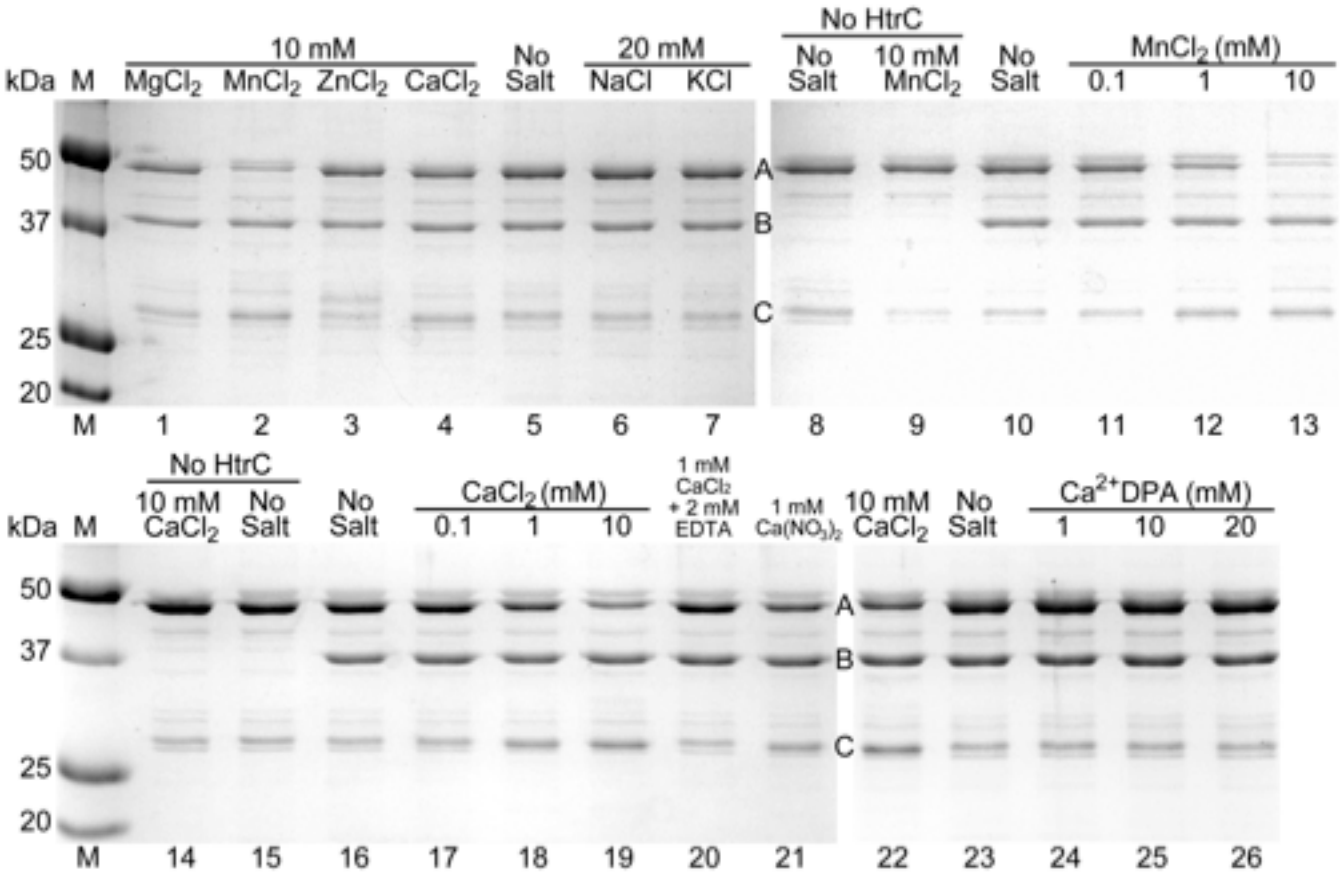

Figure 3.8. *In vitro* cleavage of YpeB by HtrC. Purified $YpeB_{21\text{-}446}$ (A) (6 μM) was incubated for 4 h with purified $HtrC_{45\text{-}391}$ (B) (1 μM), unless otherwise indicated, with the indicated small molecule additions. Reactions were terminated using SDS and heat. Samples were separated by SDS-PAGE and proteins, including the YpeB cleavage product (C), were detected by staining with Coomassie Brilliant Blue. Protein concentrations were 12 μM $YpeB_{21\text{-}446}$ and 2 μM $HtrC_{45\text{-}391}$ in lanes 22-26. Lanes 1-7, 8-13, and 14-21, and 22-26 are from four different gels. Masses of standard proteins (M) are indicated on the left.

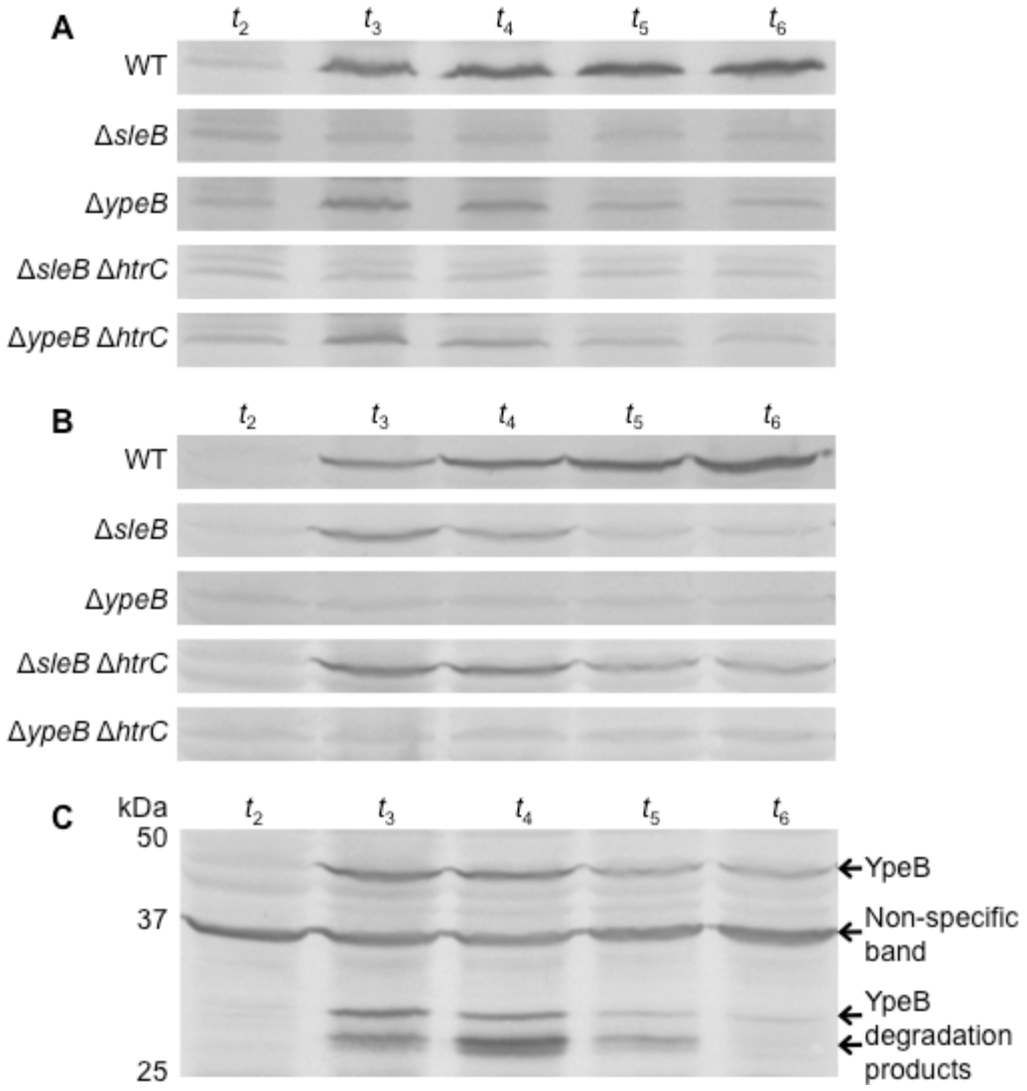

Figure 3.9. SleB and YpeB production during sporulation. Wild-type (WT), Δ*sleB*, Δ*ypeB*, Δ*sleB* Δ*htrC*, and Δ*ypeB* Δ*htrC* strains of *B. anthracis* were grown in modified G broth at 37°C, and sporangia collected during sporulation were subjected to western blot analysis. Labels t_2 through t_6 designate hours since the initiation of sporulation. (A) Sporangia probed with anti-SleB antibodies. (B) Sporangia probed with anti-YpeB antibodies. (C) Sporangia from the Δ*sleB* Δ*htrC* strain probed with anti-YpeB antibodies. The positions of the molecular weight marker proteins (not shown) are indicated on the left.

CHAPTER 4

The Ger receptors are not required for activation of the cortex lytic enzyme SleB during germination of *Bacillus subtilis* spores

Casey B. Bernhards and David L. Popham

ATTRIBUTIONS

Casey B. Bernhards performed the research and writing of the material presented herein, including spore preparation and germination experiments, and preparation of samples for HPLC analyses. Yan Chen operated the mass spectrometer. David L. Popham performed the HPLC analyses and was the principle investigator.

ABSTRACT

The natural process whereby bacterial spores germinate and become vegetative cells is triggered by the interaction of nutrient germinants with Ger receptors at the inner spore membrane. This event initiates a cascade, which includes the eventual degradation of cortex peptidoglycan by germination-specific lytic enzymes (GSLEs). Spores can also be made to germinate with non-nutrient germinants, such as exogenous Ca^{2+}-DPA and dodecylamine, although the Ger receptors are bypassed in these instances. Regardless of germination method, cortex hydrolysis is required for resumption of metabolism, making the activity of GSLEs paramount to the germination process. The GSLE SleB in *Bacillus* spores is one of two partially redundant enzymes responsible for the majority of cortex depolymerization. Unlike the other enzyme, CwlJ, it is unknown how SleB is activated during spore germination. One potential theory, made possible by the localization of both Ger receptors and SleB to the inner membrane of the spore, suggests that SleB activation is Ger receptor-dependent. To test this hypothesis, the current study utilized strains of *Bacillus subtilis* lacking all functional Ger receptors and/or GSLEs. Spores were germinated with L-alanine, Ca^{2+}-DPA, or dodecylamine, and released cortex fragments were analyzed by HPLC and mass spectrometry to identify products specific to SleB activity. During germination by non-nutrient means, SleB products were produced in the absence of Ger receptors and/or CwlJ, indicating SleB can be activated independent of these proteins.

INTRODUCTION

In nature, members of *Bacillus* and *Clostridium* transition between vegetative and spore forms when conditions are favorable and unfavorable, respectively, for growth. Unlike vegetative cells, spores are extremely resilient structures that are resistant to an array of environmental stresses (112, 147, 148). These resistance characteristics have made spore decontamination a challenge in hospitals, food production facilities, and sites following an act of bioterrorism. Spores are metabolically dormant, yet they are capable of sensing environmental cues to indicate that growth-permitting conditions have returned. The process whereby spores become vegetative cells again is known as germination and is stimulated by the interaction of nutrient germinants with (Ger) receptors located at the inner spore membrane (15, 70, 105, 118, 139). These nutrient germinants are small molecules like amino acids, sugars, and purine nucleosides (57). The series of germination events following Ger receptor activation can be divided into two stages. First, ions and pyridine-2,6-dicarboxylic acid (dipicolinic acid, DPA) as a 1:1 chelate with Ca^{2+} (Ca^{2+}-DPA) are released from the spore core, while the core partially rehydrates with water (147). Second, germination-specific lytic enzymes (GSLEs) are activated, preferentially degrading a thick layer of peptidoglycan (PG) known as the cortex (147). The cortex functions to maintain spore dehydration, and therefore contributes to spore dormancy and resistance properties (54, 148). Thus, cortex depolymerization is not only necessary for the spore to fully rehydrate and resume metabolism, but it also results in vulnerable cells (144).

GSLEs can be classified as either spore cortex lytic enzymes (SCLEs) or cortex fragment lytic enzymes (CFLEs). SCLEs degrade intact cortex PG, and thus, play the predominant role in cortex hydrolysis, while CFLEs play an auxiliary role degrading or modifying PG fragments first generated by SCLEs (94). How GSLEs, specifically SCLEs, are activated has been a research

area of interest, since activating GSLEs at a high efficiency would result in cells that are readily killed. In *Clostrium* species, SleC is the only functional SCLE (28, 83, 122), and this enzyme is proteolytically activated by one or more Csp proteases (101, 123, 149), although how this processing is regulated is unknown. *Bacillus* species possess two partially redundant SCLEs: CwlJ (CwlJ1 in *B. anthracis*) and SleB (64, 74, 145). *B. anthracis* also contains a second CwlJ homolog, CwlJ2, but this GSLE appears to play only a minor role during germination (55, 63, 64). CwlJ is activated during germination, either directly or indirectly, by Ca^{2+}-DPA released from the spore core (117), while the mechanism by which SleB becomes active has eluded researchers. SleB, a lytic transglycosylase (23, 37, 64), is present in its mature form in the dormant spore (69, 108-110), thus proteolytic processing is not needed for activation. SleB is also not activated by Ca^{2+}-DPA; spores possessing SleB as the only SCLE do not germinate with exogenous Ca^{2+}-DPA (63, 117, 145), and SleB can become spontaneously activated in spores lacking endogenous DPA (117). One suggested model for SleB activation posits that SleB is activated in a receptor-dependent manner, either directly or indirectly by Ger receptors (36, 117, 147). In contrast to CwlJ, which localizes to the spore coats (13), placement of SleB at the inner spore membrane (36) puts SleB in the vicinity of the Ger receptors and makes such an interaction more feasible. Other models put forth for SleB activation involve changes in the stress of cortex PG during germination (52, 117, 147), changes in the fluidity to the inner membrane (125), or regulation of SleB activity by YpeB—a protein required for stable incorporation of SleB within the dormant spore (19, 36, 90) (Chapter 3).

While nutrient germinant binding to Ger receptors is likely the natural process by which germination is initiated, spores can also be triggered to germinate by alternate means. Exogenous Ca^{2+}-DPA (135) and cationic surfactants, such as dodecylamine (136, 137), are two

well-studied non-nutrient germinants that bypass interaction with Ger receptors in *Bacillus* (119, 143). Like the efflux of endogenous Ca^{2+}-DPA from the core during nutrient germination, exogenous Ca^{2+}-DPA stimulates germination by activating CwlJ (CwlJ1/CwlJ2) (63, 117, 145). Dodecylamine appears to trigger germination by opening SpoVA Ca^{2+}-DPA channels in the inner membrane (164). Utilizing these alternative methods of germination, as well as strains of *B. subtilis* without functional Ger receptors and/or GSLEs, the present study investigates the requirement of Ger receptors for SleB activation. It is concluded that SleB is activated in a manner that is independent of both Ger receptors and CwlJ, thus, shortening the list of possible ways by which SleB is activated for cortex degradation during spore germination.

MATERIALS AND METHODS

Bacterial strains and growth conditions. All *B. subtilis* strains used in this study are derivatives of strain 168 and are listed in Table 4.1. Strains were constructed by transformation (3) and grown in rich medium or on agar plates (LB, 2xYT, or 2xSG (87)) supplemented with 10 μg/ml tetracycline, 100 μg/ml spectinomycin, 3 μg/ml chloramphenicol, and/or 0.5 μg/ml erythromycin plus 12.5 μg/ml lincomycin, where appropriate. Spores were prepared in 2xSG broth without antibiotics. After 4 days of incubation at 37°C with aeration, spores were harvested and repeatedly washed with deionized water over several days. Remaining vegetative cells were heat killed at 65°C for 25 min. Spores were stored in deionized water at 4°C until analysis. All spore preparations were deemed > 95% free of vegetative cells by microscopic examination.

Spore germination. For spore germination via the nutrient germinant L-alanine, 50 OD units of spores in water were heat activated at 70°C for 30 min and quenched on ice for 5 min.

Heat activated spores were pelleted at 6,800 x *g* for 15 min at 4°C and resuspended in 5 ml 4 mM L-alanine. Following a 20 min incubation at 37°C, spores were centrifuged at 6,800 x *g* for 5 min at room temperature and resuspended in 5 ml 10 mM Tris-HCl pH 8.0. Spores were allowed to germinate at 37°C for an additional 100 min. Spore germination with 50 mM Ca^{2+}-DPA pH 8.0 was performed as described for L-alanine, except spores were not heat activated prior to germination. Germination by dodecylamine was initiated by resuspending 50 OD units of spores that were not heat activated in 5 ml 1 mM dodecylamine 20 mM KPO_4 pH 7.0. Unlike germination with L-alanine or Ca^{2+}-DPA, the buffered dodecylamine solution was not removed, and germination proceeded for 4 h at 37°C. Germination efficiency by all three germinants was assessed by phase-contrast microscopy following incubation.

Preparation of muropeptides and analysis. Following spore germination, cortex-derived muropeptides released to the exudate were purified and prepared for reverse-phase high pressure liquid chromatography (RP-HPLC) analysis. Pellet and exudate (supernatant) fractions were first separated by centrifugation at 15,800 x *g* for 2 min at room temperature. All exudates were lyophilized, and exudates from spores germinated with dodecylamine were resuspended in 500 µl H_2O and extracted three times with 500 µl of a 24:1 solution of choloform:isoamyl alcohol to remove the dodecylamine. During each extraction, samples were vortexed for 30 s, centrifuged at 15,800 x *g* for 3 min, and the aqueous (top) layer containing muropeptides was retained for subsequent steps. Half of each exudate fraction was digested with the muramidase Mutanolysin (Sigma) for 16 h at 37°C, as described previously (47, 124). Insoluble material was removed by centrifugation, and soluble muropeptides were lyophilized, resuspended in 0.25 M $Na_2B_4O_7$ pH 9.0, and reduced with $NaBH_4$ prior to HPLC analysis, as described previously (124). Muropeptides were separated as described (124). Muropeptides were collected and

purified using an acetonitrile:TFA gradient as described (124), and were analyzed by MALDI-TOF-TOF mass spectrometry as described (67).

RESULTS AND DISCUSSION

B. subtilis contains three functional operons encoding Ger receptors: *gerA*, *gerB* and *gerK* (119). The *gerA* proteins are needed for spores to germinate in response to L-alanine as the sole germinant, while genes in the *gerB* and *gerK* operons encode proteins required for spores to germinate in a mixture of asparagine, glucose, fructose, and potassium ions (AGFK) (106). Deletion of all three operons in a single strain (FB72) was previously shown to abolish germination in response to nutrients present in rich media (119), while still allowing a normal germination response with Ca^{2+}-DPA (117) or dodecylamine (143). Results from these earlier studies indicate that the mechanism of spore germination via Ca^{2+}-DPA or dodecylamine is independent of the Ger receptors. Additionally, it has been shown that Ca^{2+}-DPA initiates germination by activating the GSLE CwlJ (117), while dodecylamine opens Ca^{2+}-DPA channels in the inner membrane and can trigger germination without CwlJ and/or SleB (143, 164).

Using these alternative spore germination strategies, the work conducted in the present study sought to support or expel a potential model where SleB activation is dependent on Ger receptors. *B. subtilis* spores lacking all functional Ger receptors, and in combination with either a *sleB* or *cwlJ* deletion, were germinated with L-alanine, Ca^{2+}-DPA, or dodecylamine. Following germination, cortex muropeptides were analyzed for SleB activity by RP-HPLC. As expected, spores lacking *gerA*, *gerB*, and *gerK* (FB72, DPVB626, and DPVB627) did not germinate with L-alanine (data not shown), while spores without CwlJ (FB111 and DPVB627) did not germinate with Ca^{2+}-DPA (Fig. 4.1 and data not shown); therefore, muropeptides were

not released into the exudate. When germinated with L-alanine, wild-type spores (PS832), and those lacking SleB (FB110) or CwlJ (FB111) displayed muropeptide profiles similar to those published previously (data not shown) (8, 23, 36). Comparisons of muropeptide profiles between spores with and without SleB, led to identification of peaks corresponding to potential SleB-specific products. A muropeptide presumably resulting from SleB activity was collected and analyzed by mass spectrometry. The muropeptide produced a sodiated ion with m/z of 1362.2, which is consistent with the structure of muropeptide G9, anhydro-tetrasaccharide-tetrapeptide (Fig. 4.2), which was previously shown to result from SleB lytic transglycosylase activity (10). These results confirm that the collected peak is the result of SleB activity on cortex PG.

The aforementioned SleB-specific muropeptide was released from PS832 spores during germination with Ca^{2+}-DPA (Fig. 4.1), and from PS832 and FB111 spores germinated with dodecylamine (Fig. 4.3), but not from FB110 spores (Figs. 4.1 and 4.3). The presence of this product during germination of spores with Ca^{2+}-DPA or dodecylamine, and its absence in SleB-deficient spores, shows that SleB is active during germination by these non-nutrient means. While not an entirely surprising finding, it had previously never been conclusively shown that SleB becomes active during germination by these methods. In *B. subtilis* (117), *B. megaterium* (145), and *B. anthracis* (63), SleB-deficient spores germinate with Ca^{2+}-DPA similarly to wild-type spores, and spores possessing SleB as the only SCLE fail to germinate in response to Ca^{2+}-DPA. Based on results obtained during these earlier studies, it was possible that CwlJ (CwlJ1/CwlJ2) was the only active SCLE during Ca^{2+}-DPA-induced germination. During spore germination with dodecylamine, SleB and/or CwlJ are not required; however, the cortex is normally degraded as part of the dodecylamine germination process (143). The specific

enzymatic activities resulting in cortex hydrolysis during germination with dodecylamine had not been previously identified, so once again, it was feasible that CwlJ (CwlJ1/CwlJ2) alone was responsible. Results from the current study show that SleB is indeed active in spores germinated with Ca^{2+}-DPA or dodecylamine.

The SleB-specific muropeptide G9 was also observed following germination of FB72 spores with Ca^{2+}-DPA (Fig. 4.1) and dodecylamine (Fig. 4.3). Since these strains lack all functional Ger receptors, the major conclusion of this work is that SleB is capable of being activated independent of the Ger receptors. While there remains a possibility that SleB is activated by a different mechanism during nutrient versus non-nutrient germination, this finding strongly suggests that SleB is not directly activated by the Ger receptors during nutrient germination. The presence of lytic transglycosylase products in the exudates of DPVB627 spores germinated with dodecylamine (Fig. 4.3) also indicates that SleB can be activated independent of both Ger receptors and CwlJ. It has been well established during nutrient-induced germination that SleB is capable of completing cortex hydrolysis without CwlJ (74, 117, 145) or CwlJ1 (55, 63, 64); however, should an alternative activation strategy exist for SleB during non-nutrient germination, CwlJ is also not required.

ACKNOWLEDGEMENTS

We thank an NSF-REU supported student, Megan Silbaugh, who assisted with strain construction and analysis. We also thank Yan Chen for operating the mass spectrometer.

Table 4.1. *B. subtilis* strains.

Strain	Genotype/Phenotype [a]	Construction [b]	Source
PS832	Wild-type		P. Setlow
FB110	Δ*sleB*::Tet^r		(117)
FB111	Δ*cwlJ*::Tet^r		(117)
FB72	Δ*gerA*::Sp^r, Δ*gerB*::Cm^r, Δ*gerK*::MLS^r		(119)
DPVB626	Δ*gerA*::Sp^r, Δ*gerB*::Cm^r, Δ*gerK*::MLS^r, Δ*sleB*::Tet^r	FB110→FB72	This study
DPVB627	Δ*gerA*::Sp^r, Δ*gerB*::Cm^r, Δ*gerK*::MLS^r, Δ*cwlJ*::Tet^r	FB111→FB72	This study

[a] Tet^r, tetracycline resistance; Sp^r, spectinomycin resistance; Cm^r, chloramphenicol resistance; MLS^r, macrolide-lincosamide-streptogramin B resistance.

[b] Strains were constructed by transformation. The designation proceeding the arrow is the source of donor chromosomal DNA, while the designation following the arrow is the recipient strain.

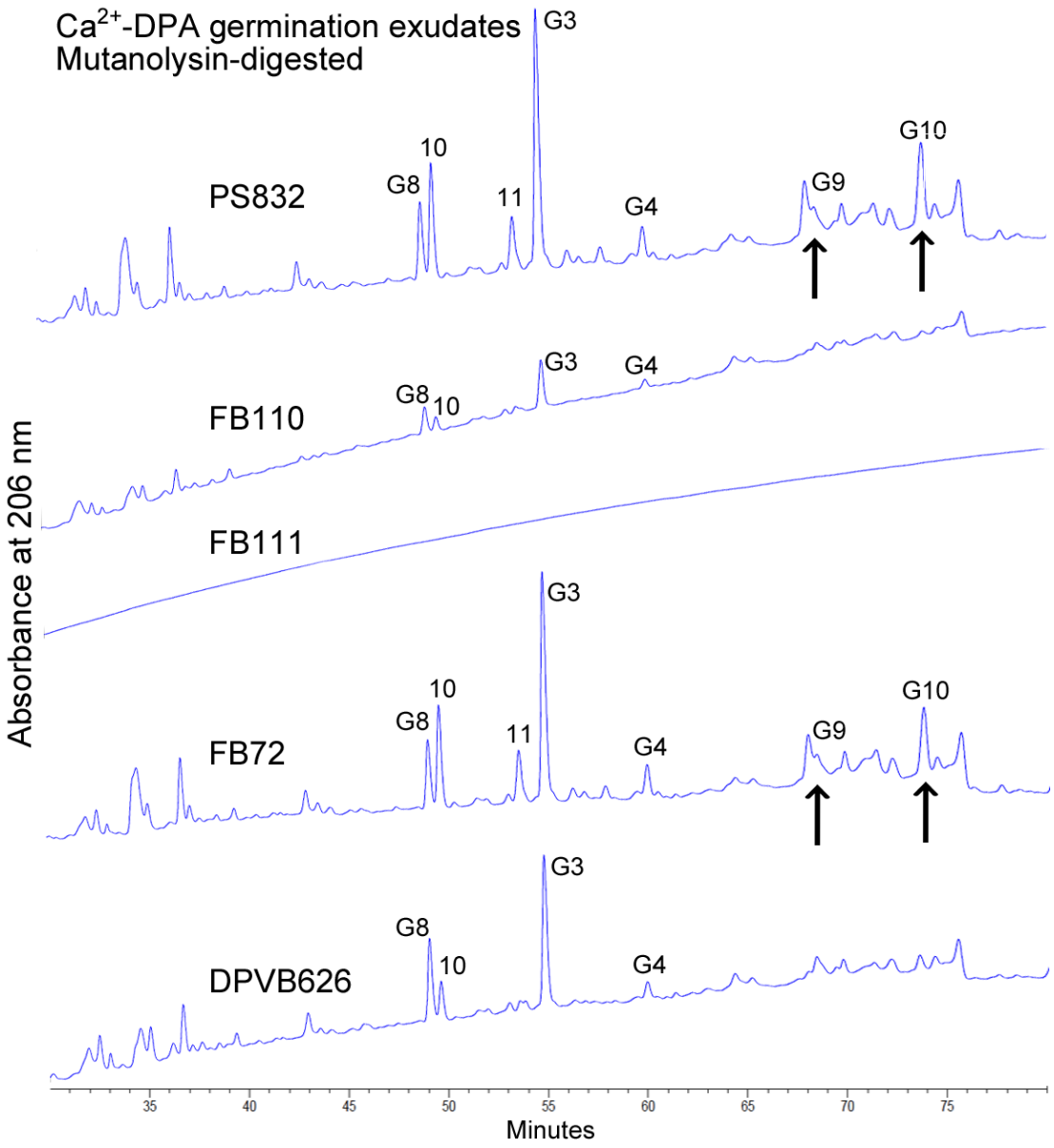

Figure 4.1. HPLC separation of Ca^{2+}-DPA germination exudate muropeptides. Spores were germinated for 120 min with 50 mM Ca^{2+}-DPA. Exudates were concentrated, digested with Mutanolysin, reduced, and separated using HPLC. Peaks are numbered as in (10). Muropeptides G9 and G10, products of SleB activity, are indicated by arrows. Muropeptide G9 was identified by mass spectrometry. DPVB627 and FB111 spores both lack *cwlJ* and do not germinate with Ca^{2+}-DPA; thus, DPVB627 results are omitted.

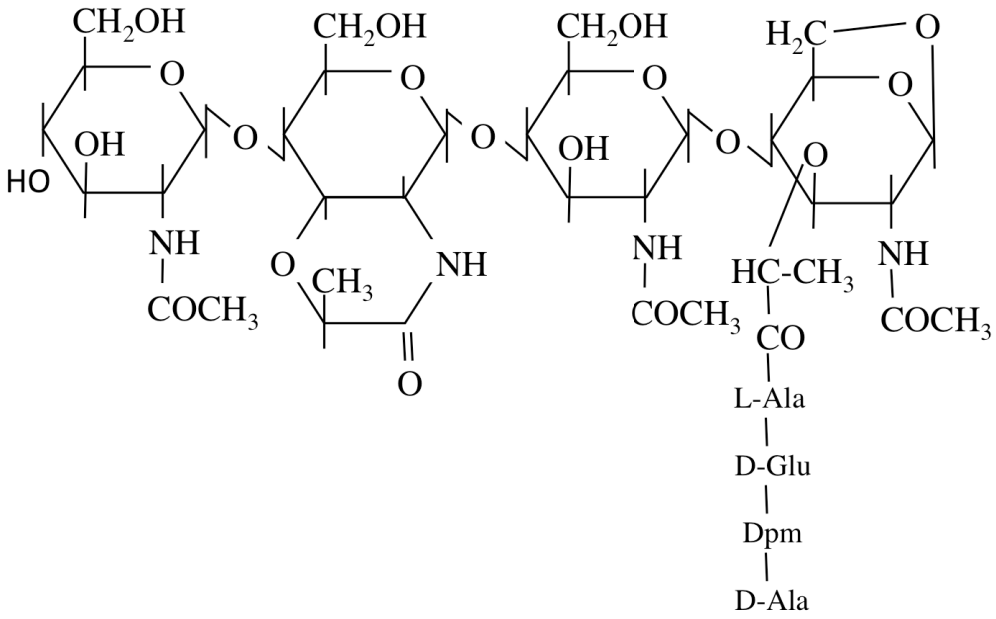

Figure 4.2. Structure of muropeptide G9: anhydro-tetrasaccharide-tetrapeptide.

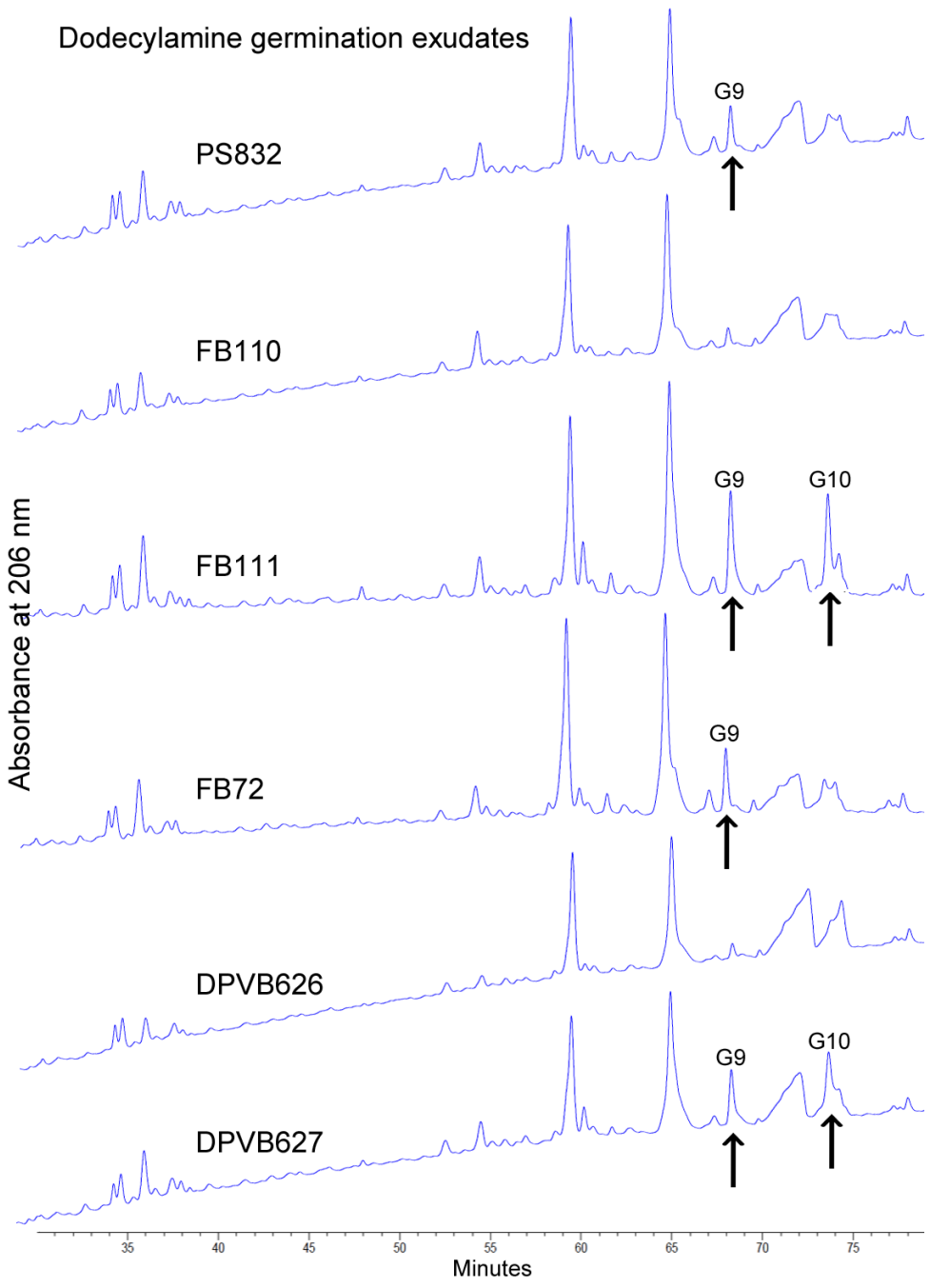

Figure 4.3. HPLC separation of dodecylamine germination exudate muropeptides. Spores were germinated for 240 min with 1 mM dodecylamine. Exudates were concentrated, reduced, and separated using HPLC. Peaks are numbered as in (10). Muropeptides G9 and G10, products of SleB activity, are indicated by arrows. Muropeptide G9 was identified by mass spectrometry.

CHAPTER 5

In vitro and *in vivo* studies of the interaction between SleB and YpeB, and investigation of the contributions of SpoIVB, YlaJ, and YhcN

Casey B. Bernhards and David L. Popham

ATTRIBUTIONS

Casey B. Bernhards performed the research, experimentation, data analysis, and writing of the material presented herein. David L. Popham was the principle investigator.

ABSTRACT

During spore germination, cortex peptidoglycan degradation is the result of germination-specific lytic enzyme (GSLE) activity. The activity of one of the *Bacillus* GSLEs, SleB, is dependent upon another protein, YpeB, expressed from the same operon. These proteins localize to the same regions of the spore and are co-dependent, where the absence of one results in the degradation of the other during spore formation. The current work further investigated the relationship between SleB and YpeB in *Bacillus anthracis* by attempting to demonstrate a physical interaction, both *in vitro* and *in vivo*. SleB and YpeB did not interact *in vitro*, and a direct interaction was not proven *in vivo*. Other proteins that may be involved with SleB and/or YpeB were also examined. SpoIVB is a potential protease involved in SleB and YpeB degradation due to its timing and location of expression. SleB was not stabilized during sporulation of a Δ*ypeB spoIVB* strain of *B. anthracis*, indicating SpoIVB cannot be solely responsible for the absence of SleB in Δ*ypeB* spores. *B. anthracis* homologs of the *B. subtilis* lipoproteins YlaJ and YhcN were also investigated, as a third gene following *sleB* and *ypeB* in the *B. anthracis* operon is similar to both proteins. Deletion of *ylaJ* and/or *yhcN* at loci BAS2560 and BAS4323, respectively, did not result in significant defects during spore germination.

INTRODUCTION

A critical step during bacterial spore germination—a process whereby a spore transforms from a dormant, highly resistant structure to a metabolically active vegetative cell—is cortex peptidoglycan (PG) depolymerization. This is accomplished by the activity of germination-specific lytic enzymes (GSLEs) within the dormant spore. SleB, a GSLE in *Bacillus* species, is a lytic transglycosylase capable of allowing complete spore germination even in the absence of other GSLEs (38, 61, 86, 97, 100, 116). SleB is expressed upstream of *ypeB*, and the arrangement with *ypeB* in an operon is highly conserved across *Bacillus* species (61, 100, 170, 200). This operon is expressed in the forespore compartment of the developing spore under the control of σ^G (23, 108). Both SleB and YpeB contain signal sequences directing their translocation across the inner forespore membrane (23, 108-110), where they would be found in the intermembrane space between the inner and outer membranes prior to cortex synthesis during sporulation. The SleB signal sequence is removed during spore formation (69, 108-110), while the YpeB signal sequence is not predicted to be cleaved, likely tethering YpeB to the inner membrane. Fittingly, at least a portion of both proteins have been localized to this membrane (36).

SleB and YpeB have a reciprocal relationship where not only is YpeB required for the presence of SleB within dormant spores, but SleB is also necessary for the presence of YpeB (19, 36, 90). In the absence of the other protein, SleB and YpeB are rapidly degraded during sporulation (19); therefore, SleB lytic activity on cortex peptidoglycan is dependent on YpeB (23). The mechanism by which SleB and YpeB stabilize one another and other possible roles of YpeB have not been determined. An interesting possibility surrounds the three putative PepSY domains at the C-terminal portion of YpeB (177). The inhibitory role of these domains in a class

of proteases could translate to inhibition of SleB activity by YpeB (177). The arrangement of *sleB* and *ypeB* in an operon, co-localization, and the co-dependent relationship between the two proteins strongly suggests that SleB and YpeB physically interact, yet such a direct interaction has not been conclusively demonstrated.

A prime candidate for a protease that may degrade SleB and YpeB in the absence of the other protein during spore formation is SpoIVB. SpoIVB is a serine protease that is involved of processing of pro-σ^K to σ^K during sporulation (168). SpoIVB cleavage of SpoIVFA (30, 46) frees SpoIVFB from its inhibitory complex with SpoIVFA and BofA (216, 222). SpoIVFB in turn processes pro-σ^K to active σ^K (134, 179). The active form of this sporulation specific sigma factor directs late stage gene expression in the mother cell compartment of the sporangium (61). As expression of *spoIVB* is induced in the forespore at the engulfment stage of sporulation under the control of σ^G (43), SpoIVB is secreted into the intermembrane space (49, 73, 263) in order to act on SpoIVFA in the outer forespore membrane (215, 222). Expression of *spoIVB* at the same time and location as *sleB* and *ypeB*, as well as translocation of all three proteins into the intermembrane space, would give SpoIVB access to SleB and YpeB during spore formation.

In *Bacillus anthracis* and other members of the *B. cereus* group, a third gene follows *sleB* and *ypeB* as part of a putative tricistronic operon (64, 125). This gene at locus BAS2560 in the *B. anthracis* chromosome, shows homology to the *B. subtilis* genes *ylaJ* and *yhcN* (19, 64). In *B. subtilis*, *ylaJ* and *yhcN* appear to be monocistronically transcribed during sporulation under the control of σ^G and encode putative membrane-anchored lipoproteins (12, 84). While YlaJ is otherwise uncharacterized, a *yhcN* mutant examined in *B. subtilis* displayed a minor defect in spore germination or outgrowth (12). Arrangement of BAS2560 in an operon with *sleB* and *ypeB*, suggests a possible relationship between the three proteins.

The goal of this study was to demonstrate a physical interaction between *B. anthracis* SleB and YpeB and potentially provide more insight into the function of YpeB. In addition, three other proteins that may play a role in the relationship between SleB and YpeB during sporulation and germination were examined. These candidate proteins included the lipoproteins YlaJ and YhcN, and the protease SpoIVB. *In vitro*, an interaction between SleB and YpeB was not observed. Likewise, a physical interaction between SleB and YpeB *in vivo* was not conclusively shown. Investigation of YlaJ and YhcN revealed that YlaJ and YhcN do not contribute significantly to SleB and YpeB stability, or to SleB activity during spore germination. Alternatively, other redundant proteins may exist in *B. anthracis*. Lastly, SleB was not stabilized during sporulation of a Δ*ypeB spoIVB* strain, indicating other proteases are capable of SleB degradation in the absence of YpeB.

MATERIAL AND METHODS

Bacterial strains and growth conditions. Strains and plasmids used are listed in Table 5.1. All *B. anthracis* strains in this study are derived from the Sterne strain 34F2 and were grown at 37°C in brain heart infusion (BHI; Difco) with 5 μg/ml erythromycin, 20 μg/ml kanamycin, or 250 μg/ml spectinomycin, where appropriate. *B. anthracis* strains maintaining pBKJ236- or pRP1028-derived plasmids extrachromosomally were incubated at 25°C. Following plasmid integration into the chromosome (at 42°C in most instances), these strains were subsequently grown at 37°C. All *B. subtilis* strains are derivatives of strain 168 and were grown at 37°C in LB, 2xYT, or 2xSG (87) with 3 μg/ml chloramphenicol, 100 μg/ml spectinomycin, or 10 μg/ml tetracycline, where appropriate. *Escherichia coli* strains used for plasmid propagation or protein overexpression were grown in LB at 37°C with 50 μg/ml

ampicillin, 30 μg/ml chloramphenicol, 500 μg/ml erythromycin, 20 μg/ml kanamycin, or 100 μg/ml spectinomycin.

***B. anthracis* mutant construction.** Primer sequences used during plasmid construction are listed in Table 5.2. All plasmids created were verified by DNA sequencing. To create a Δ*ylaJ* strain of *B. anthracis*, *ylaJ* and approximately 500-bp flanking each side of the gene were PCR amplified from the *B. anthracis* chromosome. The PCR product was inserted into the vector pBKJ236 (75) by digesting with the restriction enzymes SacII and NotI and ligating the DNA to create pDPV410. Inverse PCR of the plasmid using primers with BglI restriction sites at the 3′ ends resulted in a linear PCR product with the majority of *ylaJ* deleted, leaving only three codons from each end of the gene. Subsequent BglI digestion and ligation of the PCR product formed pDPV413. This plasmid containing the *ylaJ* deletion was introduced into *B. anthracis* using the markerless gene replacement strategy as previously described (75), except plasmid pSS4332 (21) was used for I-SceI expression in place of pBKJ223.

To create Δ*yhcN* and Δ*ylaJ* Δ*yhcN* strains, *yhcN* and approximately 500-bp on each side from the *B. anthracis* chromosome were PCR amplified. The resulting PCR product was inserted into vector pRP1028 (21) by digestion with HindIII and BamHI and ligating the DNA, creating pDPV419. Plasmid pRP1028 serves the same role as pBKJ236 during the markerless gene replacement method for gene deletion. Inverse PCR of pDPV419 was performed using primers with BglII sites at the 3′ ends, which deleted all of *yhcN* but the first 9 and last 6 codons. Plasmid pDPV420 was subsequently created by digesting the inverse PCR product with BglII and ligating the DNA. This plasmid was introduced into wild-type and Δ*ylaJ* strains of *B. anthracis* as described above, creating Δ*yhcN* and Δ*ylaJ* Δ*yhcN* strains. All gene deletions were verified by PCR amplification and sequencing.

For construction of *spoIVB* and Δ*ypeB spoIVB* strains, an approximately 500-bp internal fragment of *B. anthracis spoIVB* (BAS4077) was PCR amplified from the chromosome and inserted into pRP1028 using restriction enzymes BamHI and KpnI. The resulting plasmid, pDPV429, was moved into wild-type and Δ*ypeB* (19) strains of *B. anthracis* by conjugation, as done in the initial stages of the markerless gene replacement procedure (75). Subsequent plasmid integration and disruption of the chromosomal copy of *spoIVB* was achieved by shifting the temperature to 42°C and was verified by PCR.

***B. anthracis* spore and sporangia preparation and analysis.** Spores were prepared in modified G broth (78) at 37°C with aeration. After 3 to 4 days, dormant spores were harvested by centrifugation and repeatedly washed with deionized water over several days. Any remaining vegetative cells were heat killed at 65°C for 25 min. A 50% sodium diatrizoate (Sigma) gradient was used to further purify spores, as described previously (113). Decoated spores were prepared as previously described (19). Untreated (native) and decoated spores were stored in deionized water at 4°C until analysis. The rate of germination and outgrowth of decoated spores in liquid BHI was assessed by monitoring the change in OD_{600} as described previously (19). Germination efficiency assays, in which decoated spores were serially diluted and plated on BHI medium, were performed as previously described (19). For sporangia collection, strains were grown at 37°C in modified G broth with 100 μg/ml spectinomycin, where appropriate. Samples were collected every hour from hours 2 (t_2) through 6 (t_6) after the initiation of sporulation, as described previously (19). Dormant spore and sporangia samples were broken with glass beads and proteins extracted for western blot analysis as described previously (19).

***B. anthracis* protein expression in *E. coli* and purification.** Overexpression and purification of His_6-MBP-$SleB_{33-253}$, $SleB_{33-253}$, and $YpeB_{21-446}$ has been published previously

(19, 65). Primer sequences used for plasmid construction are given in Table 5.2. For overexpression of His_6-MBP-$YpeB_{1-446}$, the *ypeB* gene from the *B. anthracis* chromosome was amplified by PCR and inserted into a modified version of pDEST-HisMBP (11) containing a tobacco etch virus (TEV) cleavage site (pDEST-HisMBP-T) using restriction-free cloning (162). The resulting plasmid encoded an N-terminal His_6-tagged maltose binding protein (MBP) and $YpeB_{1-446}$, separated by a TEV cleavage site. Successful plasmid construction was verified by sequencing. The His_6-MBP-$YpeB_{1-446}$ fusion protein was overexpressed in *Escherichia coli* BL21 (λDE3) (pLysS Cm^r) (Novagen) and purified as described previously for His_6-MBP-$YpeB_{21-446}$ (19), except the His_6-MBP tag was not removed. Briefly, cells were grown at 37°C to an OD_{600} of 1.0, at which point protein expression was induced with 1 mM isopropyl-β-D-thiogalactopyranoside at 10°C for 16 h. Cells were lysed by sonication and purified using a Ni-Sepharose HisTrap HP affinity column (GE Healthcare). Protein was eluted with a linear gradient of 30 to 500 mM imidazole and dialyzed.

Enzymatic activity assays on spore PG. Intact spore sacculi from *B. subtilis* PS832 (wild-type) were prepared as previously described (65), except that spores were not treated with DNase or RNase. *B. anthracis* $SleB_{33-253}$ (0.25 μg), $YpeB_{21-446}$ (0.7 μg), and/or $YpeB_{21-446}$ that had first been heated to 100°C for 5 min were mixed and incubated at room temperature for 5 min. Proteins were added to 0.2 OD_{600} units/ml spore sacculi in a total volume of 1 ml buffer containing 30 mM $NaPO_4$ pH 7.0, 1 mM EDTA, 1 mM DTT, and 0.1% Triton X-100. PG hydrolysis was monitored by the change in OD_{600} over time.

***In vitro* affinity pull-down assays.** All centrifugations were performed at 1,000 x *g* for 1 min. His_6-MBP-$SleB_{33-253}$ or His_6-MBP-$YpeB_{1-446}$ (10 μg in a total of 15 μl Buffer A [50 mM NaCl, 50 mM Tris-HCl pH 7.5, 5% glycerol, 30 mM imidazole]) were immobilized on a mini-

column consisting of 15 μl packed Ni^{2+}-NTA agarose (Qiagen) equilibrated with Buffer A. After a 30 minute incubation on ice, unbound fusion proteins were removed by centrifuging and removing the supernatant, followed by two washes with 100 μl Buffer A. During each wash, the mini-column was centrifuged and the supernatant removed. The reciprocal untagged protein (5 μg of $YpeB_{21-446}$ or $SleB_{33-253}$ in a total of 15 μl Buffer A) was then added to the mini-column and incubated for 30 minutes on ice. Unbound untagged proteins were removed as described above for the fusion proteins, except the supernatant collected after the first centrifugation was saved for SDS-PAGE analysis. Bound proteins were eluted with 20 μl Buffer B (50 mM NaCl, 50 mM Tris-HCl pH 7.5, 5% glycerol, 500 mM imidazole) and collected in the supernatant after centrifugation. Unbound and bound protein samples were mixed with 4X sample loading buffer (62.5 mM Tris-HCl pH 6.8, 4% SDS, 40% glycerol, 10% β-mercaptoethanol, 0.1% bromophenol blue) to a final concentration of 1X, heated to 100°C for 5 min., and analyzed in 9% SDS-PAGE gels stained with Coomassie Brilliant Blue R-250 (Jersey Lab Supply).

Antibody resin preparation. Anti-SleB and anti-YpeB antibody resins were prepared by modifications to a published procedure (29). All centrifugations were performed at 1,500 x *g* at 4°C. For each antibody resin preparation, 1 ml of packed protein A-sepharose (BioVision) was washed three times with 5 ml cold 1X PBS. 2 ml of crude antiserum against *B. anthracis* proteins (anti-SleB or anti-YpeB (19)) were batch absorbed to the protein A-sepharose for 1 h at 4°C with gentle rocking. Antibody resins were washed four times with 5 ml cold 1X PBS, and antibodies were covalently cross-linked to the protein A-sepharose with 5 mM suberic acid bis (Sigma-Aldrich) in a total volume of 2 ml. Cross-linking was allowed to proceed for 30 min at room temperature with gentle rocking, followed by addition of Tris-HCl pH 7.5 to a final concentration of 100 mM to quench the reaction. After a 15 min incubation at room temperature

with gentle rocking, three washes with 2 ml 100 mM glycine pH 2.5 were performed to remove uncross-linked antibodies. Between each glycine wash, antibody resins were neutralized with 5 ml cold 1X PBS with gentle rocking at 4°C for 10 min. Antibody resins were stored at 4°C as a 50% slurry in 1X PBS with 0.02% sodium azide.

Construction of *B. subtilis* strains for inducible expression of *B. anthracis* proteins. Primer sequences used for plasmid construction are listed in Table 5.2. Correct plasmid construction was verified with DNA sequencing. To create *B. subtilis* strains for inducible expression of *B. anthracis* SleB and/or YpeB, *sleB* and *ypeB*, along with ribosome-binding site upstream of *sleB*, were PCR amplified from the *B. anthracis* chromosome. The PCR product was inserted into pSWEET-*bgaB* (20) downstream of a xylose-inducible promoter (*xylAp*) by digestion with NotI and PacI and DNA ligation. The resulting plasmid was designated pDPV439. To create Δ*sleB ypeB* and *sleB* Δ*ypeB* strains, overlap extension PCR (66) was performed using pDPV439 as template to delete the majority of either *sleB* or *ypeB*. Overlap extension PCR involves multiple rounds of PCR using two internal and two external primers. The internal primers were the same primers used previously for creating Δ*sleB* (64) and Δ*ypeB* (19) strains of *B. anthracis*, leaving only the first 10 and last 9 codons of *sleB* or three codons from each end of *ypeB*. The external primers annealed to the pSWEET-*bgaB* backbone of pDPV439, outside of the *sleB ypeB* insert. Subsequent digestion of the PCR products and pDPV439 with NotI and PacI, followed by ligation, created pDPV443 and 444. Plasmids pDPV439, 443, and 444 were transformed (3) as concatemers (from a Rec^+ strain of *E. coli*) into a *sleB*::*Sp* strain of *B. subtilis*, where they integrated into the *amyE* locus of the *B. subtilis* chromosome through a double recombination. To verify *amyE* disruption, transformants were screened for the loss of α-amylase activity on 2xSG agar plates containing 1% starch using

iodine crystals, as described previously (4). The resulting strains were DPVB639, 652, and 653. In order to use the *B. subtilis* membrane protein PBP2a as a control during co-IP, FLAG-tagged *pbpA* (encoding PBP2a-FLAG) was added to these strains. The chloramphenicol resistance marker in the *pbpA*-FLAG strain of *B. subtilis* (DPVB360) (176) was first changed to tetracycline resistance using pCm::Tc, as previously described (153). Chromosomal DNA from this strain, DPVB679, was used to transform (3) DPVB639, 652, and 653, producing DPVB680, 681, and 682, respectively. Final strain construction was verified by PCR amplification.

Expression of *B. anthracis* proteins and preparation of *B. subtilis* membranes. *B. subtilis* strains were grown in 100 ml LB medium with appropriate antibiotics to an OD_{600} of 0.3. To induce *B. anthracis* SleB and YpeB expression, xylose was added to a final concentration of 2% in the presence of 1 mM PMSF. Cultures were induced for 2 h, after which cells were harvested by centrifugation at room temperature. Cells were washed with 10 ml 1X SMM + PMSF (0.5 M sucrose, 20 mM $MgCl_2$, 20 mM maleic acid pH 6.5, 1 mM PMSF), and interacting proteins were cross-linked with 1% formaldehyde in 10 ml 1X SMM + PMSF for 10 min at room temperature. Protoplasts and membranes were prepared by modifications to a published procedure (29). Protoplasts were first created by resuspending cells in 10 ml 1X SMM + PMSF + 1 mg/ml lysozyme and incubating at 37°C for 10 min. Protoplasts were harvested by centrifugation at room temperature and flash frozen in liquid N_2. Osmotic lysis of thawed protoplasts occurred by addition of 2.5 ml hypotonic buffer (Buffer H) (20 mM HEPES pH 8, 200 mM NaCl, 1 mM DTT, 1 mM PMSF, 0.5 μg/ml leupeptin, 0.7 μg/ml pepstatin A). Next, lysates were treated with 10 μg/ml DNase I and 20 μg/ml RNase A in the presence of 1 mM $MgCl_2$ and 1 mM $CaCl_2$ for 1 h on ice. Membrane fractions were separated by centrifugation at 100,000 x *g* for 1 h at 4°C and homogenized in 200 μl Buffer G (Buffer H + 10% glycerol).

Homogenized membranes were flash frozen in liquid N_2. Homogenized membranes were diluted 5-fold with Buffer S (Buffer H + 20% glycerol + 100 μg/ml lysozyme), and membrane proteins were solubilized with 1% Triton X-100 with rotation for 1 h at 4°C. Soluble membrane proteins were separated by centrifugation at 100,000 x *g* for 1 h at 4°C.

Co-immunoprecipitation of proteins from solubilized *B. subtilis* membranes. Co-immunoprecipitation (co-IP) was performed from solubilized membranes by modifications to a published procedure (29). Anti-SleB resin, anti-YpeB resin, or protein-A sepharose without antibodies was washed with cold 1X PBS, and 20 μl packed resin was mixed with half of the soluble fraction (the load) from Triton X-100 treated membranes. Mixtures were rotated for 4 h at 4°C and centrifuged at 2,700 x *g* for 5 min at 4°C to separate unbound proteins in supernatants (the flow-through) from resins. Resins were washed four times with 1 ml Buffer S + 1% Triton X-100, and immunoprecipitated proteins were eluted with 50 μl of elution buffer (150 mM NaCl, 25 mM Tris-HCl pH 6.8, 2% SDS, 10 mM EDTA, 0.75% Triton X-100, 20% glycerol) at 50°C for 15 min. Following centrifugation at 2,300 x *g* for 2 min at room temperature, β-mercaptoethanol and bromophenol blue were added to supernatants (the IP) to final concentrations of 2.5%. Approximately 250-300 μl of the remaining load and flow-through fractions were concentrated ~5.5-fold using Amicon Ultra 3K 0.5 ml centrifugal filters (Millipore) according to the manufacturer's instructions. To concentrated and unconcentrated load and flow-through fractions, 4X sample loading buffer was added to a final concentration of 1X, and Triton X-100 was added to a final concentration of 0.75% to concentrated fractions only. All load, flow-through, and IP fractions were heated to 100°C for 5 min to reverse formaldehyde cross-links, and fractions were analyzed by western blot.

Western blot analysis. Polyclonal antibodies raised in rabbits against *B. anthracis* SleB and YpeB (19) were used for detection of SleB and YpeB in western blots. Polyclonal rabbit anti-FLAG antibodies (Sigma) were used for detection of PBP2a-FLAG. Anti-SleB antibodies were used at a 1:500 or 1:1,000 dilution, anti-YpeB antibodies were used at a 1:1,000 or 1:3,000 dilution, and anti-FLAG antibodies were used at a 1:900 dilution. Secondary goat anti-rabbit-HRP antibodies (Bio-rad) were used at a 1:5,000 (cat. #166-2408) or 1:200,000 (cat. #170-6515) dilution. Where indicated, Clean-Blot IP detection reagent HRP (Pierce) was used at a 1:200 dilution in place of secondary antibodies. Western blots utilized Amersham Hybond-P (PVDF) membranes (GE Healthcare), and antibody detection was carried out using colorimetric (BM Blue POD Substrate, Precipitating; Roche) or chemiluminescent (Amersham ECL Prime Western Blotting Detection Reagent; GE Healthcare) substrates.

RESULTS

Enzymatic activity assays on spore PG. To determine if YpeB can inhibit SleB activity on spore PG *in vitro*, purified *B. anthracis* $YpeB_{21-446}$ and/or $SleB_{33-253}$ were mixed with PS832 spore sacculi and the change in OD_{600} monitored (Fig. 5.1). *B. anthracis* and *B. subtilis* have essentially identical spore PG structures (47); thus, *B. subtilis* spore PG has routinely been used to assess *B. anthracis* GSLE activity due to the ease in which *B. subtilis* spores and PG are purified (65, 86). As demonstrated previously (65), $SleB_{33-253}$ activity on PS832 spore sacculi resulted in a rapid decrease in OD_{600} (Fig. 5.1). As anticipated, since exogenous YpeB from other species had no effect on decoated spores (90), $YpeB_{21-446}$ alone did not exhibit any lytic activity on spore PG (Fig. 5.1). When an excess of $YpeB_{21-446}$ (0.7 μg) was preincubated with 0.25 μg $SleB_{33-253}$ for 5 min prior to addition to spore sacculi, no inhibition of SleB activity was

observed (Fig. 5.1). Even when 2 μg of $YpeB_{21-446}$ and 0.05 μg $SleB_{33-253}$ were used, SleB activity was not inhibited (data not shown).

***In vitro* SleB and YpeB affinity pull-down assays.** In an attempt to show a physical interaction between *B. anthracis* SleB and YpeB *in vitro*, $YpeB_{21-446}$ or $SleB_{33-253}$ were added to mini-columns consisting of His_6-MBP-$SleB_{33-253}$ or His_6-MBP-$YpeB_{1-446}$, respectively, bound to Ni^{2+}-NTA agarose. After a 30 min incubation on ice, unbound proteins were collected and bound proteins were eluted with 500 mM imidazole. Unbound and bound proteins were analyzed by SDS-PAGE and stained with Coomassie blue (Fig. 5.2). $YpeB_{21-446}$ did not bind to His_6-MBP-$SleB_{33-253}$, as evident by the presence of $YpeB_{21-446}$ exclusively in the unbound protein fraction. Even when the experiment was performed with an incubation temperature of 30°C, binding was not observed (data not shown). In the reciprocal experiment, $SleB_{33-253}$ was only present in the unbound protein fraction, indicating it did not bind to His_6-MBP-$YpeB_{1-446}$.

***In vivo* SleB and YpeB co-IP.** To demonstrate an interaction between SleB and YpeB *in vivo*, the *sleB* and *ypeB* genes from *B. anthracis* were cloned into a *sleB*::*Sp* strain of *B. subtilis*, in which the mutation has a polar effect that significantly reduces the expression of *ypeB* (90), under the control of an inducible promoter. Co-expression of the *B. anthracis* proteins was induced with xylose during vegetative growth, and interacting proteins were cross-linked with formaldehyde to capture weak and transient interactions, as well as interactions that might be disrupted during subsequent experimental manipulations. Membrane fractions were isolated, solubilized with Triton X-100, and used for co-IP experiments. When the proteins were co-expressed and anti-SleB antibody resin used, the majority of SleB was immunoprecipitated and some of YpeB was co-immunoprecipitated (Fig. 5.3A and B). When SleB or YpeB was expressed alone, low levels of SleB or YpeB, respectively, were detected in the load; however,

only SleB was immunoprecipitated (Fig. 5.3A and B). Similar results were obtained during a reciprocal experiment using anti-YpeB antibody resin; when co-expressed, most of YpeB was immunoprecipitated and a smaller fraction of SleB was co-immunoprecipitated (Fig. 5.4A and B). Likewise, low levels of YpeB or SleB were detected in the absence of their partner protein, but only YpeB was immunoprecipitated (Fig. 5.4A and B). Neither protein was immunoprecipitated using protein-A sepharose without bound antibodies (Figs. 5.3 and 5.4), demonstrating the specificity of the proteins for their cognate antibody.

As a control, a FLAG-tagged version of the *B. subtilis* membrane protein PBP2a was included in the strains used for co-IP. When the same IP samples that had showed co-immunoprecipitation of SleB and YpeB were probed with anti-FLAG antibodies, PBP2a-FLAG was also detected, albeit not as clearly (Figs. 5.3C and 5.4C). The high level of background seen in IP samples probed with anti-FLAG antibodies was thought to be antibody heavy and light chain contamination from the anti-SleB and anti-YpeB antibody resins, even though the antibodies had been cross-linked to the protein A-sepharose. Therefore, Clean-Blot IP detection reagent HRP, which only recognizes native primary antibodies used during western blotting and not denatured antibodies, was used. While this reagent significantly diminished the background present in IP samples probed with anti-SleB and anti-YpeB antibodies (compare Fig. 5.3A and B with Fig. 5.4A and B), the background seen in IP samples probed with anti-FLAG antibodies was not reduced.

Effect of *ylaJ* and *yhcN* deletions on spore germination. In *B. anthracis*, BAS2560 is the gene following *sleB* and *ypeB* in a putative tricistronic operon (64). BAS2560 shows homology with genes *ylaJ* (51% identity/ 71% similarity) and *yhcN* (30% identity/ 49% similarity) in *B. subtilis*, both of which are expressed during sporulation and encode putative

lipoproteins. BAS4323, which appears to be monocistronic in *B. anthracis*, also shows homology with *B. subtilis yhcN* (26% identity/ 47% similarity). BAS2560 and BAS4323 will henceforth be referred to as *ylaJ* and *yhcN*, respectively. Genes *ylaJ* and *yhcN*, alone and in conjunction, were deleted from the *B. anthracis* chromosome to determine what effect they may have on SleB and/or YpeB. When Δ*ylaJ*, Δ*yhcN*, and Δ*ylaJ* Δ*yhcN* spores were germinated in BHI medium and germination monitored spectrophotometrically, mutant spores displayed germination rates indistinguishable from that of wild-type spores in assays using native (data not shown) and decoated spores (Fig. 5.5). In a decoated spore plating efficiency assay, mutant spores produced similar amounts of colonies as wild-type spores, with less than a 2-fold reduction in plating efficiency (Table 5.3). To see if YlaJ and/or YhcN affect SleB and/or YpeB stability over time, the plating assay was repeated on spores after 4 months, but similar results were obtained (Table 5.3). As another assessment of SleB and YpeB stability in mutant spores, proteins were extracted from broken spores and probed with anti-SleB and anti-YpeB antibodies (Fig. 5.6). Similar levels of SleB and YpeB were observed across all strains, indicating SleB and YpeB stability was not affected by the gene deletions.

Effect of a *spoIVB* mutation on SleB stability. In the absence of YpeB, SleB is rapidly degraded during spore formation, and the reverse is also true (19). SpoIVB, a protease with similar temporal and spatial expression patterns as SleB and YpeB, is a candidate protease for their proteolysis. At the time of this study, anti-YpeB antibodies had not been obtained; thus, only SpoIVB proteolysis of SleB was examined. To determine if SpoIVB is responsible for SleB degradation in a Δ*ypeB* strain, *spoIVB* and Δ*ypeB spoIVB* mutant strains were constructed in *B. anthracis*. A complication in this line of experimentation is that SpoIVB is part of the cascade that leads to processing of pro-σ^K to σ^K during sporulation (30). As such, *spoIVB* mutants are

defective in cortex and coat formation and do not form dormant spores (43). To circumvent this issue, the stability of SleB in mutant strains was investigated in sporulating cells rather than dormant spores. As demonstrated previously (19), in a wild-type strain SleB was strongly detected from 3 hours (t_3) onward after the initiation of sporulation, while only miniscule levels were detected during early *sleB* expression from a Δ*ypeB* strain (Fig. 5.7). In a *spoIVB* mutant, low levels of SleB were observed at t_5 and t_6 (Fig. 5.7). This reduction in SleB expression compared with wild-type can likely be attributed to the sporulation defect in this strain. In a Δ*ypeB spoIVB* mutant, SleB was not restored, even to the low levels seen during sporulation of the *spoIVB* mutant (Fig. 5.7); thus, SpoIVB cannot be solely responsible for the degradation of SleB during spore formation in the absence of YpeB.

DISCUSSION

In vitro experiments aimed at showing a physical interaction between SleB and YpeB in *Bacillus* species have been largely unsuccessful. In the current study, affinity pull-down assays using His_6-MBP-$YpeB_{1-446}$ and untagged $SleB_{33-253}$, and inversely, His_6-MBP-$SleB_{33-253}$ and untagged $YpeB_{21-446}$ were performed; however, binding between the proteins was not observed. Li et al. performed a more extensive series of affinity pull-down assays using various forms of *B. cereus* and *B. megaterium* SleB and YpeB purified from *E. coli*, but again, an interaction was not seen (90). One possible rationale for the lack of interaction *in vitro* is that the proteins likely interact as they are co-expressed and co-translated; however, even when pull-down assays were performed using cell extracts from *E. coli* or *Lactococcus lactis* in which SleB and YpeB were co-expressed, the two proteins did not interact (90). It's also feasible that both proteins in their entirety are needed to mediate an interaction. With the exception of the His_6-MBP-$YpeB_{1-446}$

fusion protein used in this study, all forms of SleB and YpeB tested in the present work and by Li et al. lacked their signal sequences. In sporulating cells, the SleB signal sequence is rapidly removed following transport across the inner forespore membrane (69, 108, 110), but an interaction with YpeB may occur before or during transport. The YpeB signal sequence is not predicted to be cleaved and presumably anchors YpeB to the inner membrane, but it could also play a role in an interaction with SleB. TEV protease was unable to cleave His_6-MBP-$YpeB_{1-446}$, which is why $YpeB_{21-446}$ was used in reciprocal experiments with His_6-MBP-$SleB_{33-253}$. In addition, signal sequence removal greatly facilitates protein purification. It's also possible that affinity tags on either protein impeded an interaction; however the use of multiple types and both N-terminal and C-terminal tags by Li et al. (90), suggests otherwise.

Whereas $YpeB_{21-446}$ also failed to inhibit $SleB_{33-253}$ activity on spore PG during *in vitro* enzymatic activity assays in the current study, Li et al. did observe some inhibition of *B. cereus* SleB activity on decoated spores by YpeB (90). $YpeB^M$ (residues 23-447) and $YpeB^C$ (residues 214-447) exhibited an inhibitory effect on the C-terminal, catalytic domain of SleB ($SleB^C$, residues 136-259), but had little effect on mature SleB ($SleB^M$, residues 32-259) (90). Interestingly, $YpeB^N$ (residues 23-204), containing none of the inhibitory PepSY domains, resulted in the greatest inhibition of all forms of SleB tested (90). These results are the first possible evidence of an interaction between SleB and YpeB *in vitro*.

Due to the inability of the present study to demonstrate a physical interaction between *B. anthracis* SleB and YpeB *in vitro*, *in vivo* approaches were explored. In addition to the possible need for protein co-expression, any interaction may occur as SleB and YpeB are translocated across the inner forespore membrane. Thus, a membrane or another component not represented in the *in vitro* studies may be necessary for the interaction to occur. Co-IP of SleB and YpeB

from developing or dormant *B. anthracis* spores was not possible due to the hardy nature of the spore structure. SleB and YpeB could not be successfully solubilized from the spore without methods that would disrupt any protein interactions. To overcome this obstacle, the interaction was reprogrammed to occur in vegetative cells. *B. anthracis* SleB and YpeB were co-expressed and cross-linked in vegetative *B. subtilis* cells because a xylose-inducible expression system had already been developed in this species (20). In control strains expressing SleB or YpeB alone, low levels of SleB or YpeB, respectively, were detected even in the absence of the partner protein. While these results are still consistent with instability of SleB and YpeB in Δ*ypeB* and Δ*sleB* spores, respectively (19), the detection of even low levels of these proteins in vegetative *B. subtilis* cells can be explained by the fact that the cell cytoplasm encountered in the co-IP experiments is not completely identical to the environment encountered by SleB and YpeB during spore formation. The same protease(s) that normally degrades SleB and YpeB during sporulation may not be expressed during vegetative cell growth. Additionally, SleB and YpeB expression is not under the control of their native promoter; thus, there is likely a higher level of protein expression under the xylose expression system than in the developing spore. When SleB and YpeB were co-expressed, the proteins were co-immunoprecipitated with both anti-SleB and anti-YpeB antibody resins. While these were initially promising results, an unrelated *B. subtilis* membrane protein, PBP2a, was also co-immunoprecipitated, indicating that the small amount of SleB or YpeB co-immunoprecipitated was not above the level of background that is normal for co-IP experiments.

Other proteins that were investigated for a potential relationship with SleB and YpeB include YlaJ, YhcN, and SpoIVB. YlaJ is expressed from the *sleB ypeB* operon in *B. anthracis*, suggesting a possible relationship. The genes encoding YlaJ and another, possibly redundant

protein, YhcN, were deleted from the *B. anthracis* chromosome, but no obvious phenotype was observed in dormant spores or during germination of these mutant spores. Either these lipoproteins play only a minor role during spore germination or outgrowth, or there may be additional redundant proteins masking the effects of the deletions. The gene encoding SpoIVB was also disrupted to see if this protease was responsible for SleB proteolysis in Δ*ypeB* spores. While hindered by the inability of *spoIVB* mutants to make dormant spores, it appeared that such a mutation did not stabilize SleB during Δ*ypeB spoIVB* sporulation. It's possible that multiple proteases are responsible for degrading SleB and YpeB during spore formation, as it appears multiple proteases, including HtrC, degrade YpeB during germination (Chapter 3). SpoIVB may be one of the proteases involved, but this cannot be conclusively determined based on the experiment presented in this study. Unfortunately, many of the proteases present during sporulation are required at various stages of spore formation; thus, analysis of SleB and YpeB stability in these mutants or in a multiple protease-deficient strain is not currently possible.

ACKNOWLEDGEMENTS

We thank Roger Plaut and Scott Stibitz for the gift of plasmids pSS4332 and pRP1028. We also thank the MAOP and REU undergraduate students who assisted with strain constructions and analyses: Brittany Aeschlimann, Maralis Butler, and Crystal Thomas.

Table 5.1. Bacterial strains and plasmids.

Strain or plasmid	Relevant genotype/phenotype [a]	Construction [b]	Source
E. coli			
DPVE13	BL21 (λDE3) pLysS (Cm^r)		Novagen
DPVE439	pDPV425 (His_6-MBP-$YpeB_{1-446}$ Amp^r) Cm^r	pDPV425→DPVE13	This study
B. anthracis			
Sterne 34F2	$pXO1^+$ $pXO2^-$		P. Hanna
DPBa89	Δ*ypeB*		(19)
DPBa105	Δ*ylaJ*	pDPV413→34F2	This study
DPBa116	Δ*yhcN*	pDPV420→34F2	This study
DPBa119	Δ*ylaJ* Δ*yhcN*	pDPV420→DPBa105	This study
DPBa130	*spoIVB*::pDPV429 Sp^r	pDPV429→34F2	This study
DPBa131	Δ*ypeB spoIVB*::pDPV429 Sp^r	pDPV429→DPBa89	This study
B. subtilis			
PS832	Wild-type		P. Setlow
FB112	*sleB*::Sp^r		(117)
DPVB152	*sleB*::Sp^r	FB112→PS832	This study
DPVB360	*pbpA*-FLAG Cm^r		(176)
DPVB639	*sleB*::Sp^r, *amyE*::*xylAp-sleB ypeB* Cm^r	pDPV439→DPVB152	This study
DPVB652	*sleB*::Sp^r, *amyE*::*xylAp*-Δ*sleB ypeB* Cm^r	pDPV443→DPVB639	This study
DPVB653	*sleB*::Sp^r, *amyE*::*xylAp-sleB* Δ*ypeB* Cm^r	pDPV444→DPVB639	This study
DPVB679	*pbpA*-FLAG Tet^r	pCm::Tc→DPVB360	This study
DPVB680	*sleB*::Sp^r, *amyE*::*xylAp-sleB ypeB* Cm^r, *pbpA*-FLAG Tet^r	DPVB679→DPVB639	This study
DPVB681	*sleB*::Sp^r, *amyE*::*xylAp*-Δ*sleB ypeB* Cm^r, *pbpA*-FLAG Tet^r	DPVB679→DPVB652	This study
DPVB682	*sleB*::Sp^r, *amyE*::*xylAp-sleB* Δ*ypeB* Cm^r, *pbpA*-FLAG Tet^r	DPVB679→DPVB653	This study
Plasmids			
pBKJ236	Er^r *ori*(Ts)		(75)
pRP1028	Sp^r *ori*(Ts), TurboRFP		(21)
pSS4332	Kan^r, I-SceI, AmCyan		(21)
pCm::Tc	Cm^r::Tet^r, Amp^r		(153)
pDEST-HisMBP-T	His_6-MBP, Amp^r Cm^r		F. Schubot
pSWEET-*bgaB*	*xylAp-bgaB*, Amp^r Cm^r		(20)
pDPV392	Δ*ypeB*		(19)
pDPV410	$ylaJ^+$	pBKJ236::*ylaJ*	This study
pDPV413	Δ*ylaJ*	pBKJ236::Δ*ylaJ*	This study
pDPV419	$yhcN^+$	pRP1028::*yhcN*	This study
pDPV420	Δ*yhcN*	pRP1028::Δ*yhcN*	This study
pDPV425	His_6-MBP-$YpeB_{1-446}$	pDEST-HisMBP-T::$ypeB_{1-446}$	This study
pDPV429	*spoIVB′*	pRP1028::*spoIVB′*	This study
pDPV439	*xylAp-sleB ypeB*	pSWEET-*bgaB*::*sleB ypeB*	This study
pDPV443	*xylAp*-Δ*sleB ypeB*	pSWEET-*bgaB*::Δ*sleB ypeB*	This study
pDPV444	*xylAp-sleB* Δ*ypeB*	pSWEET-*bgaB*::*sleB* Δ*ypeB*	This study

[a] Cm^r, chloramphenicol resistance; Amp^r, ampicillin resistance; Sp^r, spectinomycin resistance; Tet^r, tetracycline resistance; Er^r, erythromycin resistance; *ori*(Ts), temperature-sensitive origin of replication; Kan^r, kanamycin resistance.

[b] *E. coli* and *B. anthracis* strains were constructed by conjugation or electroporation, where the designation preceding the arrow is the plasmid and the designation following the arrow is the recipient strain. *B. subtilis* strains were constructed by transformation (3), where the designation preceding the arrow is the donor plasmid or chromosomal DNA and the designation following the arrow is the recipient strain.

Table 5.2. Primer sequences.

Plasmid constructed	Primer name	Sequence 5′ to 3′ [a]
pDPV410	462	CAGACCCGCGGAGGCGGATATCCAATTTGGG
	463	CAGACGCGGCCGCCCCTGTATGTATGTTCATGC
pDPV413	464	CAGCCCGCGCGGCGATTTTCATTATTCTCACCACTTTA
	465	CAGCCGCGCGGGCCAATAAATAAAGATAACCTTAACCCT
pDPV419	483	CGCCCAAAGCTTTGGCAAATGCCATATCAGCAAGG
	484	CGCGGATCCGGATGAACGTCTCATTCTGC
pDPV420	485	CGCAGATCTAGCAATCACTTTTACTTTCG
	486	CGCAGATCTACTGGTACAGTGCGATAAC
pDPV425	510	***GTGGAGAACCTGTACTTCCAGGGT***ATGTTACGAGGTATTATAATCGTATTATTAAC
	511	*CCACTTTGTACAAGAAAG*TTGCATTGCTTTAATCATAAATTTTTTCAACAGCC
pDPV429	527	CGCGGATCCCATCCCCGAAACAACTTGTTG
	528	CGCGGTACCGGTGTTAACTTAGTGCGAATATGC
pDPV439	577	CGCTTAATTAAGGAGGGAAATTTATGCGCCAAAAAGC
	578	CGCGCGGCCGCTCACCACTTTACCATTAAAGTTTAATC
pDPV443	104	AATGAGGTTAAGAGTATTCC
	105	ATCTTGATAATAAGGGTAAC
	289	GCCCGCGCGGCACCTCCCTGCTATTTTAAAAATAGCTT
	290	GGGAGGTGCCGCGCGGGCAAGATCGGGAAACATATTTTC
pDPV444	444	GCCCGCGCGGCTCGTAACATAGTTCCACCTCCGCTC
	445	AGCCGCGCGGGCTATGATTAAACTTTAATGGTAAAGT
	104, 105	

[a] Restriction sites are underlined, TEV cleavage site regions of pDEST-HisMBP-T are italicized and in bold, and *att*R2.1 regions of pDEST-HisMBP-T are italicized and underlined.

Table 5.3. Decoated spore plating efficiencies for *ylaJ* and *yhcN* deletion mutants.

Strain	Genotype	Initial CFU/OD_{600} [a]	CFU/OD_{600} [b]
34F2	wild-type	6.9×10^7	7.9×10^7
DPBa105	Δ*ylaJ*	3.9×10^7	6.7×10^7
DPBa116	Δ*yhcN*	5.0×10^7	5.9×10^7
DPBa119	Δ*ylaJ* Δ*yhcN*	3.7×10^7	6.1×10^7

[a] Values obtained are from an assay performed on purified spores stored in deionized water at 4°C for 2 weeks prior to decoating.

[b] Values obtained are from an assay performed on purified spores stored in deionized water at 4°C for 4 months prior to decoating.

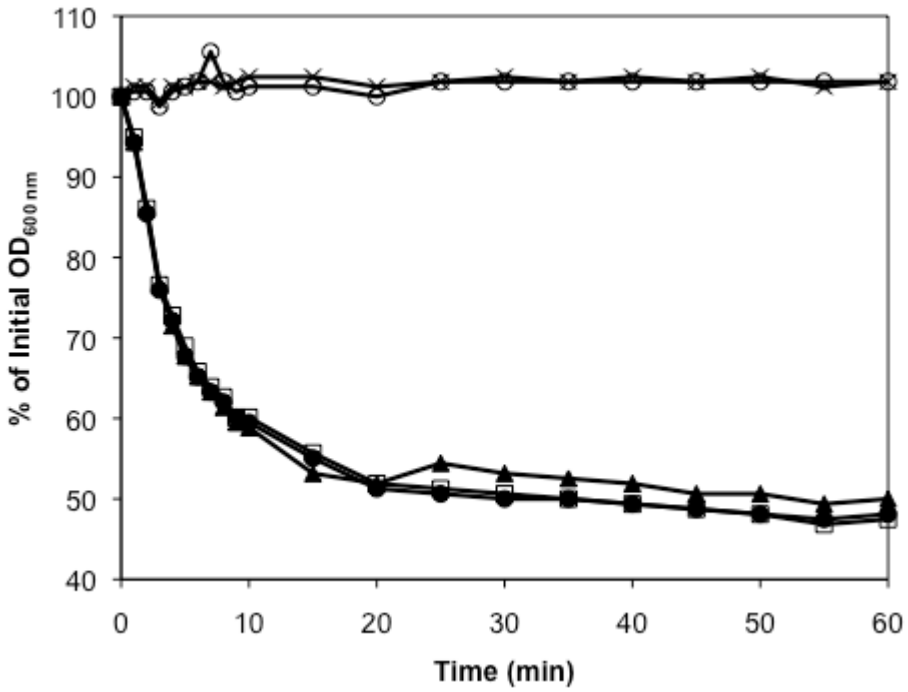

Figure 5.1. YpeB does not inhibit SleB activity *in vitro*. Purified PS832 spore sacculi was mixed with 0.25 μg $SleB_{33\text{-}253}$ (●), 0.7 μg $YpeB_{21\text{-}446}$ (○), 0.25 μg $SleB_{33\text{-}253}$ preincubated with 0.7 μg $YpeB_{21\text{-}446}$ (□), 0.25 μg $SleB_{33\text{-}253}$ preincubated with 0.7 μg inactivated $YpeB_{21\text{-}446}$ (▲), or buffer (×) and the OD_{600} was measured over time.

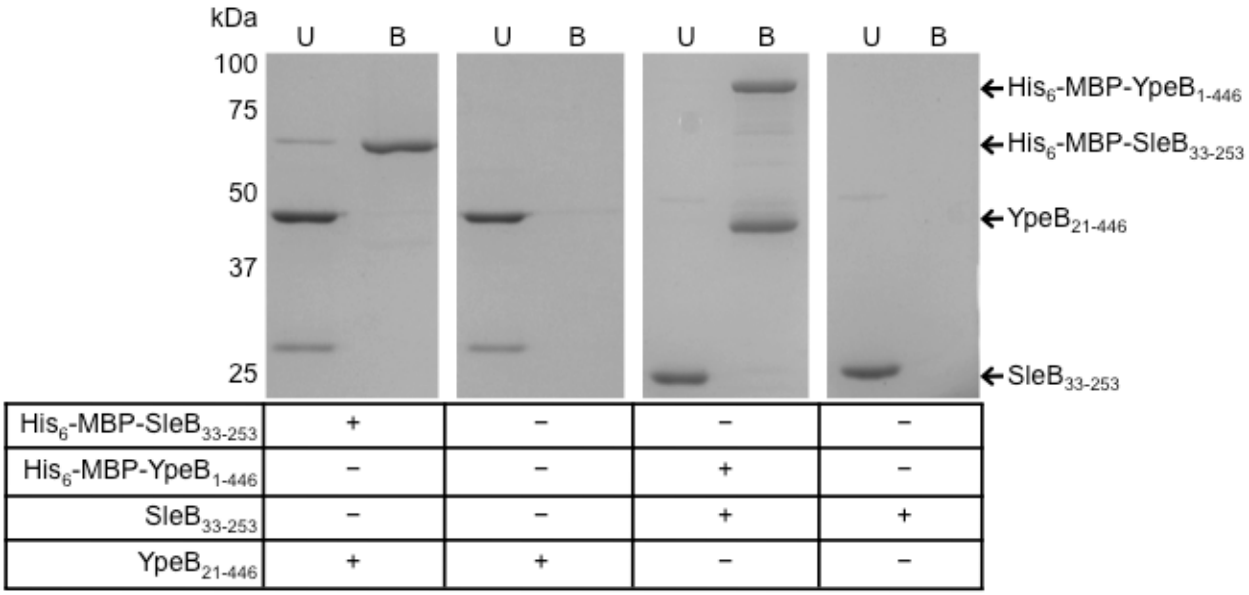

His_6-MBP-$SleB_{33-253}$	+	−	−	−
His_6-MBP-$YpeB_{1-446}$	−	−	+	−
$SleB_{33-253}$	−	−	+	+
$YpeB_{21-446}$	+	+	−	−

Figure 5.2. SleB and YpeB do not interact *in vitro*. Where indicated, His_6-MBP-$SleB_{33-253}$ or His_6-MBP-$YpeB_{1-446}$ was first immobilized on Ni^{2+}-NTA agarose, and $YpeB_{21-446}$ or $SleB_{33-253}$, respectively, was added. Unbound (U) proteins and bound (B) proteins eluted with imidazole were separated by SDS-PAGE and stained with Coomassie blue. The first two panels are from one SDS-PAGE gel, while the last two panels are from a second SDS-PAGE gel. Intervening lanes between panels 1 and 2, and between panels 3 and 4 were removed for clarity. The positions of molecular weight marker proteins (not shown) are indicated on the left. His_6-MBP-$YpeB_{1-446}$, His_6-MBP-$SleB_{33-253}$, $YpeB_{21-446}$, and $SleB_{33-253}$ have predicted molecular weights of 93.3, 67.4, 47.9, and 24.2 kDa, respectively. Unlabeled bands are likely protein degradation products.

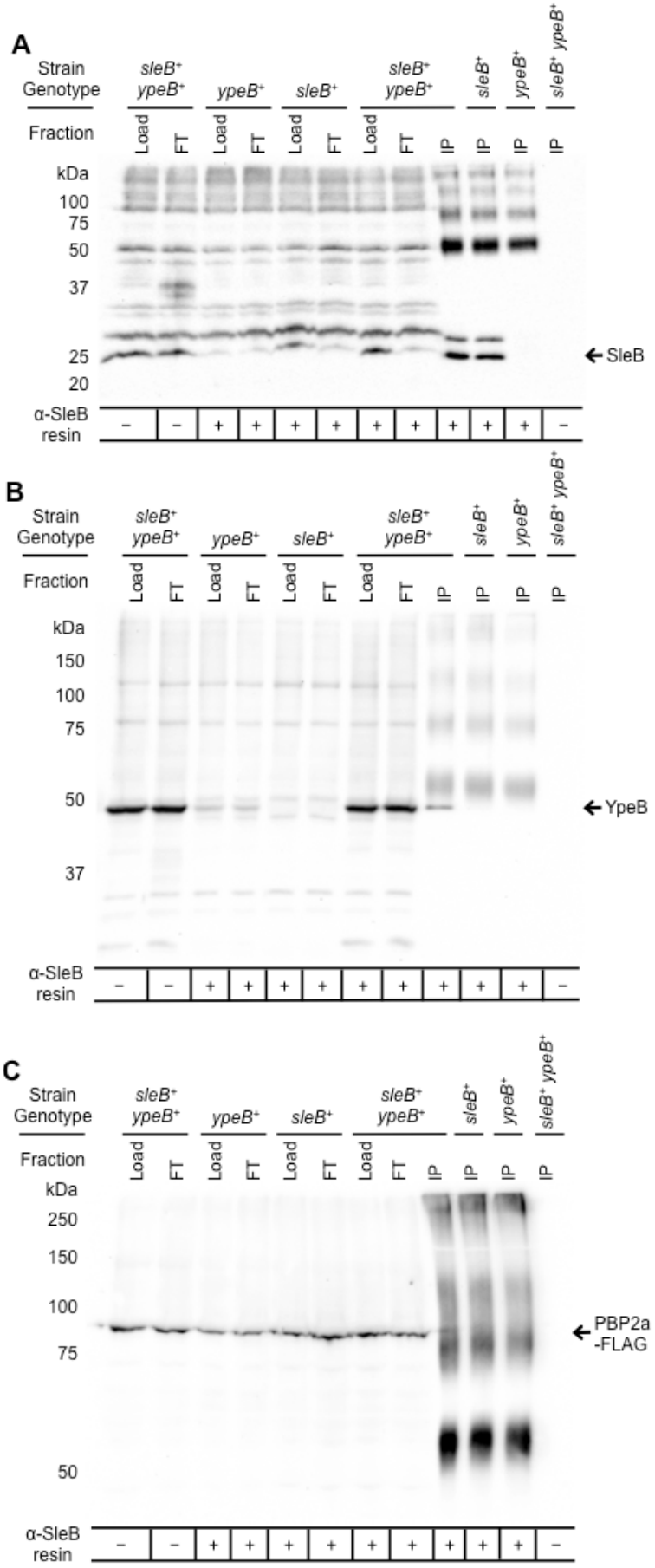
A
Strain Genotype
sleB+ ypeB+
ypeB+
sleB+
sleB+ ypeB+
sleB+
ypeB+
sleB+ ypeB+
Fraction
Load
FT
IP
kDa
100
75
50
37
25
20
SleB
α-SleB resin
B
YpeB
150
C
PBP2a -FLAG
250

Figure 5.3. Co-IP of SleB and YpeB with anti-SleB resin. *B. anthracis* SleB and/or YpeB were expressed and cross-linked in *B. subtilis* strains DPVB680 (*sleB*$^+$ *ypeB*$^+$), DPVB681 (*ypeB*$^+$), and DPVB682 (*sleB*$^+$) during vegetative growth. Proteins solubilized from *B. subtilis* membranes were immunoprecipitated with *B. anthracis* anti-SleB antibodies cross-linked to protein A-sepharose, or with protein A-sepharose without bound antibodies. Proteins before immunoprecipitation (Load), unbound proteins in the flow-through (FT), and immunoprecipitated proteins (IP) were analyzed in western blots using a chemiluminescent detection substrate. (A) Concentrated load and FT samples, and unconcentrated IP samples run on a 12% SDS-PAGE gel, transferred to PVDF membrane, and probed with anti-SleB antibodies. (B) Unconcentrated load, FT, and IP samples run on a 7.5% SDS-PAGE gel, transferred to PVDF membrane, and probed with anti-YpeB antibodies. (C) Concentrated load and FT samples, and unconcentrated IP samples run on a 7.5% SDS-PAGE gel, transferred to PVDF membrane, and probed with anti-FLAG antibodies. (A) and (B) utilized secondary goat anti-rabbit-HRP antibodies, while (C) used Clean-Blot IP detection reagent HRP. The positions of molecular weight marker proteins (not shown) are indicated on the left. SleB, YpeB, and PBP2a-FLAG have predicted molecular weights of 24.1, 50.0, and 81.1 kDa, respectively.

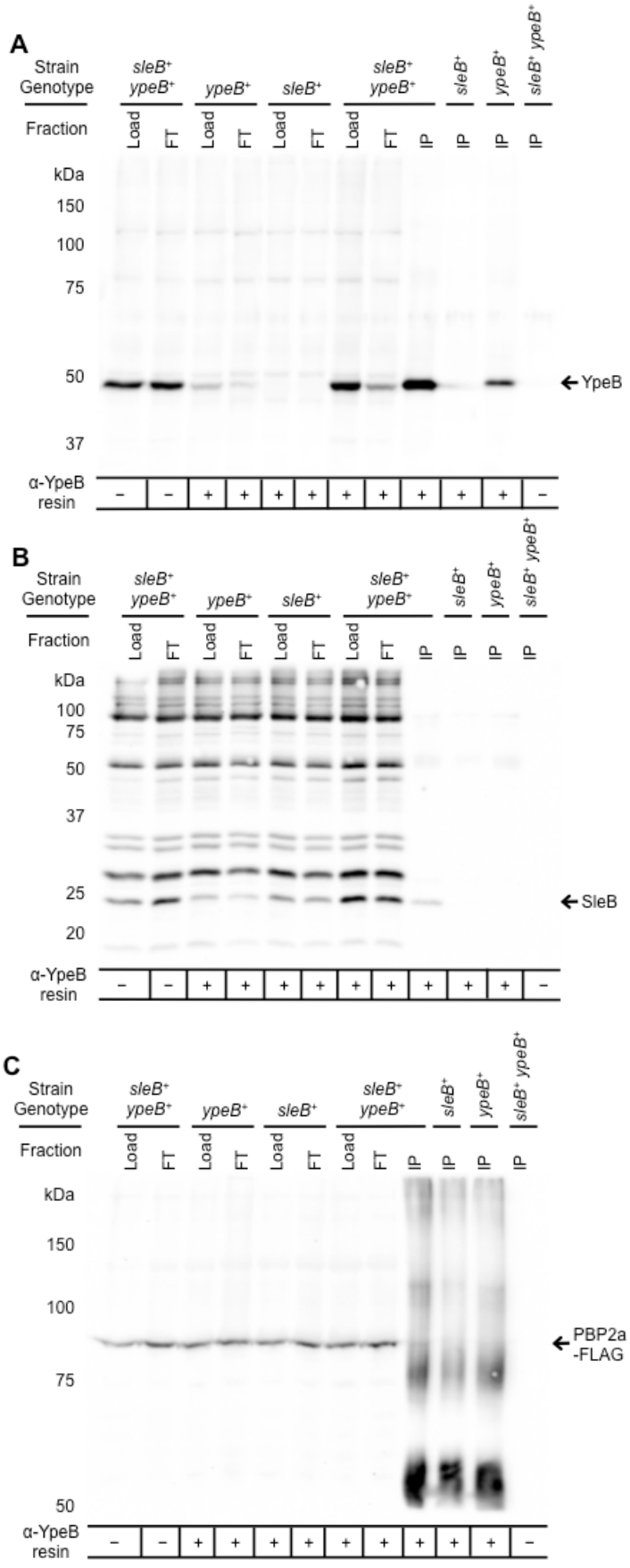
A
Strain Genotype
sleB+ ypeB+
ypeB+
sleB+
sleB+ ypeB+
sleB+
ypeB+
sleB+ ypeB+
Fraction
Load
FT
IP
kDa
150
100
75
50
37
YpeB
α-YpeB resin
B
SleB
25
20
C
PBP2a -FLAG

Figure 5.4. Co-IP of SleB and YpeB with anti-YpeB resin. *B. anthracis* SleB and/or YpeB were expressed and cross-linked in *B. subtilis* strains DPVB680 (*sleB*$^+$ *ypeB*$^+$), DPVB681 (*ypeB*$^+$), and DPVB682 (*sleB*$^+$) during vegetative growth. Proteins solubilized from *B. subtilis* membranes were immunoprecipitated with *B. anthracis* anti-YpeB antibodies cross-linked to protein A-sepharose, or with protein A-sepharose without bound antibodies. Proteins before immunoprecipitation (Load), unbound proteins in the flow-through (FT), and immunoprecipitated proteins (IP) were analyzed in western blots using Clean-Blot IP detection reagent HRP and chemiluminescent detection substrate. (A) Unconcentrated load, FT, and IP samples run on a 7.5% SDS-PAGE gel, transferred to PVDF membrane, and probed with anti-YpeB antibodies. (B) Unconcentrated load, FT, and IP samples run on a 12% SDS-PAGE gel, transferred to PVDF membrane, and probed with anti-SleB antibodies. (C) Concentrated load and FT samples, and unconcentrated IP samples run on a 7.5% SDS-PAGE gel, transferred to PVDF membrane, and probed with anti-FLAG antibodies. The positions of molecular weight marker proteins (not shown) are indicated on the left. SleB, YpeB, and PBP2a-FLAG have predicted molecular weights of 24.1, 50.0, and 81.1 kDa, respectively.

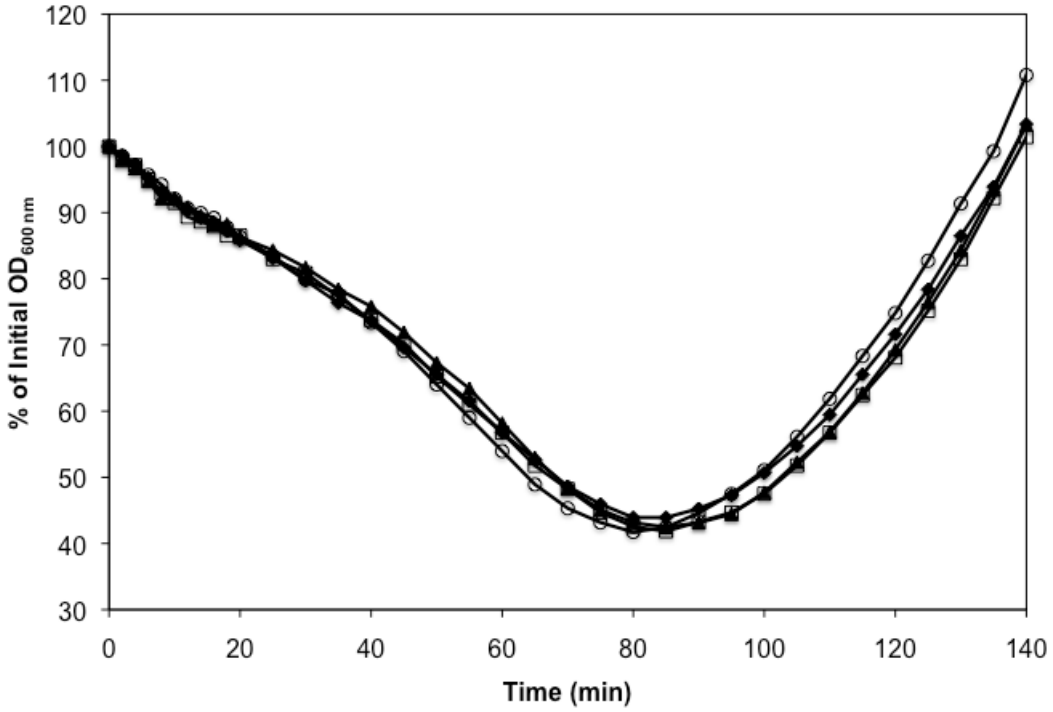

Figure 5.5. Germination and outgrowth of decoated spores are not affected by *ylaJ* and/or *yhcN* deletions. Decoated wild-type (◆), Δ*ylaJ* (□), Δ*yhcN* (○), and Δ*ylaJ* Δ*yhcN* (▲) spores were heat activated and germinated in BHI medium at 37°C.

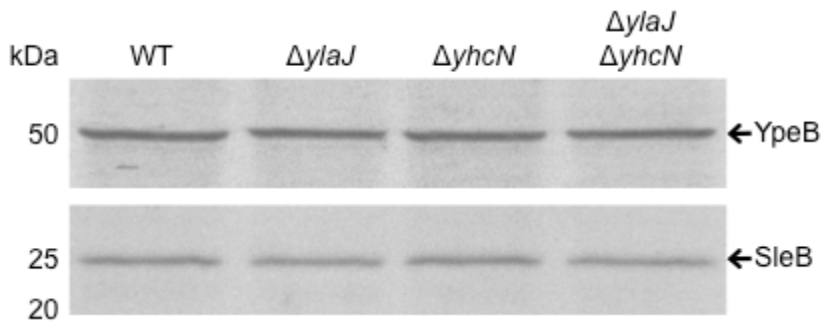

Figure 5.6. SleB and YpeB stability are not affected by *ylaJ* and/or *yhcN* deletions. Dormant wild-type (WT), Δ*ylaJ*, Δ*yhcN*, and Δ*ylaJ* Δ*yhcN* spores were broken and proteins extracted for western blot analysis. Blots were probed with anti-YpeB (top) and anti-SleB (bottom) antibodies, and a colorimetric substrate was used for detection. The positions of molecular weight marker proteins (not shown) are indicated on the left. YpeB has a predicted molecular weight of 50.0 kDa, while mature SleB without its signal sequence has a predicted molecular weight of 24.1 kDa.

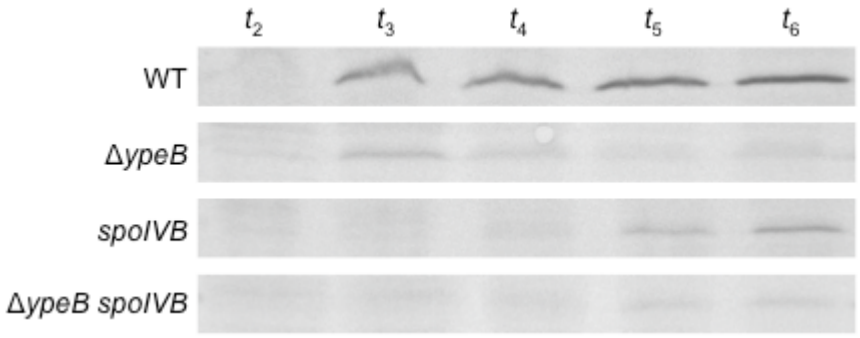

Figure 5.7. Disruption of *spoIVB* does not stabilize SleB during Δ*ypeB* spore formation. Wild-type (WT), Δ*ypeB*, *spoIVB*, and Δ*ypeB spoIVB* strains were sporulated in modified G broth at 37°C, and samples were collected from 2-6 hours (t_2-t_6) after the initiation of sporulation. Immunoblots were probed with anti-SleB antibodies, and a colorimetric substrate was used for detection.

CHAPTER 6

Final Discussion

The 2001 anthrax attacks, in which letters containing *Bacillus anthracis* spores were mailed in the United States, exposed the true social and economic consequences stemming from the use of *B. anthracis* as a bioweapon. As spores are extremely resilient structures, there remains a need for efficient spore decontamination strategies that are easier, safer, and cheaper than the methods currently employed. One potential solution involves exploiting the natural process of spore germination, whereby spores lose their resistance properties as they become vegetative cells. Triggering spore germination at a high efficiency would result in cells that are easily killed using simplified decontamination methods. Germination-specific lytic enzymes (GSLEs) are attractive targets for such approaches as they are required for complete spore germination and resumption of metabolism. Unfortunately, there are still large gaps in our understanding of the spore germination process that have prevented the real-world application of germination-mediated decontamination. Key remaining questions center around GSLE regulation, including how they remain inactive in the dormant spore and how they are subsequently activated during germination. With knowledge of how GSLE activity is controlled, GSLEs or proteins that modulate their activity could become targets to elicit spore germination at a high rate.

The work presented in this dissertation aims to address these questions surrounding GSLE regulation, specifically regulation of SleB. Chapters 2 and 3 focus on how SleB stability in the dormant spore and SleB activity during germination are regulated by its partner protein, YpeB. In Chapter 2, it was shown using Δ*sleB* and Δ*ypeB* strains of *B. anthracis* that SleB and YpeB are co-dependent. In the absence of the other protein, SleB and YpeB are expressed but rapidly degraded during sporulation, resulting in dormant spores that lack both proteins. Therefore, Δ*sleB* and Δ*ypeB* spores exhibit essentially identical germination phenotypes, as SleB

activity during spore germination is dependent on YpeB. Regions in both the N- and C- terminal domains of YpeB are required for the stability of SleB, and certain highly conserved residues within the YpeB C-terminal PepSY domains contribute to the stability of both proteins.

The size and stability of SleB remain unchanged during spore germination; however, as demonstrated in Chapter 3, YpeB is cleaved to form two stable products during spore germination. Additionally, both stable products contain the C-terminal PepSY domains. The two specific cleavage sites resulting in the observed YpeB products were determined, and it was shown both *in vivo* and *in vitro* that their production is the result of the protease HtrC. It's unclear if HtrC is also involved in SleB and YpeB proteolysis during sporulation, but at minimum, HtrC is not solely responsible. The ability to determine whether YpeB processing by HtrC plays a prominent role in SleB activation was hampered by the inability of cleavage site mutations to block YpeB degradation, and the presence of other proteases in the spore that are capable of degrading YpeB in the absence of HtrC. The existence of apparent "back-up" mechanisms that ensure YpeB is degraded during germination may suggest that YpeB processing is an important element during the germination cascade. It has also been shown that protease inhibitors can halt the progression of germination at various stages (24-26, 40). While the precise germination events blocked by these protease inhibitors are generally not known, it's clear that proteases are integral to the process of spore germination.

The typically inhibitory PepSY domains of YpeB, coupled with YpeB cleavage during spore germination, makes the possibility of YpeB involvement in SleB inhibition and/or activation hard to overlook. In a model where YpeB is involved in both activities, SleB and YpeB likely physically interact, stabilizing each other and holding SleB inactive. Degradation of SleB during spore formation could serve as a fail-safe mechanism to prevent any SleB not in a

complex with YpeB from degrading cortex PG prior to spore germination. The PepSY domains may function to inhibit SleB activity until germination is triggered, at which point HtrC and other proteases become active and cleave YpeB. HtrC may be activated by the efflux of ions from the spore core, just as CwlJ is activated by release of Ca^{2+}-DPA (117). YpeB processing by HtrC would then release SleB from its inhibitory interaction with YpeB, allowing SleB to degrade cortex PG.

Other models proposed to explain how SleB remains inactive in the dormant spore and is activated during spore germination involve the Ger receptors, the stress of cortex PG, and the fluidity of the inner forespore membrane. In the first alternate model, upon germinant contact with receptors at the inner membrane, SleB is activated in a Ger receptor-dependent manner. Work detailed in Chapter 4 indicates that SleB can be activated in the absence of Ger receptors and argues against this proposal. The cortex PG stress theory posits that in the dormant spore, SleB is not active on cortex PG because the PG is not in a conformation recognized by SleB. During germination, as the core begins to rehydrate and turgor pressure increases, the cortex PG changes to a stressed conformation that SleB is able to cleave. In disagreement with this model, Heffron et al. found that *B. anthracis* SleB purified from *Escherichia coli* was active on a variety of cortex PG substrates (decoated spores, spore sacculi, and cortex fragments) with various levels of cortical stress (65). While it's possible that SleB purified from *E. coli* is more active than native SleB, other studies have shown that SleB isolated from germinated spore exudates is active on decoated spores (52, 93), which are thought to have the same cortical stress as dormant spores (65). Yet another scheme suggests that SleB is inactive in the dormant spore due to immobility of the lipids (42) that comprise the inner spore membrane. Upon initiation of germination, fluidity returns to the inner membrane (42), permitting SleB activity. This

hypothesis fails to address how SleB is held inactive during sporulation, prior to immobilization of the lipid bilayer. Additionally, SleB (and YpeB) have been localized to both the inner membrane and the outer region of the cortex (36, 108). If the fraction of SleB located in the cortex is functional, how is its activity regulated?

A model involving YpeB is a logical explanation that could account for both the inactivity of SleB in the dormant spore and SleB activation during germination. A key piece missing from the puzzle is conclusive evidence that SleB and YpeB physically interact—a likely requirement for this model. Experiments performed in Chapter 5 aimed at demonstrating a direct interaction between SleB and YpeB *in vivo* and *in vitro* were unsuccessful. While similar attempts by other groups have been largely unfruitful, Li et al. did observe inhibition of *Bacillus cereus* SleB activity on decoated spores by YpeB *in vitro* (90). Interestingly, the N-terminal domain of YpeB ($YpeB^N$, residues 23-204), containing none of the PepSY domains, resulted in the greatest inhibition of all forms of SleB tested (90). YpeB lacking its signal sequence ($YpeB^M$, residues 23-447) and the C-terminus of YpeB ($YpeB^C$, residues 214-447) did exhibit an inhibitory effect on the C-terminal, catalytic domain of SleB ($SleB^C$), but had little effect on SleB without its signal sequence ($SleB^M$) (90). Clearly more work is needed to substantiate these results *in vivo* and explain the basis for SleB inhibition, or lack there of, by various forms of YpeB. Perhaps it's actually the critical N-terminal region of YpeB that binds and inhibits SleB activity via an unknown mechanism, and the PepSY domains serve to mediate protease activity in the surrounding environment.

There are many challenges associated with further characterization of the relationship between SleB and YpeB. The strict co-dependency of the two proteins complicates matters, as a mutation that destabilizes one will almost certainly destabilize the other. The involvement of

proteases in SleB and YpeB degradation during sporulation and YpeB processing during germination adds another complexity. As many of the proteases present during sporulation and germination are critical to spore formation itself, protease-deficient strains are of limited use to study the SleB and YpeB interaction. Lastly, the environment where a potential physical interaction is taking place is difficult to recreate *in vitro*. As discussed in Chapter 2, SleB and YpeB may need to be co-expressed, co-folded, and/or co-translocated across the inner forespore membrane to interact, although in the study discussed above, in which Li et al. observed some inhibition of SleB activity by YpeB, the various forms of *B. cereus* SleB and YpeB tested were separately expressed and purified from *E. coli* and added exogenously to decoated spores (90). An interaction may also require the presence of a membrane, and/or other proteins that help to mediate an interaction, although as indicated in Chapter 5, it appears at least YlaJ and YhcN are not essential.

Based on the importance of both SleB and YpeB to spore germination, this intriguing relationship merits further investigation. There is a wealth of compelling circumstantial evidence in support of a direct interaction between SleB and YpeB, including co-dependency and apparent co-localization of the proteins. A scenario where YpeB interacts directly with proteases and not SleB, does not address how SleB is also able to stabilize YpeB. Due to the many complexities of the SleB-YpeB interaction, *in vivo* approaches aimed at demonstrating a physical interaction are more likely to be successful. Studies are underway to demonstrate a direct interaction within the *B. anthracis* spore using FRET analysis of fluorescently labeled SleB and YpeB. In addition, crystallization of YpeB will likely offer more insight. While the primary structure of YpeB is not homologous to other proteins of known function, perhaps its tertiary structure will resemble that of better-studied proteins. YpeB structure determination may reveal

binding clefts, surfaces used to mediate protein-protein interactions, or other novel structural elements, providing additional clues as to the mechanisms by which YpeB is able to regulate SleB.

APPENDIX

Extension of Chapter 2 Discussion: The role of YpeB in cortex hydrolysis during germination of *Bacillus anthracis* spores

It was discovered that the *ypeB* deletion created in the *B. anthracis* chromosome was in fact not in-frame as intended. Primers 444 and 445 (Table 2.2) each contain BglI restriction sites. When these primers were used to perform inverse PCR on pBKJ326::*ypeB* (pDPV388), and the PCR product was subsequently digested with BglI and ligated, the resulting plasmid (pDPV392) contained the first and last 3 codons of *ypeB*, separated by a BglI site. As the BglI site is an 11-bp sequence and not a multiple of 3, this resulted in a frame-shift at the Δ*ypeB* site in the chromosome once allelic exchange was complete. In *B. subtilis*, where *ypeB* is the last gene in a bicistronic operon with *sleB*, this would not be an issue, but in *B. anthracis*, *ypeB* is the second gene in a putative tricistronic operon and a frame-shift has the potential for a polar effect on expression of downstream BAS2560. However, with the frame-shift another stop codon is encountered just 7-bp downstream from the start of the native stop codon. Additionally, translation of *ypeB* and BAS2560 are likely not coupled, as the intergenic distance between the two genes is 26-bp. Thus, the Δ*ypeB* frameshift should not interfere with the binding of ribosomes to the Shine-Delgarno sequence upstream of BAS2560 and should not affect BAS2560 expression. Lastly, deletion of BAS2560 had no significant effect on spore germination (Chapter 5).

While it's anticipated the out-of-frame *ypeB* deletion has no effect on BAS2560 transcription or translation, when feasible, this possibility was ruled out when integrating the *ypeB* complementation plasmid and derivatives into the Δ*ypeB* chromosome. For the *ypeB* complementation strain (DPBa113) and YpeB PepSY domain point mutants (DPBa143, DPBa144, DPBa148, DPBa149, and DPBa150), PCR was used to verify plasmid integration occurred within the homologous region downstream of Δ*ypeB* on the chromosome. This ensured that the chromosomal, full-length copy of BAS2560 was downstream of *ypeB* or *ypeB* derivative

with its native promoter, and not downstream of Δ*ypeB*. Therefore, there is no question that these strains express BAS2560 normally, and any observed germination defect cannot be the result of altered BAS2560 expression. Since it was not possible to integrate plasmids containing His_6-tagged versions of *ypeB* in the same manner, as described in the materials and methods, YpeB PepSY domain truncation mutants (DPBa124, DPBa125, DPBa126, and DPBa127) and YpeB internal deletion mutants (DPBa158, DPBa159, DPBa160, and DPBa161) do contain BAS2560 just downstream of Δ*ypeB*.

To ensure that the absence of YpeB from Δ*sleB* spores was not the result of a polar effect on downstream *ypeB*, this region of the chromosome was PCR amplified and sequenced to verify the *sleB* deletion was in-frame. Additionally, in the *sleB* complementation strain (DPBa134), in which YpeB was restored in western blots (Fig. 2.2), the complementation plasmid was integrated into the chromosome in such a way that the only full-length copy of *ypeB* was immediately downstream of Δ*sleB*.

The use of decoated spores in this study highlights the activity of SleB during spore germination, since the decoating procedure is thought to inactivate CwlJ1, CwlJ2, and SleL (64). It should be noted that the CFU/OD reported here for decoated Δ*sleB* spores (Table 2.3) was less than that observed by Heffron et al., which was 1 x 10^5 CFU/OD (64). One possible explanation is the use of different methods for decoating between the two studies. Heffron et al. incubated spores in an alkaline buffer with detergent (0.1 M NaOH, 0.1 M NaCl, 1% sodium dodecyl sulfate, 0.1 M dithiothreitol at 70°C for 30 min (64, 119)), while this work employed a urea buffer with detergent (50 mM Tris-HCl pH 8, 8 M urea, 1% SDS, 50 mM DTT at 37°C for 2 h

(124)). It was observed that the former alkaline method resulted in greater aggregation of spores (data not shown), which is why the latter method utilizing urea was selected. It's possible that spore aggregation resulted in more carry over of spores during serial dilutions for Heffron et al., or perhaps the use of urea in the current study more completely inactivated the GSLEs in and near the coat layers. Another possibility, which has been addressed previously, is that differences in amounts of exogenous lytic enzymes present in batches of BHI could account for inconsistent CFU/OD values between studies (63).

REFERENCES

1. **Adams, C. M., B. E. Eckenroth, E. E. Putnam, S. Doublie, and A. Shen.** 2013. Structural and functional analysis of the CspB protease required for *Clostridium* spore germination. PLoS Pathog. **9:**e1003165.

2. **Altschul, S. F., W. Gish, W. Miller, E. W. Myers, and D. J. Lipman.** 1990. Basic local alignment search tool. J. Mol. Biol. **215:**403-410.

3. **Anagnostopoulos, C., and J. Spizizen.** 1961. Requirements for transformation in *Bacillus subtilis*. J. Bacteriol. **81:**741-746.

4. **Astolfi-Filho, S., E. V. Galembeck, J. B. Faria, and A. C. S. Frascino.** 1986. Stable yeast transformants that secrete functional α-amylase encoded by cloned mouse pancreatic cDNA. Nat. Biotechnol. **4:**311-315.

5. **Atrih, A., G. Bacher, G. Allmaier, M. P. Williamson, and S. J. Foster.** 1999. Analysis of peptidoglycan structure from vegetative cells of *Bacillus subtilis* 168 and role of PBP 5 in peptidoglycan maturation. J. Bacteriol. **181:**3956-3966.

6. **Atrih, A., G. Bacher, R. Körner, G. Allmaier, and S. J. Foster.** 1999. Structural analysis of *Bacillus megaterium* KM spore peptidoglycan and its dynamics during germination. Microbiol. **145:**1033-1041.

7. **Atrih, A., and S. J. Foster.** 2001. Analysis of the role of bacterial endospore cortex structure in resistance properties and demonstration of its conservation amongst species. J. Appl. Microbiol. **91:**364-372.

8. **Atrih, A., and S. J. Foster.** 2001. *In vivo* roles of the germination-specific lytic enzymes of *Bacillus subtilis* 168. Microbiol. **147:**2925-2932.

9. **Atrih, A., P. Zöllner, G. Allmaier, and S. J. Foster.** 1996. Structural analysis of *Bacillus subtilis* 168 endospore peptidoglycan and its role during differentiation. J. Bacteriol. **178:**6173-6183.

10. **Atrih, A., P. Zöllner, G. Allmaier, M. P. Williamson, and S. J. Foster.** 1998. Peptidoglycan structural dynamics during germination of *Bacillus subtilis* 168 endospores. J. Bacteriol. **180:**4603-4612.

11. **Austin, B. P., S. Nallamsetty, and D. S. Waugh.** 2009. Hexahistidine-tagged maltose-binding protein as a fusion partner for the production of soluble recombinant proteins in *Escherichia coli*. Methods Mol. Bio. **498:**157-172.

12. **Bagyan, I., M. Noback, S. Bron, M. Paidhungat, and P. Setlow.** 1998. Characterization of *yhcN*, a new forespore-specific gene of *Bacillus subtilis*. Gene **212:**179-188.

13. **Bagyan, I., and P. Setlow.** 2002. Localization of the cortex lytic enzyme CwlJ in spores of *Bacillus subtilis*. J. Bacteriol. **184:**1219-1224.

14. **Baillie, L. W. J.** 2006. Past, imminent and future human medical countermeasures for anthrax. J. Appl. Microbiol. **101:**594-606.

15. **Banawas, S., D. Paredes-Sabja, G. Korza, Y. Li, B. Hao, P. Setlow, and M. R. Sarker.** 2013. The *Clostridium perfringens* germinant receptor protein GerKC is located in the spore inner membrane and is crucial for spore germination. J. Bacteriol. **195:**5084-5091.

16. **Barlass, P. J., C. W. Houston, M. O. Clements, and A. Moir.** 2002. Germination of *Bacillus cereus* spores in response to L-alanine and to inosine: the roles of *gerL* and *gerQ* operons. Microbiol. **148:**2089-2095.

17. **Beaman, T. C., J. T. Greenamyre, T. R. Corner, H. S. Pankratz, and P. Gerhardt.** 1982. Bacterial spore heat resistance correlated with water content, wet density, and protoplast/sporoplast volume ratio. J. Bacteriol. **150:**870-877.

18. **Bergman, N. H., E. C. Anderson, E. E. Swenson, M. M. Niemeyer, A. D. Miyoshi, and P. C. Hanna.** 2006. Transcriptional profiling of the *Bacillus anthracis* life cycle in vitro and an implied model for regulation of spore formation. J. Bacteriol. **188:**6092-6100.

19. **Bernhards, C. B., and D. L. Popham.** 2014. The role of YpeB in cortex hydrolysis during germination of *Bacillus anthracis* spores. J. Bacteriol. **In Press, 196**.

20. **Bhavsar, A. P., X. Zhao, and E. D. Brown.** 2001. Development and characterization of a xylose-dependent system for expression of cloned genes in *Bacillus subtilis*: conditional complementation of a teichoic acid mutant. Appl. Environ. Microbiol. **67:**403-410.

21. **Bishop-Lilly, K. A., R. D. Plaut, P. E. Chen, A. Akmal, K. M. Willner, A. Butani, S. Dorsey, V. Mokashi, A. J. Mateczun, C. Chapman, M. George, T. Luu, T. D. Read, R. Calendar, S. Stibitz, and S. Sozhamannan.** 2012. Whole genome sequencing of phage resistant *Bacillus anthracis* mutants reveals an essential role for cell surface anchoring protein CsaB in phage AP50c adsorption. Virol. J. **9:**246.

22. **Blackburn, N. T., and A. J. Clarke.** 2001. Identification of four families of peptidoglycan lytic transglycosylases. J. Mol. Evol. **52:**78-84.

23. **Boland, F. M., A. Atrih, H. Chirakkal, S. J. Foster, and A. Moir.** 2000. Complete spore-cortex hydrolysis during germination of *Bacillus subtilis* 168 requires SleB and YpeB. Microbiol. **146:**57-64.

24. **Boschwitz, H., L. Gofshtein-Gandman, H. O. Halvorson, A. Keynan, and Y. Milner.** 1991. The possible involvement of trypsin-like enzymes in germination of spores of *Bacillus cereus* T and *Bacillus subtilis* 168. J. Gen. Microbiol. **137:**1145-1153.

25. **Boschwitz, H., H. O. Halvorson, A. Keynan, and Y. Milner.** 1985. Trypsinlike enzymes from dormant and germinated spores of *Bacillus cereus* T and their possible involvement in germination. J. Bacteriol. **164:**302-309.

26. **Boschwitz, H., Y. Milner, A. Keynan, H. O. Halvorson, and W. Troll.** 1983. Effect of inhibitors of trypsin-like proteolytic enzymes *Bacillus cereus* T spore germination. J. Bacteriol. **153:**700-708.

27. **Buist, G., A. Steen, J. Kok, and O. P. Kuipers.** 2008. LysM, a widely distributed protein motif for binding to (peptido)glycans. Mol. Microbiol. **68:**838-847.

28. **Burns, D. A., J. T. Heap, and N. P. Minton.** 2010. SleC is essential for germination of *Clostridium difficile* spores in nutrient-rich medium supplemented with the bile salt taurocholate. J. Bacteriol. **192:**657-664.

29. **Campo, N., K. A. Marquis, and D. Z. Rudner.** 2008. SpoIIQ anchors membrane proteins on both sides of the sporulation septum in *Bacillus subtilis*. J. Biol. Chem. **283:**4975-4982.

30. **Campo, N., and D. Z. Rudner.** 2006. A branched pathway governing the activation of a developmental transcription factor by regulated intramembrane proteolysis. Mol. Cell **23:**25-35.

31. **Campo, N., and D. Z. Rudner.** 2007. SpoIVB and CtpB are both forespore signals in the activation of the sporulation transcription factor sigmaK in *Bacillus subtilis*. J. Bacteriol. **189:**6021-6027.

32. **Canter, D. A.** 2005. Remediating anthrax-contaminated sites: Learning from the past to protect the future. Chem. Health and Safety **12:**13-19.

33. **CDC.** 2001. Update: Investigation of bioterrorism-related anthrax and interim guidelines for exposure management and antimicrobial therapy, October 2001. JAMA **286:**2226-2232.

34. **Chen, Y., S. Fukuoka, and S. Makino.** 2000. A novel spore peptidoglycan hydrolase of *Bacillus cereus*: biochemical characterization and nucleotide sequence of the corresponding gene, *sleL*. J. Bacteriol. **182:**1499-1506.

35. **Chen, Y., S. Miyata, S. Makino, and R. Moriyama.** 1997. Molecular characterization of a germination-specific muramidase from *Clostridium perfringens* S40 spores and nucleotide sequence of the corresponding gene. J. Bacteriol. **179:**3181-3187.

36. **Chirakkal, H., M. O'Rourke, A. Atrih, S. J. Foster, and A. Moir.** 2002. Analysis of spore cortex lytic enzymes and related proteins in *Bacillus subtilis* endospore germination. Microbiol. **148:**2383-2392.

37. **Christie, G., F. I. Üstok, Q. Lu, L. C. Packman, and C. R. Lowe.** 2010. Mutational analysis of *Bacillus megaterium* QM B1551 cortex-lytic enzymes. J. Bacteriol. **192:**5378-5389.

38. **Clausen, T., C. Southan, and M. Ehrmann.** 2002. The HtrA family of proteases: implications for protein composition and cell fate. Mol. Cell. **10:**443-455.

39. **Clouston, J. G., and P. A. Wills.** 1969. Initiation of germination and inactivation of *Bacillus pumilus* spores by hydrostatic pressure. J. Bacteriol. **97:**684-690.

40. **Cortezzo, D. E., B. Setlow, and P. Setlow.** 2004. Analysis of the action of compounds that inhibit the germination of spores of *Bacillus* species. J. Appl. Microbiol. **96:**725-741.

41. **Cote, C. K., D. J. Chabot, A. Scorpio, T. E. Blank, W. A. Day, S. L. Welkos, and J. A. Bozue.** 2006. *Bacillus anthracis*: Agent of Bioterror and Disease, p. 83-120. *In* H. F. Burt Anderson, and Mauro Bendinelli (ed.), Microorganisms and Bioterrorism. Springer US.

42. **Cowan, A. E., E. M. Olivastro, D. E. Koppel, C. A. Loshon, B. Setlow, and P. Setlow.** 2004. Lipids in the inner membrane of dormant spores of *Bacillus* species are largely immobile. Proc. Natl. Acad. Sci. USA **101:**7733-7738.

43. **Cutting, S., A. Driks, R. Schmidt, B. Kunkel, and R. Losick.** 1991. Forespore-specific transcription of a gene in the signal transduction pathway that governs Pro-σ^K processing in *Bacillus subtilis*. Genes Dev. **5:**456-466.

44. **Dalbey, R. E., P. Wang, and J. M. van Dijl.** 2012. Membrane proteases in the bacterial protein secretion and quality control pathway. Microbiol. Mol. Biol. Rev. **76:**311-330.

45. **Das, D., R. D. Finn, D. Carlton, M. D. Miller, P. Abdubek, T. Astakhova, H. L. Axelrod, C. Bakolitsa, C. Chen, H. J. Chiu, M. Chiu, T. Clayton, M. C. Deller, L. Duan, K. Ellrott, D. Ernst, C. L. Farr, J. Feuerhelm, J. C. Grant, A. Grzechnik, G. W. Han, L. Jaroszewski, K. K. Jin, H. E. Klock, M. W. Knuth, P. Kozbial, S. S. Krishna, A. Kumar, D. Marciano, D. McMullan, A. T. Morse, E. Nigoghossian, A. Nopakun, L. Okach, C. Puckett, R. Reyes, C. L. Rife, N. Sefcovic, H. J. Tien, C. B. Trame, H. van den Bedem, D. Weekes, T. Wooten, Q. Xu, K. O. Hodgson, J. Wooley, M. A. Elsliger, A. M. Deacon, A. Godzik, S. A. Lesley, and I. A. Wilson.** 2010. The structure of BVU2987 from *Bacteroides vulgatus* reveals a superfamily of bacterial periplasmic proteins with possible inhibitory function. Acta. Crystallogr. Sect. F Struct. Biol. Cryst. Commun. **66:**1265-1273.

46. **Dong, T. C., and S. M. Cutting.** 2003. SpoIVB-mediated cleavage of SpoIVFA could provide the intercellular signal to activate processing of Pro-σ^K in *Bacillus subtilis*. Mol. Microbiol. **49:**1425-1434.

47. **Dowd, M. M., B. Orsburn, and D. L. Popham.** 2008. Cortex peptidoglycan lytic activity in germinating *Bacillus anthracis* spores. J. Bacteriol. **190:**4541-4548.

48. **Driks, A.** 1999. *Bacillus subtilis* spore coat. Microbiol. Mol. Biol. Rev. **63:**1-20.

49. **Driks, A.** 2002. Maximum shields: the assembly and function of the bacterial spore coat. Trends Microbiol. **10:**251-254.

50. **Fabret, C., and J. A. Hoch.** 1998. A two-component signal transduction system essential for growth of *Bacillus subtilis*: implications for anti-infective therapy. J. Bacteriol. **180:**6375-6383.

51. **Fittipaldi, N., T. Sekizaki, D. Takamatsu, M. de la Cruz Dominguez-Punaro, J. Harel, N. K. Bui, W. Vollmer, and M. Gottschalk.** 2008. Significant contribution of the *pgdA* gene to the virulence of *Streptococcus suis*. Mol. Microbiol. **70:**1120-1135.

52. **Foster, S. J., and K. Johnstone.** 1987. Purification and properties of a germination-specific cortex-lytic enzyme from spores of *Bacillus megaterium* KM. Biochem. J. **242:**573-579.

53. **Gao, X., J. Wang, D. Q. Yu, F. Bian, B. B. Xie, X. L. Chen, B. C. Zhou, L. H. Lai, Z. X. Wang, J. W. Wu, and Y. Z. Zhang.** 2010. Structural basis for the autoprocessing of zinc metalloproteases in the thermolysin family. Proc. Natl. Acad. Sci. USA **107:**17569-17574.

54. **Gerhardt, P., and R. E. Marquis.** 1989. Spore Thermoresistance Mechanisms, p. 43-63. *In* I. Smith, R. A. Slepecky, and P. Setlow (ed.), Regulation of Prokaryotic Development. American Society for Microbiology, Washington, D.C.

55. **Giebel, J. D., K. A. Carr, E. C. Anderson, and P. C. Hanna.** 2009. The germination-specific lytic enzymes SleB, CwlJ1, and CwlJ2 each contribute to *Bacillus anthracis* spore germination and virulence. J. Bacteriol. **191:**5569-5576.

56. **González-Castro, M. J., J. López-Hernández, J. Simal-Lozano, and M. J. Oruña-Concha.** 1997. Determination of amino acids in green beans by derivitization with phenylisothiocyanate and high-performance liquid chromatography with ultraviolet detection. J. Chrom. Sci. **35:**181-185.

57. **Gould, G. W.** 2006. History of science-spores. J. Appl. Microbiol. **101:**507-513.

58. **Gould, G. W., and A. D. Hitchins.** 1963. Sensitization of bacterial spores to lysozyme and to hydrogen peroxide with agents which rupture disulphide bonds. J. Gen. Microbiol. **33:**413-423.

59. **Granger, A. C., E. K. Gaidamakova, V. Y. Matrosova, M. J. Daly, and P. Setlow.** 2011. Effects of Mn and Fe levels on *Bacillus subtilis* spore resistance and effects of Mn^{2+}, other divalent cations, orthophosphate, and dipicolinic acid on protein resistance to ionizing radiation. Appl. Environ. Microbiol. **77:**32-40.

60. **Gutelius, D., K. Hokeness, S. M. Logan, and C. W. Reid.** 2014. Functional analysis of SleC from *Clostridium difficile*: an essential lytic transglycosylase involved in spore germination. Microbiol. **160:**209-216.

61. **Haldenwang, W. G.** 1995. The sigma factors of *Bacillus subtilis*. Microbiol. Rev. **59:**1-30.

62. **Hanna, P.** 1999. Lethal toxin actions and their consequences. J. Appl. Microbiol. **87:**285-287.

63. **Heffron, J. D., E. A. Lambert, N. Sherry, and D. L. Popham.** 2010. Contributions of four cortex lytic enzymes to germination of *Bacillus anthracis* spores. J. Bacteriol. **192:**763-770.

64. **Heffron, J. D., B. Orsburn, and D. L. Popham.** 2009. Roles of germination-specific lytic enzymes CwlJ and SleB in *Bacillus anthracis*. J. Bacteriol. **191:**2237-2247.

65. **Heffron, J. D., N. Sherry, and D. L. Popham.** 2011. *In vitro* studies of peptidoglycan binding and hydrolysis by the *Bacillus anthracis* germination-specific lytic enzyme SleB. J. Bacteriol. **193:**125-131.

66. **Ho, S. N., H. D. Hunt, R. M. Horton, J. K. Pullen, and L. R. Pease.** 1989. Site-directed mutagenesis by overlap extension using the polymerase chain reaction. Gene **77:**51-59.

67. **Ho, T. D., K. B. Williams, Y. Chen, R. F. Helm, D. L. Popham, and C. D. Ellermeier.** 2014. *Clostridium difficile* extracytoplasmic function σ factor σ^V regulates lysozyme resistance and is necessary for pathogenesis in the hamster model of infection. Infect. Immun. **82:**2345-2355.

68. **Horsburgh, G. J., A. Atrih, and S. J. Foster.** 2003. Characterization of LytH, a differentiation-associated peptidoglycan hydrolase of *Bacillus subtilis* involved in endospore cortex maturation. J. Bacteriol. **185:**3813-3820.

69. **Hu, K., H. Yang, G. Liu, and H. Tan.** 2007. Cloning and identification of a gene encoding spore cortex-lytic enzyme in *Bacillus thuringiensis*. Curr. Microbiol. **54:**292-295.

70. **Hudson, K. D., B. M. Corfe, E. H. Kemp, I. M. Feavers, P. J. Coote, and A. Moir.** 2001. Localization of GerAA and GerAC germination proteins in the *Bacillus subtilis* spore. J. Bacteriol. **183:**4317-4322.

71. **Hunter, S., P. Jones, A. Mitchell, R. Apweiler, T. K. Attwood, A. Bateman, T. Bernard, D. Binns, P. Bork, S. Burge, E. de Castro, P. Coggill, M. Corbett, U. Das, L. Daugherty, L. Duquenne, R. D. Finn, M. Fraser, J. Gough, D. Haft, N. Hulo, D. Kahn, E. Kelly, I. Letunic, D. Lonsdale, R. Lopez, M. Madera, J. Maslen, C. McAnulla, J. McDowall, C. McMenamin, H. Mi, P. Mutowo-Muellenet, N. Mulder, D. Natale, C. Orengo, S. Pesseat, M. Punta, A. F. Quinn, C. Rivoire, A. Sangrador-Vegas, J. D. Selengut, C. J. Sigrist, M. Scheremetjew, J. Tate, M. Thimmajanarthanan, P. D. Thomas, C. H. Wu, C. Yeats, and S. Y. Yong.** 2012. InterPro in 2011: new developments in the family and domain prediction database. Nucleic Acids Res. **40:**D306-312.

72. **Imae, Y., and J. L. Strominger.** 1976. Relationship between cortex content and properties of *Bacillus sphaericus* spores. J. Bacteriol. **126:**907-913.

73. **Imamura, D., R. Kuwana, H. Takamatsu, and K. Watabe.** 2010. Localization of proteins to different layers and regions of *Bacillus subtilis* spore coats. J. Bacteriol. **192:**518-524.

74. **Ishikawa, S., K. Yamane, and J. Sekiguchi.** 1998. Regulation and characterization of a newly deduced cell wall hydrolase gene (*cwlJ*) which affects germination of *Bacillus subtilis* spores. J. Bacteriol. **180:**1375-1380.

75. **Janes, B. K., and S. Stibitz.** 2006. Routine markerless gene replacement in *Bacillus anthracis*. Infect. Immun. **74:**1949-1953.

76. **Jing, X., H. R. Robinson, J. D. Heffron, D. L. Popham, and F. D. Schubot.** 2012. The catalytic domain of the germination-specific lytic transglycosylase SleB from *Bacillus anthracis* displays a unique active site topology. Proteins **80:**2469-2475.

77. **Kapust, R. B., J. Tozser, J. D. Fox, D. E. Anderson, S. Cherry, T. D. Copeland, and D. S. Waugh.** 2001. Tobacco etch virus protease: mechanism of autolysis and rational design of stable mutants with wild-type catalytic proficiency. Protein Eng. **14:**993-1000.

78. **Kim, H. U., and J. M. Goepfert.** 1974. A sporulation medium for *Bacillus anthracis*. J. Appl. Bacteriol. **37:**265-267.

79. **Klimpel, K. R., N. Arora, and S. H. Leppla.** 1994. Anthrax toxin lethal factor contains a zinc metalloprotease consensus sequence which is required for lethal toxin activity. Mol. Microbiol. **13:**1093-1100.

80. **Kodama, T., H. Takamatsu, K. Asai, K. Kobayashi, N. Ogasawara, and K. Watabe.** 1999. The *Bacillus subtilis yaaH* gene Is transcribed by SigE RNA polymerase during sporulation, and its product is involved in germination of spores. J. Bacteriol. **181:**4584-4591.

81. **Korza, G., and P. Setlow.** 2013. Topology and accessibility of germination proteins in the *Bacillus subtilis* spore inner membrane. J. Bacteriol. **195:**1484-1491.

82. **Kroos, L., B. Zhang, H. Ichikawa, and Y. T. Yu.** 1999. Control of sigma factor activity during *Bacillus subtilis* sporulation. Mol. Microbiol. **31:**1285-1294.

83. **Kumazawa, T., A. Masayama, S. Fukuoka, S. Makino, T. Yoshimura, and R. Moriyama.** 2007. Mode of action of a germination-specific cortex-lytic enzyme, SleC, of *Clostridium perfringens* S40. Biosc. Biotech. Biochem. **71:**884-892.

84. **Kuwana, R., Y. Kasahara, M. Fujibayashi, H. Takamatsu, N. Ogasawara, and K. Watabe.** 2002. Proteomics characterization of novel spore proteins of *Bacillus subtilis*. Microbiol. **148:**3971-3982.

85. **Lambert, E. A., and D. L. Popham.** 2008. The *Bacillus anthracis* SleL (YaaH) protein is an *N*-acetylglucosaminidase involved in spore cortex depolymerization. J. Bacteriol. **190:**7601-7607.

86. **Lambert, E. A., N. Sherry, and D. L. Popham.** 2012. *In vitro* and *in vivo* analyses of the *Bacillus anthracis* spore cortex lytic protein SleL. Microbiol. **158:**1359-1368.

87. **Leighton, T. J., and R. H. Doi.** 1971. The stability of messenger ribonucleic acid during sporulation in *Bacillus subtilis*. J. Biol. Chem. **254:**3189-3195.

88. **Leppla, S. H.** 1982. Anthrax toxin edema factor: a bacterial adenylate cyclase that increases cyclic AMP concentrations of eukaryotic cells. Proc. Natl. Acad. Sci. USA **79:**3162-3166.

89. **Lewis, J. C., N. S. Snell, and H. K. Burr.** 1960. Water permeability of bacterial spores and the concept of a contractile cortex. Science **132:**544-545.

90. **Li, Y., X. Y. Butzin, A. Davis, B. Setlow, G. Korza, F. I. Üstok, G. Christie, P. Setlow, and B. Hao.** 2013. Activity and regulation of various forms of CwlJ, SleB, and YpeB proteins in degrading cortex peptidoglycan of spores of *Bacillus* species *in vitro* and during spore germination. J. Bacteriol. **195:**2530-2540.

91. **Li, Y., K. Jin, B. Setlow, P. Setlow, and B. Hao.** 2012. Crystal structure of the catalytic domain of the *Bacillus cereus* SleB protein important in cortex peptidoglycan degradation during spore germination. J. Bacteriol. **194:**4537-4545.

92. **Liu, H., N. H. Bergman, B. Thomason, S. Shallom, A. Hazen, J. Crossno, D. A. Rasko, J. Ravel, T. D. Read, S. N. Peterson, J. Yates, III, and P. C. Hanna.** 2004. Formation and composition of the *Bacillus anthracis* endospore. J. Bacteriol. **186:**164-178.

93. **Makino, S., N. Ito, T. Inoue, S. Miyata, and R. Moriyama.** 1994. A spore-lytic enzyme released from *Bacillus cereus* spores during germination. Microbiol. **140:**1403-1410.

94. **Makino, S., and R. Moriyama.** 2002. Hydrolysis of cortex peptidoglycan during bacterial spore germination. Med. Sci. Mon. **8:**119-127.

95. **Masayama, A., H. Fukuoka, S. Kato, T. Yoshimura, M. Moriyama, and R. Moriyama.** 2006. Subcellular localization of a germination-specific cortex-lytic enzyme, SleB, of Bacilli during sporulation. Genes Genet. Syst. **81:**163-169.

96. **Masayama, A., K. Hamasaki, K. Urakami, S. Shimamoto, S. Kato, S. Makino, T. Yoshimura, M. Moriyama, and R. Moriyama.** 2006. Expression of germination-related enzymes, CspA, CspB, CspC, SleC, and SleM, of *Clostridium perfringens* S40 in the mother cell compartment of sporulating cells. Genes Genet. Syst. **81:**227-234.

97. **Mastny, M., A. Heuck, R. Kurzbauer, A. Heiduk, P. Boisguerin, R. Volkmer, M. Ehrmann, C. D. Rodrigues, D. Z. Rudner, and T. Clausen.** 2013. CtpB assembles a gated protease tunnel regulating cell-cell signaling during spore formation in *Bacillus subtilis*. Cell **155:**647-658.

98. **McKenney, P. T., A. Driks, H. A. Eskandarian, P. Grabowski, J. Guberman, K. H. Wang, Z. Gitai, and P. Eichenberger.** 2010. A distance-weighted interaction map reveals a previously uncharacterized layer of the *Bacillus subtilis* spore coat. Curr. Biol. **20:**934-938.

99. **Meador-Parton, J., and D. L. Popham.** 2000. Structural analysis of *Bacillus subtilis* spore peptidoglycan during sporulation. J. Bacteriol. **182:**4491-4499.

100. **Miyata, S., S. Kozuka, Y. Yasuda, Y. Chen, R. Moriyama, K. Tochikubo, and S. Makino.** 1997. Localization of germination-specific spore-lytic enzymes in *Clostridium perfringens* S40 spores detected by immunoelectron microscopy. FEMS Microbiol. Lett. **152:**243-247.

101. **Miyata, S., R. Moriyama, N. Miyahara, and S. Makino.** 1995. A gene (*sleC*) encoding a spore-cortex-lytic enzyme from *Clostridium perfringens* S40 spores; cloning, sequence analysis and molecular characterization. Microbiol. **141:**2643-2650.

102. **Miyata, S., R. Moriyama, K. Sugimoto, and S. Makino.** 1995. Purification and partial characterization of a spore cortex-lytic enzyme of *Clostridium perfringens* S40 spores. Biosci. Biotech. Biochem. **59:**514-515.

103. **Mock, M., and A. Fouet.** 2001. Anthrax. Annu. Rev. Microbiol. **55:**647-671.

104. **Moir, A.** 2006. How do spores germinate? J. Appl. Microbiol. **101:**526-530.

105. **Moir, A., B. M. Corfe, and J. Behravan.** 2002. Spore germination. Cell. Mol. Life Sci. **59:**403-409.

106. **Moir, A., and D. A. Smith.** 1990. The genetics of bacterial spore germination. Annu. Rev. Microbiol. **44:**531-553.

107. **Monroe, A., and P. Setlow.** 2006. Localization of the transglutaminase cross-linking sites in the *Bacillus subtilis* spore coat protein GerQ. J. Bacteriol. **188:**7609-7616.

108. **Moriyama, R., H. Fukuoka, S. Miyata, S. Kudoh, A. Hattori, S. Kozuka, Y. Yasuda, K. Tochikubo, and S. Makino.** 1999. Expression of a germination-specific amidase,

SleB, of Bacilli in the forespore compartment of sporulating cells and its localization on the exterior side of the cortex in dormant spores. J. Bacteriol. **181:**2373-2378.

109. **Moriyama, R., A. Hattori, S. Miyata, S. Kudoh, and S. Makino.** 1996. A gene (*sleB*) encoding a spore cortex-lytic enzyme from *Bacillus subtilis* and response of the enzyme to L-alanine-mediated germination. J. Bacteriol. **178:**6059-6063.

110. **Moriyama, R., S. Kudoh, S. Miyata, S. Nonobe, A. Hattori, and S. Makino.** 1996. A germination-specific spore cortex-lytic enzyme from *Bacillus cereus* spores: cloning and sequencing of the gene and molecular characterization of the enzyme. J. Bacteriol. **178:**5330-5332.

111. **Myers, G. S. A., D. A. Rasko, J. K. Cheung, J. Ravel, R. Seshadri, R. T. DeBoy, Q. Ren, J. Varga, M. M. Awad, L. M. Brinkac, S. C. Daugherty, D. H. Haft, R. J. Dodson, R. Madupu, W. C. Nelson, M. J. Rosovitz, S. A. Sullivan, H. Khouri, G. I. Dimitrov, K. L. Watkins, S. Mulligan, J. Benton, D. Radune, D. J. Fisher, H. S. Atkins, T. Hiscox, B. H. Jost, S. J. Billington, J. G. Songer, B. A. McClane, R. W. Titball, J. I. Rood, S. B. Melville, and I. T. Paulsen.** 2006. Skewed genomic variability in strains of the toxigenic bacterial pathogen, *Clostridium perfringens*. Genome Res. **16:**1031-1040.

112. **Nicholson, W. L., N. Munakata, G. Horneck, H. J. Melosh, and P. Setlow.** 2000. Resistance of *Bacillus* endospores to extreme terrestrial and extraterrestrial environments. Microbiol. Mol. Biol. Rev. **64:**548-572.

113. **Nicholson, W. L., and P. Setlow.** 1990. Sporulation, germination, and outgrowth, p. 391-450. *In* C. R. Harwood and S. M. Cutting (ed.), Molecular Biological Methods for *Bacillus*. John Wiley and Sons Ltd., Chichester, England.

114. **Okamura, S., K. Urakami, M. Kimata, T. Aoshima, S. Shimamoto, R. Moriyama, and S. Makino.** 2000. The N-terminal prepeptide is required for the production of spore cortex-lytic enzyme from its inactive precursor during germination of *Clostridium perfringens* S40 spores. Mol. Microbiol. **37:**821-827.

115. **Orsburn, B., S. B. Melville, and D. L. Popham.** 2008. Factors contributing to heat resistance of *Clostridium perfringens* endospores. Appl. Environ. Microbiol. **74:**3328-3335.

116. **Ou, L.-T., and R. E. Marquis.** 1970. Electromechanical interactions in cell walls of Gram-positive cocci. J. Bacteriol. **101:**92-101.

117. **Paidhungat, M., K. Ragkousi, and P. Setlow.** 2001. Genetic requirements for induction of germination of spores of *Bacillus subtilis* by Ca^{2+}-dipicolinate. J. Bacteriol. **183:**4886-4893.

118. **Paidhungat, M., and P. Setlow.** 2001. Localization of a germinant receptor protein (GerBA) to the inner membrane of *Bacillus subtilis* spores. J. Bacteriol. **183:**3982-3990.

119. **Paidhungat, M., and P. Setlow.** 2000. Role of Ger proteins in nutrient and nonnutrient triggering of spore germination in *Bacillus subtilis*. J. Bacteriol. **182:**2513-2519.

120. **Papanikolau, Y., G. Prag, G. Tavlas, C. E. Vorgias, A. B. Oppenheim, and K. Petratos.** 2001. High resolution structural analyses of mutant chitinase A complexes with

substrates provide new insight into the mechanism of catalysis. Biochem. **40:**11338-11343.

121. **Paredes-Sabja, D., P. Setlow, and M. R. Sarker.** 2011. Germination of spores of *Bacillales* and *Clostridiales* species: mechanisms and proteins involved. Trends Microbiol. **19:**85-94.

122. **Paredes-Sabja, D., P. Setlow, and M. R. Sarker.** 2009. SleC is essential for cortex peptidoglycan hydrolysis during germination of spores of the pathogenic bacterium *Clostridium perfringens*. J. Bacteriol. **191:**2711-2720.

123. **Paredes-Sabja, D., P. Setlow, and M. R. Sarker.** 2009. The protease CspB is essential for initiation of cortex hydrolysis and dipicolinic acid (DPA) release during germination of spores of *Clostridium perfringens* type A food poisoning isolates. Microbiol. **155:**3464-3472.

124. **Popham, D., J. Helin, C. Costello, and P. Setlow.** 1996. Analysis of the peptidoglycan structure of *Bacillus subtilis* endospores. J. Bacteriol. **178:**6451-6458.

125. **Popham, D. L., and C. B. Bernhards.** 2015. Spore Peptidoglycan, In Press. *In* A. Driks and P. Eichenberger (ed.), The Bacterial Spore: From Molecules to Systems. ASM Press, Washington, D.C.

126. **Popham, D. L., M. E. Gilmore, and P. Setlow.** 1999. Roles of low-molecular-weight penicillin-binding proteins in *Bacillus subtilis* spore peptidoglycan synthesis and spore properties. J. Bacteriol. **181:**126-132.

127. **Popham, D. L., J. D. Heffron, and E. A. Lambert.** 2012. Degradation of Spore Peptidoglycan During Germination, p. 121-142. *In* E. Abel-Santos (ed.), Bacterial Spores: Current Research and Applications. Caister Academic Press, Norwich, UK.

128. **Popham, D. L., J. Helin, C. E. Costello, and P. Setlow.** 1996. Muramic lactam in peptidoglycan of *Bacillus subtilis* spores is required for spore outgrowth but not for spore dehydration or heat resistance. Proc. Natl. Acad. Sci. USA **93:**15405-15410.

129. **Popham, D. L., B. Illades-Aguiar, and P. Setlow.** 1995. The *Bacillus subtilis dacB* gene, encoding penicillin-binding protein 5*, is part of a three-gene operon required for proper spore cortex synthesis and spore core dehydration. J. Bacteriol. **177:**4721-4729.

130. **Popham, D. L., J. Meador-Parton, C. E. Costello, and P. Setlow.** 1999. Spore peptidoglycan structure in a *cwlD dacB* double mutant of *Bacillus subtilis*. J. Bacteriol. **181:**6205-6209.

131. **Psylinakis, E., I. G. Boneca, K. Mavromatis, A. Deli, E. Hayhurst, S. J. Foster, K. M. Varum, and V. Bouriotis.** 2005. Peptidoglycan N-acetylglucosamine deacetylases from *Bacillus cereus*, highly conserved proteins in *Bacillus anthracis*. J. Biol. Chem. **280:**30856-30863.

132. **Ragkousi, K., P. Eichenberger, C. van Ooij, and P. Setlow.** 2003. Identification of a new gene essential for germination of *Bacillus subtilis* spores with Ca^{2+}-dipicolinate. J. Bacteriol. **185:**2315-2329.

133. **Ragkousi, K., and P. Setlow.** 2004. Transglutaminase-mediated cross-linking of GerQ in the coats of *Bacillus subtilis* spores. J. Bacteriol. **186:**5567-5575.

134. **Resnekov, O., and R. Losick.** 1998. Negative regulation of the proteolytic activation of a developmental transcription factor in *Bacillus subtilis*. Proc. Natl. Acad. Sci. USA **95:**3162-3167.

135. **Riemann, H., and Z. J. Ordal.** 1961. Germination of bacterial endospores with calcium and dipicolinic acid Science **133:**1703-1704.

136. **Rode, L. J., and J. W. Foster.** 1960. Germination of bacterial spores by long-chain alkyl amines. Nature **188:**1132-1134.

137. **Rode, L. J., and J. W. Foster.** 1961. Germination of bacterial spores with alkyl primary amines. J. Bacteriol. **81:**768-779.

138. **Rode, L. J., and J. W. Foster.** 1960. The action of surfactants on bacterial spores. Archiv für Mikrobiologie **36:**67-94.

139. **Ross, C., and E. Abel-Santos.** 2010. The Ger receptor family from sporulating bacteria. Curr. Issues Mol. Biol. **12:**147-158.

140. **Scheurwater, E., C. W. Reid, and A. J. Clarke.** 2008. Lytic transglycosylases: bacterial space-making autolysins. Int. J. Biochem. Cell Biol. **40:**586-591.

141. **Schmidt, T. R., E. J. Scott, 2nd, and D. W. Dyer.** 2011. Whole-genome phylogenies of the family *Bacillaceae* and expansion of the sigma factor gene family in the *Bacillus cereus* species-group. BMC Genomics **12:**430.

142. **Sekiguchi, J., K. Akeo, H. Yamamoto, F. K. Khasanov, J. C. Alonso, and A. Kuroda.** 1995. Nucleotide sequence and regulation of a new putative cell wall hydrolase gene, *cwlD*, which effects germination in *Bacillus subtilis*. J. Bacteriol. **177:**5582-5589.

143. **Setlow, B., A. E. Cowan, and P. Setlow.** 2003. Germination of spores of *Bacillus subtilis* with dodecylamine. J. Appl. Microbiol. **95:**637-648.

144. **Setlow, B., E. Melly, and P. Setlow.** 2001. Properties of spores of *Bacillus subtilis* blocked at an intermediate stage in spore germination. J. Bacteriol. **183:**4894-4899.

145. **Setlow, B., L. Peng, C. A. Loshon, Y. Q. Li, G. Christie, and P. Setlow.** 2009. Characterization of the germination of *Bacillus megaterium* spores lacking enzymes that degrade the spore cortex. J. Appl. Microbiol. **107:**318-328.

146. **Setlow, P.** 2014. Germination of spores of *Bacillus* species: what we know and do not know. J. Bacteriol. **196:**1297-1305.

147. **Setlow, P.** 2003. Spore germination. Curr. Opin. Microbiol. **6:**550-556.

148. **Setlow, P.** 2006. Spores of *Bacillus subtilis*: their resistance to and killing by radiation, heat and chemicals. J. Appl. Microbiol. **101:**514-525.

149. **Shimamoto, S., R. Moriyama, K. Sugimoto, S. Miyata, and S. Makino.** 2001. Partial characterization of an enzyme fraction with protease activity which converts the spore peptidoglycan hydrolase (SleC) precursor to an active enzyme during germination of *Clostridium perfringens* S40 spores and analysis of a gene cluster involved in the activity. J. Bacteriol. **183:**3742-3751.

150. **Slepecky, R., and J. W. Foster.** 1959. Alterations in metal content of spores of *Bacillus megaterium* and the effect on some spore properties. J. Bacteriol. **78:**117-123.

151. **Spencer, R. C.** 2003. *Bacillus anthracis*. J. Clin. Pathol. **56:**182-187.

152. **Stackebrandt, E., and F. A. Rainey.** 1997. Phylogenetic Relationships, p. 3-20. *In* J. I. Rood, B. A. McClane, J. G. Songer, and R. W. Titball (ed.), The Clostridia: Molecular Biology and Pathogenesis. Academic Press, San Diego, CA.

153. **Steinmetz, M., and R. Richter.** 1994. Plasmids designed to alter the antibiotic resistance expressed by insertion mutations in *Bacillus subtilis*, through in vivo recombination. Gene **142:**79-83.

154. **Sweeney, D. A., C. W. Hicks, X. Cui, Y. Li, and P. Q. Eichacker.** 2011. Anthrax infection. Am. J. Respir. Crit. Care Med. **184:**1333-1341.

155. **Terry, C., A. Shepherd, D. S. Radford, A. Moir, and P. A. Bullough.** 2011. YwdL in *Bacillus cereus*: its role in germination and exosporium structure. PLoS One **6:**e23801.

156. **Thompson, J. D., D. G. Higgins, and T. J. Gibson.** 1994. CLUSTAL W: improving the sensitivity of progressive multiple sequence alignments through sequence weighting, position specific gap penalties and weight matrix choice. Nucleic Acids Research **22:**4673-4680.

157. **Tipper, D. J., and J. J. Gauthier.** 1972. Structure of the Bacterial Endospore, p. 3-12. *In* H. O. Halvorson, R. Hanson, and L. L. Campbell (ed.), Spores V. American Society for Microbiology, Washington, D.C.

158. **Tipper, D. J., and P. E. Linnet.** 1976. Distribution of peptidoglycan synthetase activities between sporangia and forespores in sporulating cells of *Bacillus sphaericus*. J. Bacteriol. **126:**213-221.

159. **Tjalsma, H., A. Bolhuis, J. D. H. Jongbloed, S. Bron, and J. M. van Dijl.** 2000. Signal peptide-dependent protein transport in *Bacillus subtilis*: a genome-based survey of the secretome. Microbiol. Mol. Biol. Rev. **64:**515-547.

160. **Urakami, K., S. Miyata, R. Moriyama, K. Sugimoto, and S. Makino.** 1999. Germination-specific cortex lytic enzymes from *Clostridium perfringens* S40 spore: time of synthesis, precursor structure and regulation of enzymatic activity. FEMS Microbiol. Lett. **173:**467-473.

161. **Üstok, F. I., L. C. Packman, C. R. Lowe, and G. Christie.** 2014. Spore germination mediated by *Bacillus megaterium* QM B1551 SleL and YpeB. J. Bacteriol. **196:**1045-1054.

162. **van den Ent, F., and J. Löwe.** 2006. RF cloning: a restriction-free method for inserting target genes into plasmids. J. Biochem. Biophys. Methods **67:**67-74.

163. **van Heijenoort, J.** 2001. Formation of the glycan chains in the synthesis of bacterial peptidoglycan. Glycobiol. **11:**25R-36R.

164. **Vepachedu, V. R., and P. Setlow.** 2007. Role of SpoVA proteins in release of dipicolinic acid during germination of *Bacillus subtilis* spores triggered by dodecylamine or lysozyme. J. Bacteriol. **189:**1565-1572.

165. **Vitale, G., R. Pellizzari, C. Recchi, G. Napolitani, M. Mock, and C. Montecucco.** 1998. Anthrax lethal factor cleaves the N-terminus of MAPKKs and induces

tyrosine/threonine phosphorylation of MAPKs in cultured macrophages. Biochem. Biophys. Res. Commun. **248:**706-711.

166. **Vollmer, W.** 2008. Structural variation in the glycan strands of bacterial peptidoglycan. FEMS Microbiol. Rev. **32:**287-306.

167. **Wach, A.** 1996. PCR-synthesis of marker cassettes with long flanking homology regions for gene disruptions in *S. cerevisiae*. Yeast **12:**259-265.

168. **Wakeley, P. R., R. Dorazi, N. T. Hoa, J. R. Bowyer, and S. M. Cutting.** 2000. Proteolysis of SpolVB is a critical determinant in signalling of Pro-σ^K processing in *Bacillus subtilis*. Mol. Microbiol. **36:**1336-1348.

169. **Warth, A. D.** 1985. Mechanisms of Heat Resistance, p. 209-225. *In* G. J. Dring, D. J. Ellar, and G. W. Gould (ed.), Fundamental and Applied Aspects of Bacterial Spores. Academic Press, Inc., London.

170. **Warth, A. D., and J. L. Strominger.** 1972. Structure of the peptidoglycan from spores of *Bacillus subtilis*. Biochem. **11:**1389-1396.

171. **Warth, A. D., and J. L. Strominger.** 1971. Structure of the peptidoglycan from vegetative cell walls of *Bacillus subtilis*. Biochem. **10:**4349-4358.

172. **Warth, A. D., and J. L. Strominger.** 1969. Structure of the peptidoglycan of bacterial spores: occurrence of the lactam of muramic acid. Proc. Natl. Acad. Sci. USA **64:**528-535.

173. **Westphal, A. J., P. B. Price, T. J. Leighton, and K. E. Wheeler.** 2003. Kinetics of size changes of individual *Bacillus thuringiensis* spores in response to changes in relative humidity. Proc. Natl. Acad. Sci. USA **100:**3461-3466.

174. **White, D.** 2007. Microbial Development and Physiological Adaptation: Varied Responses to Environmental Cues and Intercellular Signals, p. 467-598, The Physiology and Biochemistry of Prokaryotes, 3rd ed. Oxford University Press, New York, NY.

175. **Wuytack, E. Y., J. Soons, F. Poschet, and C. W. Michiels.** 2000. Comparative study of pressure- and nutrient-induced germination of *Bacillus subtilis* spores. Appl. Environ. Microbiol. **66:**257-261.

176. **Xue, Y.** 2008. Effects of protein domains on localization of penicillin-binding proteins 2a and 2b in *Bacillus subtilis*. Master's Thesis. Virginia Polytechnic Institute and State University, Blacksburg, VA.

177. **Yeats, C., N. D. Rawlings, and A. Bateman.** 2004. The PepSY domain: a regulator of peptidase activity in the microbial environment? Trends Biochem. Sci. **29:**169-172.

178. **Zhang, P., S. Thomas, Y. Q. Li, and P. Setlow.** 2012. Effects of cortex peptidoglycan structure and cortex hydrolysis on the kinetics of Ca^{2+}-dipicolinic acid release during *Bacillus subtilis* spore germination. J. Bacteriol. **194:**646-652.

179. **Zhou, R., C. Cusumano, D. Sui, R. M. Garavito, and L. Kroos.** 2009. Intramembrane proteolytic cleavage of a membrane-tethered transcription factor by a metalloprotease depends on ATP. Proc. Natl. Acad. Sci. USA **106:**16174-16179.